Assessment of Steel Structures Subjected to Fire Conditions

By

Phillip Oosthuizen

Supervisor

Dr. Alvin Masarira

Department of Civil Engineering

University of Cape Town

P/Bag Rondebosch 7701

Cape Town

This thesis is submitted in partial fulfillment of the requirements for award of the Master of Science Degree in Engineering at the University of Cape Town.

February 2010

DECLARATION

I know the meaning of plagiarism and declare that all the work in the document, save for that which is properly acknowledged, is my own.

ACKNOWLEDGEMENTS

My sincerest appreciation and gratitude goes to the following;

To Dr. Alvin Masarira, for the guidance and support in all aspects of my studies and for believing in my abilities.

To the staff of The Civil Engineering Department and for my fellow students for making the postgraduate studies so much more bearable.

To my wife, Katrina, a huge and special thank you, for bearing with me and taking care of our children, Phillippa and Brandon-Lee.

Above all, it was only through the grace and help of God that this thesis could be accomplished. Therefore may the glory and honor of God be evident in this thesis.

To God is the glory, for the things He hath done!

Table of Contents

List of Figures

List of Tables

1. Introduction

1.1 General

When structural steel frames or buildings are subjected to fire conditions, they suffer a loss of stiffness and strength. Members tested in isolation in the standard fire test behave different to members forming part of complete structural systems subjected to real fire conditions [1]. Member end fixity conditions and thermal restraint offered by connections and cooler adjacent structure have a major influence on the capacity of these members [2]. Coupled to this is the effect of the bracing system. Members located at considerable distances from the fire compartment are significantly affected in a frame with a flexible bracing system as opposed to a frame with an infinitely rigid bracing core [3].

Under real conditions, fire normally develops in a compartment and gas temperatures vary from the compartment floor level to the ceiling level. This usually causes temperature variations in members enclosing the fire compartment. The temperature of members under fire conditions can be uniform, non-uniform or have a temperature gradient along their lengths and/or have a cross sectional temperature gradient. Temperature distribution has a major effect on the capacity of these members [4]. Joints in steel framed buildings heat up at a slower rate than the material at mid span of a slower rate than the material at mid span of a beam or column and could be as much as 62 to 88% lower in temperature [5].

1.2 Historical Background

Applying fire protection to steel framed buildings remains the traditional means to satisfy the fire resistance requirements of these structures [5]. In addition Al-Jabri et al. [5] stated that it is more rational to design a structure to withstand fire as a load case, rather than to design the structure for ambient temperature conditions and applying fire protection afterwards.

Over the past two decades, many studies have been conducted and papers published on techniques of dealing with structures under fire conditions. The British Steel Corporation [6] tested various individual members in the standard fire test, subjected to both convective and radiative heat transfer processes in order to assess the heating rate of these members and their failure loads at various temperature levels.

1.3 Limitations

The research is based on finite element modelling using the analysis software package, ADINA [7], due to the extensive costs of conducting laboratory tests.

2. Introduction and Literature Review

2.1 Introduction

The collapse of the World Trade Centre in New York, USA, on September 11, 2001, prompted engineers to consider the effect of temperature on steel in more detail. As a result the central focus of researches conducted over the past decade was to investigate the effect of heat on the stiffness and strength of structural steel.

Laboratory experiments were conducted on isolated members and a limited number were conducted on complete frames at the Cardington Laboratory [1] and at other institutions in the USA and Britain etc.

This thesis will look at the experiments and research conducted over the past two decades. The development of temperature in isolated members and members forming part of complete frames are discussed in this chapter under section 2.1, `Steel Heating Rates and Observations'. The developments around analysis and design techniques are also considered in this chapter under section 2.2 ` Analysis and Design Techniques'.

These research are critically reviewed in this chapter and will form the basis of the types of steel members and steel frames to be modelled in the finite element program, ADINA [7].

2.2 Literature Review

2.2.1 Steel Heating Rates and Observations

The fire resistance of a structural member is defined by its resistance time when subjected to different load levels and increasing heat under controlled conditions in a standard fire test. Analytical techniques for this calculation are based on empirical, predictive equations derived from data, obtained from a large number of specimens tested in the standard fire test procedure.

T.R Kay, BR Kirby and RR Preston [8] noted in their comments on the European code of practice for "actions on structures exposed to fire", ENV.1991-2-7[9], that different furnaces heat up test specimens at different rates due to differences of net heat flux provided at the specimen. ENV.1991-2-7[9] allows designers to choose curve-fitting factors, γ_C and γ_r to ensure heating rates in alignment with approved fire-resistance testing furnaces in the UK. The authors also discuss, evaluate and recommend values for furnaces and structural steel emissivity (ε_f and

ε_m), the furnace gas temperature (Θ_g) and the configuration factor (Φ). In order to predict the temperature rise in members correctly, it is important to use suitable values for these factors.

It must also be stated, that the standard fire resistance test is much concerned with the fire resistance time i.e. the time it takes for a member to reach its critical temperature. This is understandable from a safety concern with regards to the safe evacuation of people and valuables. But focus must remain with the criteria to design buildings appropriately to withstand these temperatures in order to minimize damage to property. It is quite difficult to predict the heating rate of members in frames / structures as a large number of conditions play a major role in the intensity of a fire as well as direction of spread. Isolated members observed in the standard fire test behave vastly different from members forming part of building frames. This approach also assumes that the emissivity does not change with temperature.

The standard heat transfer model proposed by EN 1993-1-2: 2005 [10] does not include the effect of combustion products on the rate of heat transfer from the fire to structural elements and consequently over estimates the temperature increase of structural members.

This effect was investigated by J.I. Ghojel and M.B. Wong [11] and proposed a model with a particular medium. The model assumes a grey enclosure i.e. steel, the inside of which is filled with an isothermal non-grey gas. The model takes into account the thickness of the gas layer as thin layers transmit more radiation than thick layer. It is also assumed that the steel is a black body which does not emit heat. This can be true at the beginning of the heating process when the steel is cold and major process is heat absorption. But as the process progresses, the gas steel temperature becomes almost equal so that the steel might emit heat and even more so when the steel temperature is higher than that of the gas.

Kang-Hai et al. [12] mentioned in his review that observations made during the Cardington tests, revealed that steel members in a building frame heated up at a much slower rate than in the standard fire test. Observations from the Cardington test also revealed interactions between frame members and that steel columns possibly experience both axial and rotational restraint. It was also speculated that initial imperfections affect the failure time of steel columns under the effect of increased temperatures. Kang-Hai Tan, Wee-Siang Toh, Zhan –Fei Haung and Gaun-Hwee Phng [12] decided to verify these observations with experiments.

Column crookedness, load eccentricities and longitudinal temperatures development were measured in these experiments. Steel columns, having different slenderness ratios, and subjected to different degrees of axial restraints stiffness were tested under increasing temperature conditions. The columns were first tested under ambient temperature conditions to determine

their load capacity (P_u^{20}) and were subjected to a constant working load that was taken as 50% of P_u^{20}.

Kang-Hai Tan, Wee-Siang Toh, Zhan –Fei Haung and Gaun-Hwee Phng [12] observed that column imperfections and load eccentricities markedly reduce the column failure times. The column axial loads were significantly increased by axial restraints, resulting in a reduced column failure time. From these experimental results, the authors developed a simple Rankine approach to compute column failure times which compared well with test results. In the experiments, the steel columns were heated all-round, so that the cross sectional temperature of the steel columns were uniform. Again, this will most likely not be the case for columns under real fire conditions.

Fire compartments are used in buildings to stop the spread of fire, resulting in a zone of structural members at a higher temperature than the surrounding structure outside of this compartment. These weaker structural members are supported by the cooler surrounding structure providing alternative load paths and thus preventing collapse of the complete structure. The cooler and stiffer surrounding structures also prevent the thermal expansion of the heated members in the fire compartment inducing additional internal axial forces and moments. Members subjected to these forces will have lower failure strength than members tested in isolation in the standard fire test. Again, this might not be entirely true as YC Wang and JM Davies [13] stated that applied moment had no effect on the failure load of columns.

Compartment fire test were conducted by the Building Research Establishment on a full scale eight storey building in their Cardington Laboratory in 1995 and 1996. C.G. Bailey, D.B. Moore and T. Lennon [14] observed that heat protected columns were subjected to moments caused by the lateral displacements of heated beams. Moments calculated by using the standard slope-deflection equations were significantly lower than the recorded column moments. Purpose written computer software [15] was employed to model the frame in figure 2.1 and the predicted moments compared well to the test results. The model stiffened with steel cross-bracing indicated that the whole structure was affected by the expansion of the heated beam which induced moments in columns located some distance outside the fire compartment. Using infinite horizontal restraint in the centre of the frame by using shear walls resulted in a localised effect induced by the heated beam causing lateral deflection in the direction of least horizontal restraint. It was also noted that the axial stiffness of the beam has a huge impact on the amount of deflection induced in the column.

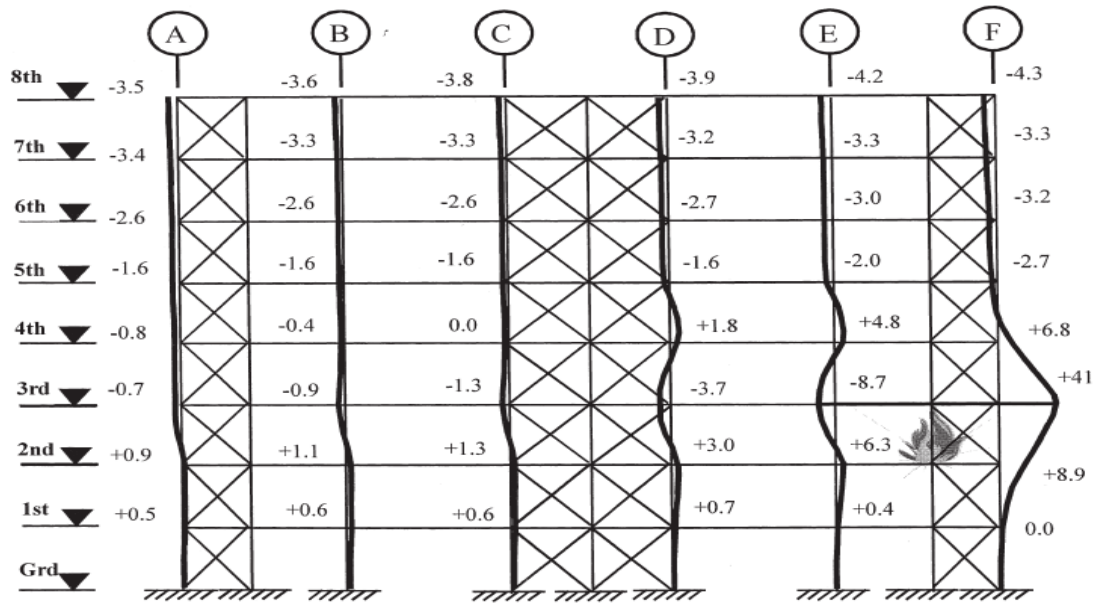

Figure 2.1: Predicted Lateral displacements of the two-dimensional frame representing the structure along gridline 4 [14]

Very little observation is made about the contribution of the column stiffness towards axial and rotational restraint. It must also be noted that the moments in columns are also induced by unbalanced loading on beams especially end columns. This might explain why moments determined from the slope-deflection equations were lower than actual recorded readings.

Structural steel frames experience a reduction in strength for the duration of a fire which can result in permanent deformations while the strength of these frames will be regained after the duration of the fire. Structural steel subjected to constant loading will deform permanently at temperatures in excess of 450 degrees due to creep and this was noted by Kirby and Preston [16]. Although almost no loss of stiffness and strength occur at low temperature levels, stresses of significant magnitude will lead to plasticity and fatigue of critical members in statically indeterminate structures.

These phenomena were studied by Lyle P. Carden and Ahmad M Itani [17] at the University of Nevada on a single level steel structure used as a training facility to extinguish fires. The structure was approximately 5 years old at the time of the study and was subjected to approximately three (3) fire simulations a week. The structure was also equipped with a sprinkler system to cool the areas of steel that had the highest temperatures. Based on physical measurements, the frame was analyzed for uniform cross-sectional temperature and for a temperature gradient across the cross section in both the x and y directions.

For a uniform temperature increase in the members of the steel frame, the resulting ultimate loads were very low compared to a differential temperature applied to the member cross-sections over the full length. Differential temperatures often result in permanent deformations in moment and eccentrically loaded frames (Figure 2.2). Hardening of the steel was evident at temperatures below the transition temperature and was caused by plastic strains induced by thermal actions in the structural members.

Figure 2.2: Permanently deformed column caused by different temperature between the west and east face [17].

The difference in temperature between the opposite faces of a structural member is kept constant through out the length of the members. This cannot be true for real structures, but definitely shed some light on structures subjected to repeated fires.

2.2.2 Analysis and Design Techniques

Steel frames under fire conditions experience an interaction of an elastic form of failure as well as a plastic form of failure and can be described by the Merchant Rankine formula. The critical load for the stability of these frames is in the non-linear range and the non-linear model of heated steel must be accounted for in the analysis. W Skowronski [18], has proposed a method for describing the behaviour of columns in a fire.

Skowronski [18] used the force method of analysis for the assemblage of a displacement matrix which consists of displacement components for columns externally loaded and for beams not axially loaded. For columns that are not axially load, the elements of the displacement matrix were calculated by taking the non-elastic effect of the heated steel into account. The elements for axially loaded columns were computed by taking into account the tangent modulus (E) to obtain linearized equations.

The method proposed by Skowronski [18] is reasonably accurate in the approach to the solution, but does not take into account the thermal expansion of steel. The assumption that the column behaves linearly elastic cannot be true. Some columns are either directly or indirectly affected by heat and depending on the level of load may or may not be in the linear elastic range.

Members of structural steel frames under fire conditions behave different to the simply supported members tested in the standard fire test. Y.C. Wang and D.B. Moore [1] developed a finite element computer program to include the behaviour of semi-rigid beam column connections, second-order geometrical nonlinearity, residual stresses and initial deflections. They also noted that both gas and steel temperatures recorded on a full-scale portal frame tested in a natural fire by the Fire Research Station (FRS) and the British Steel Corporation [19] at the FRS Cardington Laboratory differed quite remarkably from the standard fire exposure. It must be noted that the full-scale tests were carried out under specific fire conditions i.e. specific fire load, specific ventilation conditions, etc.

Advanced finite element analysis programs do not solve problems in a fashion in which the interaction of the governing parameters is clear. These finite element programs also do not allow for code prescribed equations that are of use in structural designs. M.A. Bradford, T. K. Luu and A. Heidarpour [20] addressed this issue in 2007 by using a fundamental mechanics approach based on virtual work.

M.A. Bradford, T. K. Lun and A. Heidarpour [20] derived an equation based on the principle of virtual work to describe all possible degrees of displacement as follows;

$$\int_{-L}^{L} \int_{A} (\sigma.\delta_{\varepsilon})\, dA dZ + (k_L\, \omega_L.\, \delta_{\omega L} + k_R\, \omega_R.\, \delta_{\omega R} + r_L v_L'.\, \delta v_L' + r_R v_R'.\, \delta v_R') - \int_{-L}^{L} q\,(z).\, \delta v dz = 0 \qquad (2.1)$$

Where k_L and k_R are the elastic spring stiffness of the supports, r_L and r_R are the elastic rotational spring stiffness of the supports ωL and ω_R is the deformation in the z-direction, ν_L and ν_R are the end transverse displacements and δ is the deflection and the direction of the deflection is defined by the subscripts ν_L, ν_R, ω_L and ω_R. δ_ε is the deflection induced by strain and σ is the stress in the member. The superscripts in ν_L' and ν_R' define the first derivative of the transverse displacements. The subscripts L and R refer to z at –L and L respectively.

The substitution of the thermal and mechanical components of the nonlinear strain- displacement relationship, together with the stress-strain relationship at elevated temperature, into this equation results in a formulation of the principles of virtual work. This equation is slightly improved by enforcing an arbitrary reference axis at the centroid of the cross sectional area at a given temperature.

The arbitrary variations in both the transverse and axial directions in the integrand of this equation can be used to derive the familiar beam-column or tie-beam deformation equation. The transverse displacement can be obtained from the analytical solution of the differential equation together with the kinematical end conditions and static boundary conditions. The equations of equilibrium are based on the strain at the reference level and the static boundary conditions which can be solved to produce the axial force in a member.

Although the above approach allows transparency of the influence of the various parameters of the structural behaviour, it still requires a high level of mathematical skill to solve and develop these equations especially for more complex sub-frames. Also sub-frames as proposed by this method, do not really take into account the influence of members on the outside of the sub-frame.

Finite element analysis is often used to model both the mechanical and thermal response of structures under fire conditions. However, this method sometimes becomes too complex and time consuming for many practising engineers. On the other hand, the simple calculations model is more widely used but the results obtained are often very inaccurate and conservative.

M B Wong and M Szafranski [21] developed a simple elastic method to fill the gap between the simple and advanced calculation models. The method is based on the following equation which defines the degree of utilization of a member;

$$\eta_{fi} = \frac{E_{fi.d.t}}{R_d} \qquad (2.2)$$

Where $E_{fi,d}$ is the design effect of fire actions and $R_{fi,d,t}$ is the design resistance of the steel member. The equation is used to establish the interaction relationship for pure bending and for axial bending through which the limiting temperature can be obtained. The method assumes a uniform temperature increment for all members of the frame or structure. This is not acceptable as all members in a frame or structure will not be heated up at the same rate and there will be a temperature gradient across the length of the member or its cross-section. This assumption will result in axial deformation of members only and will not take care of the curvature induced by the cross-sectional temperature gradient.

The method also does separate analyses for both static and thermal loading. One would think that these two processes are inter-related and by separation may not reflect the true behaviour of the structure. The method has shown by way of examples that as the complexity of the failure criterion increases, the limiting temperature for a frame or structure reduces.

Structures subjected to fire experience geometrical and material non-linear behaviour as well as thermal straining effects. It is important to understand the failure mechanism or progressive collapse of these structures under thermal loading. To this end Y.B.Yang, I.J. Lin, L.J. Leu and C.W. Huang [22] presented a finite element procedure for the inelastic post-bucking analysis of steel trusses under thermal loading.

Their method uses the basic principles of mechanics to develop a force displacement relationship for the truss members. The relationship is also presented in an incremental form to allow the loads or the temperature to be applied in increments. Fixed-end thermal loads are generated by fixing the ends of members while the member is allowed to displace in a subsequent phase by unlocking the member ends and simultaneously apply forces that are equal and opposite to these generated forces. Procedures for dealing with load and temperature changes separately are developed to overcome the instability associated with the limit points. The generalised displacement control method (GDC) is used to indicate the limit point.

The method is effective and sound in terms of current principles of mechanics. The method however assumes that the truss members experience a uniform temperature increase which cannot be entirely true. A member under non-uniform temperature will develop a moment which will influence the buckling load of the member. Also, in real fires, all members of a truss will be

at different temperatures, so that cooler members will provide restraint to thermal expansion. It is however worthy to note that this method has shown that the critical load decreases significantly with an increase in temperature.

Members of a frame experience intricate processes when exposed to fire conditions that are different from members subjected to the standard fire test. The heating conditions of the standard fire test do not match the conditions of real fires. These factors cause a change in both the boundary conditions and the load in a structural member of a frame.

This effect was investigated by Y.C.Wang [23] with the aide of a finite element computer programme. Boundary conditions for columns in a sub frame were modelled for cold conditions with various beam and column lengths. The limiting temperature was determined for the cold condition for columns with procedures recommended in Eurocode 3 Part 1.4 [24] and BS 5950 Part 8 [25]. Then limiting temperatures were obtained with the help of the finite element program. These temperatures were higher than those obtained by using Eurocode 3 procedures. New effective length ratios were calculated from the higher limiting temperatures which were close to values for fixed end boundary conditions.

The restraining effect of column continuity was also modelled in the finite element computer programme. An equation expressing the increase of the column axial compressive force was developed and validated by the author. This increased compressive load is added to the initial load in the column to give the total axial load. This load is then used to calculate the limiting temperature of the column, by using the relationship between the steel column limiting temperature and its load ratios recommended by Eurocode 3 Part 1.4 [24].

It is clear that the restraining effect of frame continuity results in the increase of the axial compressive force in the column and thus reducing the limiting temperature. An increase in the slenderness ratio also reduces the column limiting temperature. It was also noted that the effect of a column restraining a beam's thermal expansion has a very small influence on the column's limiting temperature. This is caused by the expanding beam inducing lateral deflections and movements in the column at early stages and at later stages restrains the less stiff column lateral deflections.

It must be noted that the author does not include all possible conditions that might influence the behaviour of columns. For instance a column less affected by heat than the restraining beam will cause large lateral deflections and movements in such a column.

Steel frames under fire conditions experience a degradation of strength due to the loss of strength of individual members at elevated temperatures. This effect is approximately reflected by the decrease in the elastic buckling strength of the structure. Elastic buckling of members are caused by the axial compression and bending action and will cause overall elastic buckling of the frame when these members interact with other members of the structure.

The phenomenon was thoroughly studied by M.B. Wong and N. Patterson [26] in 1995. From first principles of mechanics, they derived the axial forces in a cross-section caused by uniform temperature increase and the associated movement induced when there exists a temperature gradient across the cross-section. Based on the assumption that structures behave linearly elastic until instability occurs, the external loads were increased proportionally by a common factor, λ_c, to obtain the tangent stiffness matrix of the structure. Because of this assumption the axial loads of the geometric stiffness matrix caused by the temperature effect are separated from the axial loads caused by the external loads.

This cannot be entirely true as the axial loads induced by temperature reduce the axial force effect caused by the external loads. This might have the effect of increasing the elastic buckling load factor of the frame. The limiting temperature of the frame can also be obtained when the elastic buckling load factor is equal to unity. It is interesting to note that the results of an example frame showed little difference in the elastic buckling load factor for a uniform temperature increase across the cross-section compared to a temperature gradient across the cross-section.

Columns under fire conditions restrained against both rotation and sway has been studied extensively in theoretical format but not experimentally. Based upon this, Y.C. Wang and J.M. Davies [27], decided to observe the behaviour of restrained columns under heated conditions and under various levels of axial loads and primary bending moment levels. They noted that columns under increasing temperatures and subjected to a high primary bending moment and a low axial load, experience a reversal in the column moments shortly before failure. However, for columns under similar conditions, but subjected to a low primary bending moment and a high axial load will experience a reversal in the column moment long before failure. This can be ascribed to the P- δ effect experienced by the weakened flexible column behaving like a cable and causing a hogging moment at the stiffer beam-column connections.

Y.C. Wang and J.M. Davies [27] also developed a fifth degree polynomial equation for calculating the effective length of tested columns. It was observed that the effective length of the column increased to unity under increasing temperature and then reduced to lower values. This indicates that the beam-column connections exhibited pin-end conditions while the lower effective length values border fixed-end conditions. This observation is quite interesting as it might help to explain why members in structures under real fire conditions seem to exhibit more durability than its members tested in isolation thus far. However, in their case, the pin-end condition at the connection was enforced but the application of a moment at the connection. This also explains why the effective lengths remain unchanged when no external moment is applied.

Failure temperatures and failure loads were calculated by Y.C. Wang and J.M. Davies [27] according to BS 5950 Part 8 [25] and Eurocode 3 Part 1.2 [10], respectively. It was found that the calculated values, using BS 5950 Part 8 [24], compared well to experimental values when the bending moment was ignored and the effective length of 0.7 was increased to 1.2. The values predicted by the Eurocode 3 Part 1.2 [10], were based on effective length ratios of 1.0 and 0.7. These values were more conservative than the values predicted by BS5950 Part 8 [25], having failure loads of approximately 30% and 10 % lower than the actual failure loads obtained from experimental results.

Y.C. Wang and J.M. Davies [27] also concluded that column failure at elevated temperature was mainly due to axial load and was not affected by the connection stiffness i.e. pinned or fixed and by the initially applied bending moments. This is another interesting observation as one would expect moment in addition to axial load to reduce the strength of columns even further.

A theoretical analysis that can be performed by hand is required to enable engineers to quickly determine the buckling load of a column under fire conditions. Various experiments have been performed on columns under non-uniform longitudinal temperature conditions but these did not consider the influence of end restraints on the buckling load.

In 2006, K.H. Tan and W.F. Yuang [28], developed an analytical method for determining the buckling load of columns under non-uniform longitudinal temperature conditions. The critical buckling load is obtained from the conditions of equilibrium for bending moments based on curvature and deflection. The authors use a linear temperature distribution to determine the force P_T induced by the temperature and the restraint effect. A step temperature distribution is also used to determine the critical buckling load ($P_{c\text{-}cr}$) and the critical external buckling load ($P_{o\text{-}cr}$). It should be noted that the Young's modulus and the thermal expansion ratio are adjusted for the linear and stepped temperature distribution along the column length. In this method the

temperature is only non-uniform along the column length and the cross-sectional temperature is kept constant. This however is not acceptable as a column in real fire conditions will have a differential cross-sectional temperature.

K.H. Tan and W.F. Yuang [28] noted that if the bottom temperature is kept constant and the top temperature is increased, the value of P_T increased while the value of $P_{c\text{-}cr}$ decreased. By plotting the values of P_T and $P_{c\text{-}cr}$ divided by the Euler buckling load (P_E) at the column bottom temperature one can observe the above trends. For the case of uniform temperature it can be seen that the gradients for P_T and $P_{c\text{-}cr}$ are much steeper, so that by assuming this situation will lead to a significant under estimation of the critical buckling had as can be seen in figure 2.3.

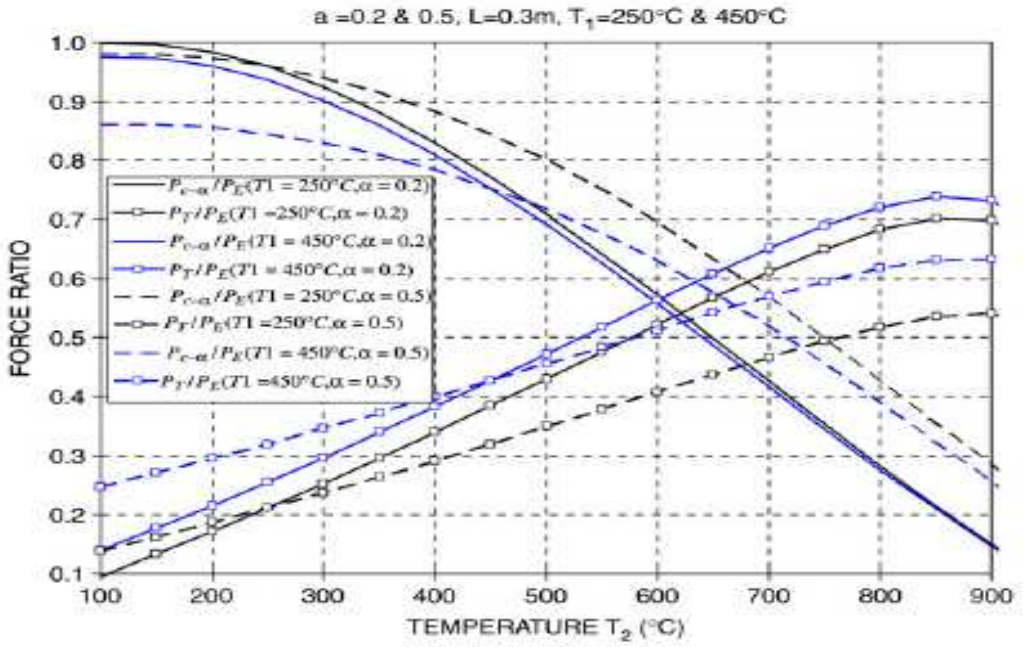

Fig. 2.3. Axial forces versus T_2: Two step distribution [28].

This analytical method however lacks the ability to analyze steel columns that experience plastic behaviour in fire. The authors also observed that the critical temperature of columns is reduced by axial restraint and is enhanced by rotational restraint.

3. Background Theory

3.1 Introduction

This chapter will discuss relevant theoretical and classical theory as background to this research. In order to achieve these objectives, this chapter will deal with the following;

i) The heat transfer model for unprotected steel members in a compartment fire.
ii) The calculation of the heating rate of an unprotected steel member in the Standard Fire Resistance Test.
iii) The material properties of structural steel at elevated temperature.
iv) The temperatures in fire based on ISO 834 [29] time-temperature curve and Eurocode 1 Part 2-2 [30].
v) The behaviour of beams and columns in furnace tests and a brief discussion on the design concepts of structural steel at elevated temperature.
vi) The basic principles of structural behaviour of elements under fire conditions.

3.2 Heat Transfer model for unprotected steel members in a standard compartment fire

3.2.1 Eurocode approach

According to Eurocode 3 [10], the temperature increase, ΔT_s during time increment Δt in the case of bare unprotected steel members in a fire through convection and radiation, is given by

$$\Delta Ts = \frac{1}{c_{ps}\,\rho_s}\left(\frac{P}{A_s}\right)\left(q_c + q_r\right)\Delta t \qquad (3.1)$$

where $c_{\rho s}$ is the specific heat of steel in J/kg K, ρ_s is the density of steel in kg/m^3 and P/A is the massivity or section factor (perimeter/ cross-sectional area). The two heat flux components: convection q_c and radiation, q_r , both in W/m^2, are represented as follows:

$$q_c = h_c\left(T_g - T_s\right) \qquad (3.2)$$

and $$qr = \varepsilon_{res}\,\sigma\left[\left(T_g + 273\right)4 - \left(T_s = 273\right)^4\right] \qquad (3.3)$$

where h_c is the heat transfer coefficient (assumed 25 W/m^2 K, T_g and T_s are the temperatures of the fire and steel, respectively (^{o} C), σ is the Stephan-Boltzmann constant (5.67 x 10 -^{8} W/m^2 K^4). The resultant emissivity ε_{res} is given by

$$\varepsilon_{res} = \frac{1}{\left(\frac{1}{\varepsilon_s}\right) + \left(\frac{1}{\varepsilon_f}\right) - 1} \tag{3.4}$$

where ε_f and ε_s are the emissivities of the fire and steel members, respectively. Emissivity is the ability of an object to emit radiation and is a function of surface finish. Equation (3.4) assumes that the fire has a constant emissivity ε_{res} and is radiating to a structural element through a perfectly transparent medium, and that the combustion products are not influencing the radiation exchange rate. Also, it is very unlikely that the resultant emissivity will not change with temperature.

3.2.2 Model with participating medium

D.K. Edwards and R. Matavosian [31] proposed the following equation to describe the radiative heat exchange between a gas and a steel member, assuming a grey (partially absorbing and emitting) enclosure filled with isothermal non-grey gas;

$$q = F_g \sigma (T_g + 273)^4 - F_s \sigma (T_s + 273)^4 \tag{3.5}$$

Where σ is the Stephan-Boltzmann constant, T_g and T_s are the temperatures of the fire and steel, respectively (^{o} C) and the transfer factors, F_g and F_s, are as follows;

$$F_g = \frac{\varepsilon_s \varepsilon_g}{1 - (1 - \varepsilon_s)\left[\left(\frac{\alpha_{g2} - \alpha_{g1}}{\alpha_{g1}}\right)\right]} \tag{3.6a}$$

$$F_g = \frac{\varepsilon_s \alpha_{sg1}}{1 - (1 - \varepsilon_s)\left[\frac{(\alpha_{g2} - \alpha_{g1})}{\alpha_{g1}}\right]} \tag{3.6b}$$

ε_s is the emissivity of the inner surface of the grey enclosure, ε_g is the total emissivity of the gaseous mixture at temperature T_g over the mean beam length of the enclosure, and α_g is the total absorptivity of the gaseous mixture for the radiation from a black surface at temperature T_s absorbed over the mean beam length by the gaseous mixture at temperature T_g. The subscript 1 denotes properties for the mean beam length of the enclosure and subscript 2 for the two mean beam length lengths including the effect of one reflection. The mean beam length is a characteristic dimension of the thickness of the gas layer transmitting radiative energy and is denoted by $L_e = 3.6\ V_c / A_c$. Where A_c and V_c are the surface area and the volume of the compartment, respectively. From the radiation property chart, the total emissivity, ε_{gs}, is first determined at atmospheric pressure as a function of the average gas temperature, partial pressure of the water vapour content and the thickness of the gas layer. This is then scaled to any pressure, up to 10 times the atmospheric pressure using a scaling component chart.

$$\alpha_{gs} = \left(T_g / T_s \right)^{\frac{1}{2}} \varepsilon_{gs} \tag{3.7}$$

For the case of a grey gas radiating to a black enclosure, ε_s =1.0 and substituting into Eqs. (3.5) and (3.6), yield the following;

$$q_r = \varepsilon_g \sigma (T_g + 273)^4 - \alpha_g \sigma (T_s + 273)^4 \tag{3.8}$$

If this equation is used for the radiation heat transfer in models, an improved correlation is found between measured and predicted temperature responses of structural members under standard and wood fire conditions (Ghojel [32], and Wong et al. [33]). By deduction, one would consider this effect to be similar for framed structures.

3.3 Calculation of the Heating Rate of an unprotected Steel Member in a Standard Fire Resistance Test

3.3.1 Introduction

Much of the work presented here is based on research carried out by T.R. Kay [8]. The fire resistance of a structural member is founded on its performance in the standard fire resistance test, EN. 1363-1 (ISO 834-1) [34 & 29] and can either be measured by testing or calculated using appropriate methods of analyses as recommended by ENV.1991-1-2-7 [9]. Due to the difficulty of testing in existing furnaces and due to financial reasons, the latter option has become more favourable in the design of structural members. The accuracy, however, is dependant on the validity of material property data used in the calculations and also on the chosen analytical model used.

In the European standard, ENV 1991-2-7 [9], for actions on structures exposed to fire, it is recommended that a standardized technique be employed to calculate the fire resistance of structural members.

Normally, the fire resistance of a load bearing structural member is calculated in two stages. First of all, the manner in which the temperature of the member increases with time, in the standard fire resistance test, must be determined (the thermal response model). The deformation of the structure/member, under the action of its applied load, can then be determined with increasing temperature (the mechanical response model).

The accuracy of the thermal response model, proves to be the most critical calculation, as most mechanical analysis types will produce similar deformations, stress values etc. with time.

3.3.2 Heating models for structural steel members

The structural member to be tested is positioned in a large furnace and is subjected to both convective heat transfers from the hot gases in the furnace and the radiative heat from the furnace inside surfaces.

The quantity of heat transferred per unit length of the test member, over a short time interval, Δt, is:

$$q = \alpha.A_m.(\theta_f - \theta_m)\Delta t \quad (3.9)$$

where α= total heat transfer coefficient (W/m^2 K), A_m = surface area per unit length exposed to fire (m^2/m), θ_f = temperature of hot gases (º C), θ_m = temperature of the test specimen (º C). If the temperature of the test specimen is increased by $\Delta\theta_m$ when q units of heat are absorbed, then

$$q = c_m m_m.\Delta\theta_m \quad (3.10)$$

Where $\Delta\theta_m = \frac{\alpha}{c_m}.\frac{A_m}{m_m}.(\theta_f - \theta_m).\Delta t$ (3.11)

Since mass is volume x density, therefore

$$\frac{A_m}{m_m} = \frac{A_m}{V \times \rho_m} \quad (3.12)$$

The ratio $A_m/V(m^{-1})$ is known as the section factor of the test piece. Substituting eqn(3.12) into eqn(3.11) gives the following expression for specimen's temperature increase;

$$\Delta\theta_m = \frac{\alpha}{c_m \rho_m}.\frac{A_m}{V}.(\theta_f - \theta_m).\Delta t \quad (3.13)$$

This equation forms the basis of the majority of existing models for the calculation of the heating rate of a structural member/structure in a standard fire resistance test. The disadvantage of eqn (3.13) is that it assumes the temperature of the test specimen is uniform and the advantage is that it takes into account the variation of the physical material properties with temperature increase. The estimation of an appropriate value for the total heat transfer coefficient, α, the variance of the density, ρ_m, and the specific heat, c_m, are of paramount importance to accurately determine the temperature increase of the structural member/structure. The total heat transfer coefficient, α, consists of two components, as follows;

$$\alpha = \alpha_c + \alpha_r \quad (3.14)$$

where α_c = the coefficient of heat transfer by convection, and α_r = the coefficient of heat transfer by radiation.

3.3.3 Convective heat transfer

The heat flux is proportional to the temperature difference between the test member, θ_m, and the furnace gases, θ_g (Newton's Law). The convective heat flux per unit surface area of the specimen is given by

$$h_c = \alpha_c(\theta_g - \theta_m) W/m^2 \qquad (3.15)$$

The coefficient of α_c is ascribed a value of 25 W/m^2 , by ENV. 1991-2-7 [9], and is not temperature dependant. Both, C. and Twilt, L., Report No. BI-89-208 [35], has suggested that the value of θ_g and θ_m becomes almost the same as time progresses and can be seen in Fig. 3.2. Therefore the effect of h_c becomes insignificant in the heating process of the structural steel member.

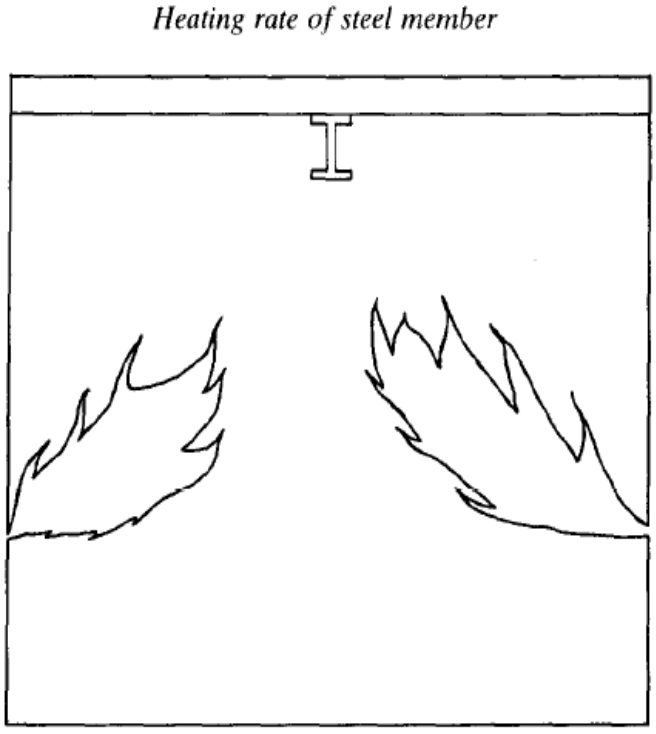

Fig. 3.1 Schematic section through a standard fire resistance test furnace [8]

3.3.4 Radiative heat transfer

As time progresses in a standard fire resistance test, radiation becomes the dominant heating process. The rate at which energy is radiated from a body is proportional to the fourth power of its absolute temperature, thus

$$h_r = \sigma(\theta + 273)^4 W/m^2 \quad (3.16)$$

where σ is the Stefan-Boltzmann constant, is 5.67 x 10-^{8} W/m^2 K^4. A body radiating this amount of heat (no body actually does), is called a black body. Only a fraction of black body radiation is emitted and is defined by the following equation;

$$h_r = \varepsilon.\sigma(\theta + 273)^4 W/m^2 \quad (3.17)$$

where ε (‹ 1) is the emissivity. Emissivity is largely dependant on surface finish, being low for polished metal surfaces and closer to unity for dull, oxidized materials. The value of ε is assumed to be independent of temperature for calculation.

The structural member under investigation, at a temperature θ_m, will emit some radiation and will receive a greater amount of radiation from the furnace, which is at a temperature of θ_f. Therefore, the net heat flux received by the member is

h_r = heat flux received from the furnace minus heat flux radiated back to the furnace

The net heat flow per unit surface area of the test member, h_r, depends on the relative sizes and positions of the test member and the furnace.

a) For very small test members (i.e. in relation to the furnace size), the radiant heat emitted by it and if ever reflected back by the furnace walls and/or gases, is the defined by

$$h_r = \varepsilon_m.\sigma\left[(\theta_f + 273)^4 - (\theta_m + 273)^4\right] W/m^2 \quad (3.18)$$

Figure 3.1 which show a test geometry conforming to this condition.

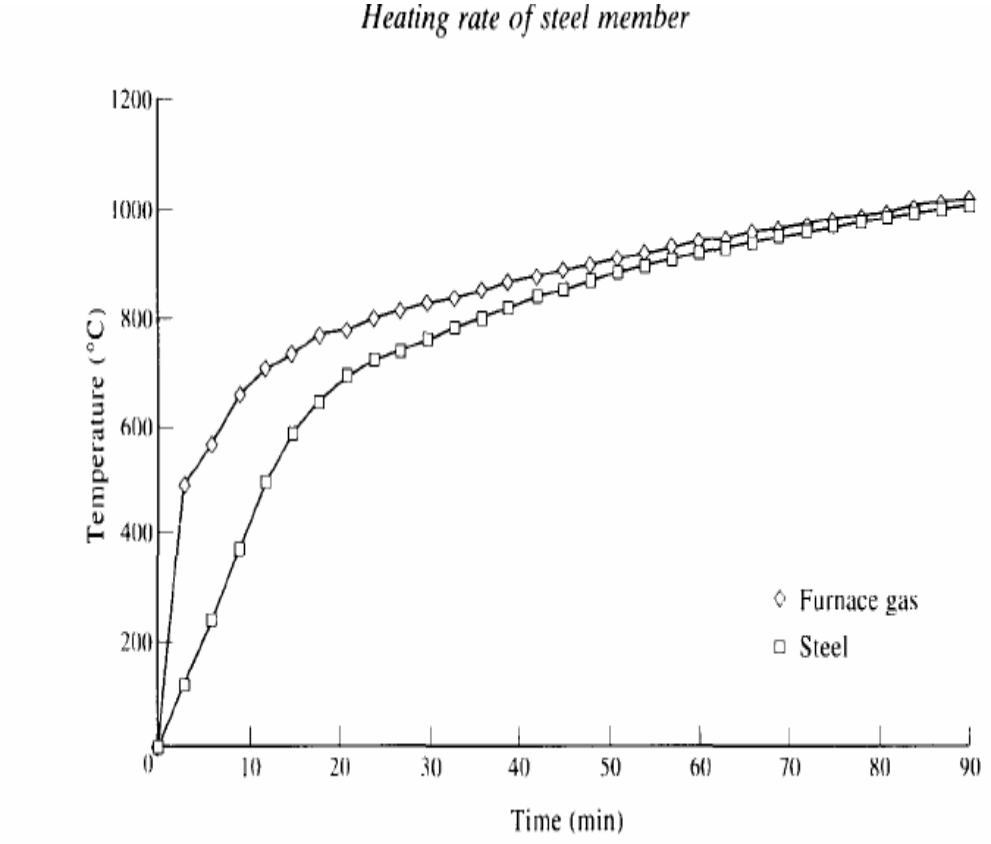

Fig. 3.2 Heating rate of a 406mm x 178mm x 54 kg/m steel beam in a standard fire resistance test [8]

b) For large test members, the emissivity of the furnace becomes dominant and the radiation emitted by the test member is absorbed or reflected back to it by the furnace, and is given by

$$h_r = \frac{\varepsilon_f . \varepsilon_m \sigma}{\varepsilon_f + \varepsilon_m - \varepsilon_f . \varepsilon_m} \left[(\theta_f + 273)^4 - (\theta_m + 273)^4 \right] W/m^2 \qquad (3.19a)$$

It was shown, by Fishenden et al. [36], Lankford et al. [37] and Thor [38], that in a standard fire resistance test on a steel member, the values of both ε_f and ε_m are approximately 0.8, thus

$$\frac{\varepsilon_f . \varepsilon_m}{\varepsilon_f + \varepsilon_m - \varepsilon_f . \varepsilon_m} = \frac{0.64}{0.96} = 0.67 \qquad (3.19b)$$

The above expression is normally replaced by

$$\varepsilon_r = \varepsilon_f . \varepsilon_m = 0.64 \qquad (3.19c)$$

This is known as the resultant emissivity and is used in EN.1991-2-7[9]. EN.1991-2-7[9] gives the radiative heat flux to a steel member in a standard fire resistance test as

$$h_r = \Phi.\varepsilon.\sigma\left[\left(\theta_f + 273\right)^4 - \left(\theta_m + 273\right)^4\right] W/m^2 \qquad (3.20)$$

where Φ is a configuration factor usually taken as one (1.0) for test members completely surrounded by flames and must be corrected by an appropriate section factor if member is not completely engulfed in flames.

According to EN.1991-2-7 [9], the total heat flux radiated to a test steel member in a standard fire resistance test is

$$h = \gamma_c.h_c + \gamma_r.h_r \qquad (3.21)$$

Where γ_c and γ_r are safety factors. The γ is a curve fitting factor chosen to ensure the prediction of a heating rate in agreement with observed heating rates in nationally approved fire-resistance-testing furnaces. The factors for determining h_c are known because:

$$\alpha_c = 25 W/m^2 \qquad (3.22)$$

and $\theta_g = 345\log_{10}\left(8t+1\right)+20$ from EN. 1363-1 [34]. (3.23)

However, to determine h_r, one has to assume values for ε_f, ε_m and θ_f. There have been many suggestions, by others, for the emissivity values of steel (Fig. 3.3) and in the range of 20-800 º C, the value of ε_m is always in excess of 0.79.

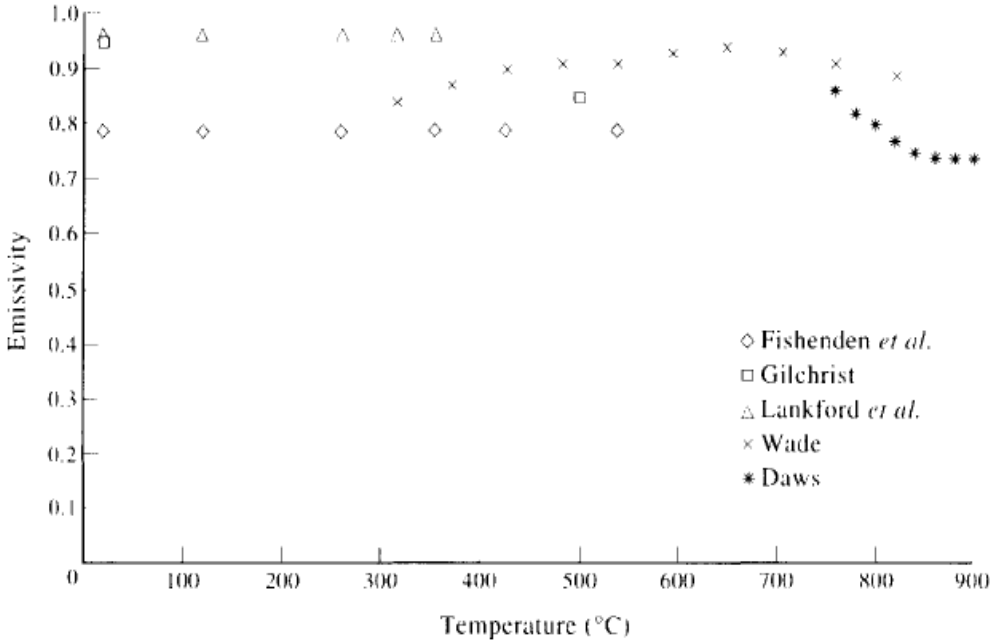

Fig. 3.3 Emissivity of dull oxidized mild steel [8].

On the other hand, the emissivity of the furnace, ε_f, is determined by its size, construction, linings and the composition of the flames. Radiant heating of the test member in a natural-gas-fire test furnace is dependant on emissions from the walls and floor of the chamber and therefore θ_f in eqn. (3.20) should describe the temperature of these surfaces rather than that of the gas, θ_g, adjacent to the test member. For oil-fired furnaces, it may be justifiable to equate θ_f to θ_g.

3.3.5 Analytical methods

From earlier discussion, it is clear that calculation, from first principles, of the heat transfer within a gas-fired furnace is a reasonably intricate problem. The normal procedure is to make a large number of observations on a particular design of furnace and then use the resulting data to develop empirical, predictive equations. Equation (3.13), which describes the heating of the test steel member, can be rearranged as follows;

$$\frac{\Delta\theta_m}{\Delta t} = \frac{A_m}{V}.\frac{h}{c_m.\rho_m} \qquad (3.24)$$

Where h is the effective heat flux, both radiative and convective, at a certain point on the test member at any instant (i.e. incident heat flux – heat flux emitted by the test member).
Thus, knowing the heating rate of a steel beam, A_m/V, in a standard fire resistance test furnace, allows one to determine the value of h at regular intervals throughout the test. This exercise has

been carried out for unprotected 254 x 146 x 43 kg/m I-section steel beams tested in the floor furnace at Warrington Fire Research Centre [8]. Figure 3.6 reflects the observed mean temperature/time values for the lower (exposed) flange of the beam. Figure 3.5 shows the effective heat flux, h, calculated from the curve shown in figure 3.6. The general shape of the curve arises from the requirement to heat the furnace gases in such a manner that they display the same temperature/time curve prescribed in ISO 834-1 (EN.1363-1) [34].

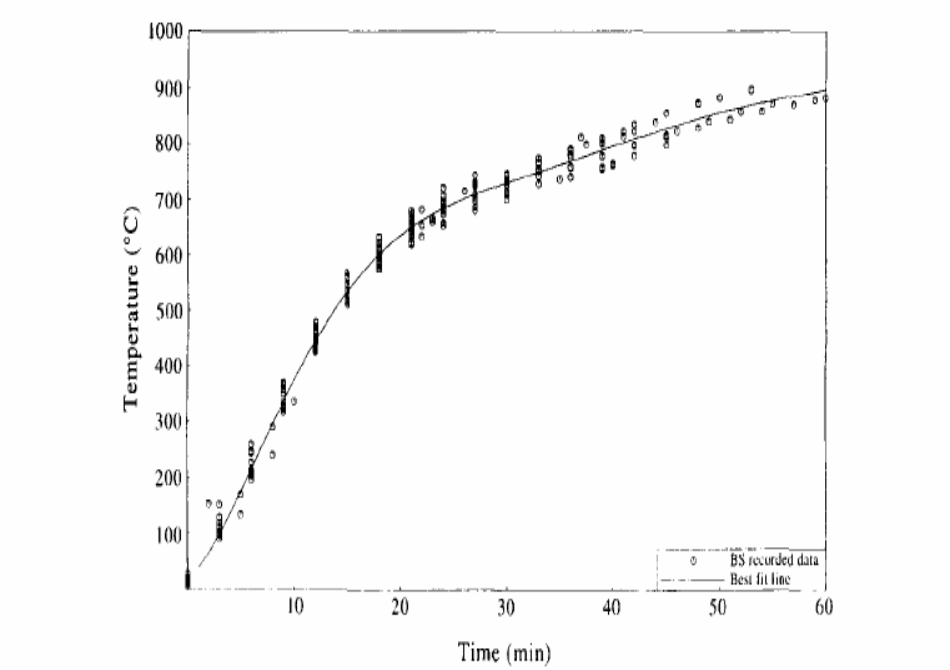

Fig. 3.4: 254 x146 x 43 kg/m unprotected beam-lower flange heating rate [8].

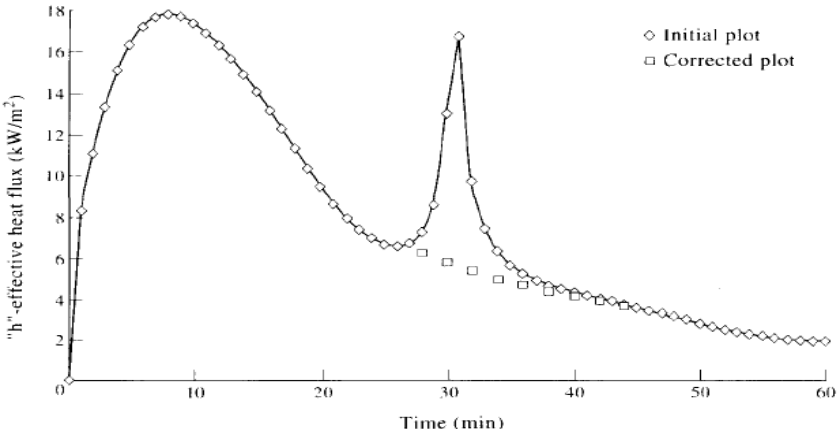

Fig. 3.5 Effective heat flux calculated from heating rate of beam in standard fire resistance test [8]

The effective heat flux = incident heat flux – heat flux emitted by the steel beam or

$$h = h_i - h_m \tag{3.25}$$

The value of h_m can be obtained from the following expression;

$$h_m = \varepsilon_m . \sigma (\theta_m + 273)^4 \tag{3.26}$$

Assuming ε_m is 0.8 (Fig. 3.3), the values of h_m, and hence h_i, have been calculated at regular intervals as shown in Fig. 3.6.

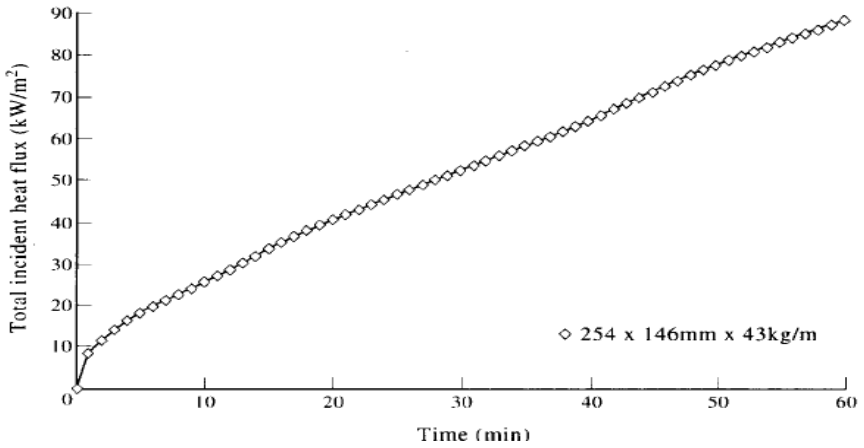

Fig. 3.6 Total incident heat flux estimated during a standard fire resistance test on a steel beam at Warrington Fire Research Centre [8]

If the above analysis is correct and furnace operation is well controlled, then calculated values of the incident heat flux, h_i, should be the same regardless of the size of the beam under test.

3.4 Discussion of EC3 - Fire Engineering Design of Steel Structures

3.4.1 Mechanical properties of steel

Most construction materials suffer a progressive loss of strength and stiffness as their temperature increases. For steel these effects can be seen in Eurocode 3 [10] stress-strain curves (Fig. 3.7) and occurs at temperatures as low as 300 º C.

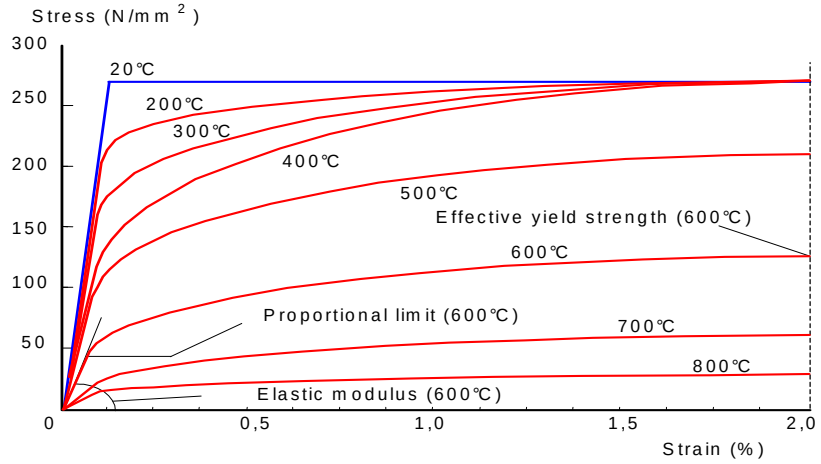

Fig. 3.7.Reduction of stress-strain properties with temperature for S275 steel [10].

3.4.2 Thermal properties of steel

3.4.2.1 Thermal expansion of steel

Top flanges of steel members experience a differential thermal expansion and this may be due to shielding of the top flange, for example a beam that supports a concrete slab which causes a heat-sink effect. In larger structures e.g. frames, it is necessary to recognize the restraining effect to thermal expansion by the structure outside of the fire compartments. It is considered necessary that one appreciates the variance of the coefficients of steel with respect to temperature (Fig. 3.8).

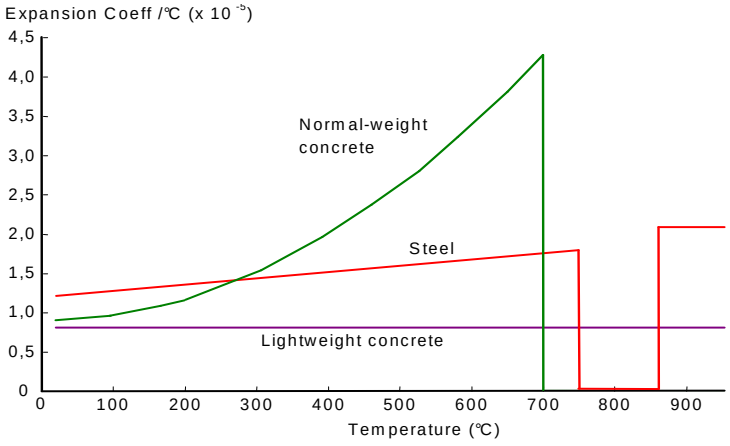

Figure 3.8 Variation of Eurocode 3 thermal expansion coefficients of steel and concrete with temperature [10].

3.4.2.2 Thermal conductivity of steel

This is a coefficient that affects the rate at which heat arriving at the steel surface is conducted through the metal (Fig. 3.9). For simple fire engineering calculations, one may use the constant conservative value of 45 W/m^{o} K.

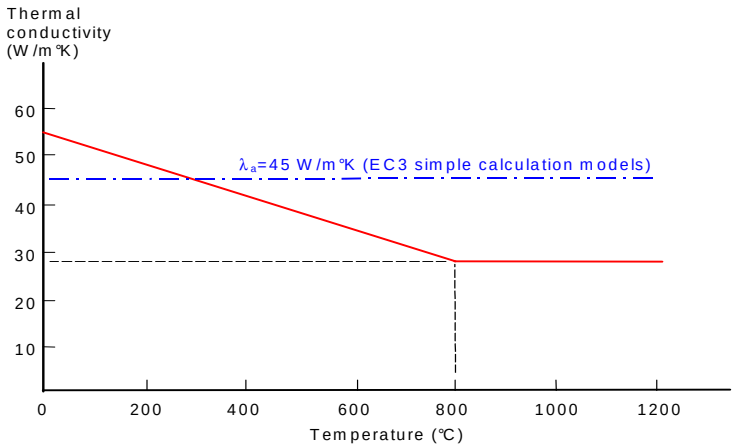

Fig. 3.9 Eurocode 3 representations of the variation of thermal conductivity of steel with temperature [10].

3.4.2.3 Specific heat of steel

The specific heat of steel is the quantity of heat required to increase the steel temperature by 1 ^{o}C. This value varies somewhat with temperature and can be observed in figure 3.10. One observes a sharp increase in this value at a temperature range of approximately 735 ^{o}C and this can be due to the fact that the material undergoes a crystal-structure phase change. Once again, for simple fire engineering calculations a value of 600 J/kg ^{0}C may be used, but does not allow for the endothermic nature of the phase change.

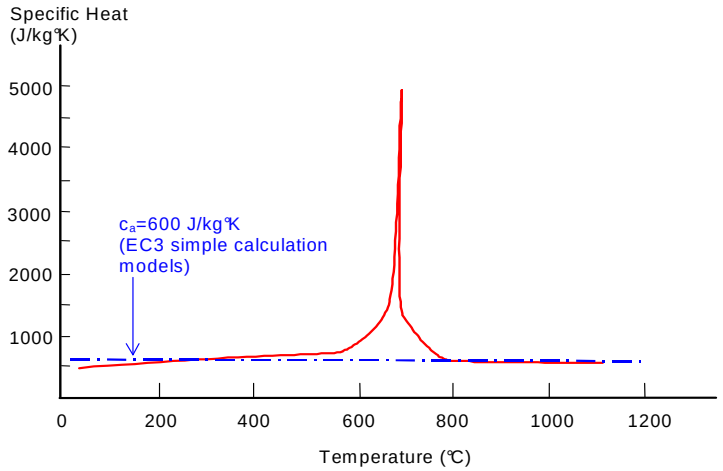

Figure 3.10 Variation of the specific heat of steel with temperature [10].

3.4.3 Temperatures in fires

Real fires in buildings grow and decay in relation to the mass and energy balance within the compartments (Fig. 3.11). The energy released depends upon the quantity and type of fuel available and also upon the ventilation conditions prevailing.

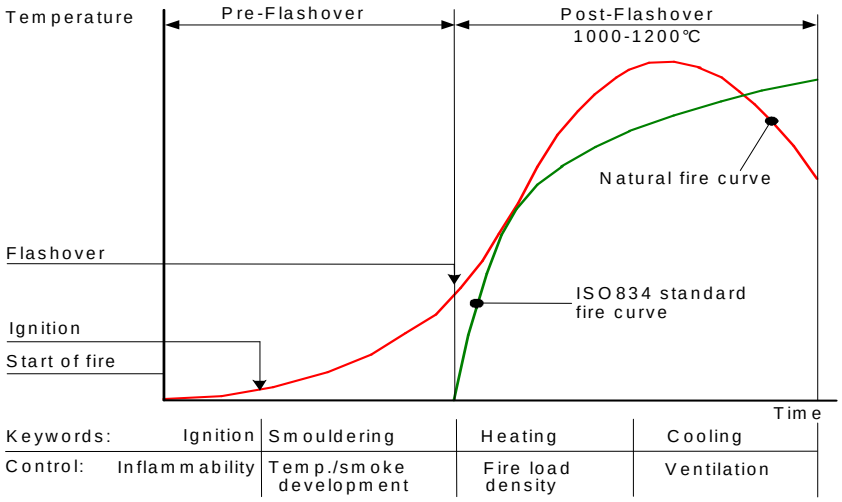

Figure 3.11 Phases of a natural fire, comparing atmosphere temperatures with the ISO834 standard fire curve [10].

Real fires can be defined by three phase's viz. growth, full development and decay. Fire resistance times stipulated in most national codes relate to the test performance of structural members when heated in accordance with an internationally agreed time-temperature curve defined in ISO 834 [34]. This curve portrays atmosphere temperatures which rise continuously with time, but at a diminishing rate (Fig. 3.12). This curve has become the standard design curve which is employed for furnace testing of structural steel members.

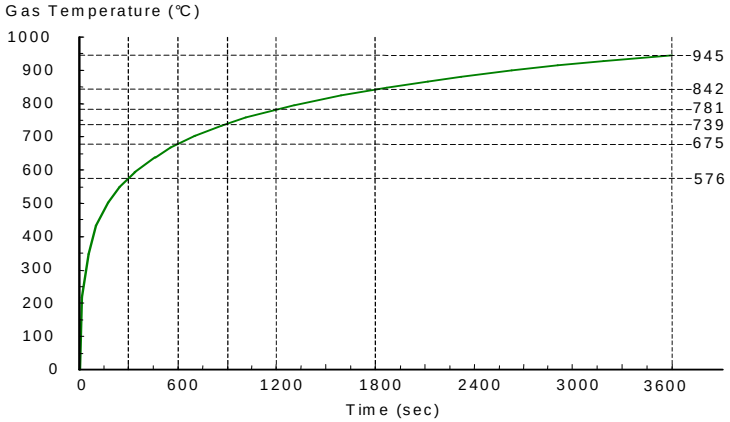

Figure 3.12 Atmosphere temperatures for ISO834 standard fire [10].

The ‘’External Fire’’ curve may be used to determine the fire resistance of structures exposed to exterior fire, which have lower atmosphere temperatures (Fig.3.13). The ‘’ Hydrocarbon Fire’’ curve on the other hand may be used in cases where buildings are used for the storage of hydrocarbon materials (Fig. 3.13).

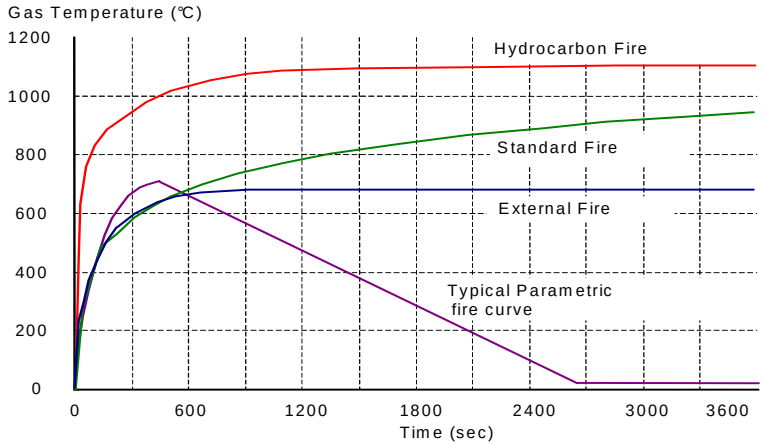

Figure 3.13. EC1 Part 2-2 nominal fire curves compared with a parametric fire [10].

An alternative method, is to attempt to model a natural fire using a ``parametric’’ fire curve for which equations are provided in EC1 Part 2-2 [30]. This enables one to compute simple models of fire temperatures in the heating and cooling phases of the post-flashover fire and the time at which the maximum temperature is attained. Data, however is required on the material properties (density, specific heat, thermal conductivity etc.) enclosing the compartment, the fire load (fuel) density and the ventilation conditions/areas when employing these equations.

When using the parametric curve, the ‘equivalent time’ can be employed to compare the severity of the fire in consistent terms and also to relate the resistance times of structural members in real fires to their resistance in the standard fire.

3.4.4 Behaviour of beams and columns in furnace tests

The behaviour of frame structural members is assessed by subjection to testing in furnaces using the standard time-temperature atmosphere curve. Full-scale testing of structural members under load is difficult due to furnace size restrictions. The only support condition of a member in a furnace is simply supported, with the member allowed to expand axially. A member normally forms part of a fire compartment in a frame/structure surrounded by adjacent members of the frame/structure, which are unaffected by the fire and consequently these members resist the thermal expansion of the heated member.

At ambient temperatures structural deflections are very small and axial restraint is very rarely an issue of significance. Axial restraint operates in various manners at different stages of a fire. In the early stages the restraint of thermal expansion is associated with the development of high compressive stresses. At later stages the weakening of the material is high and the restraint may begin to support the member by resisting pull-in. These effects cannot be reproduced in a furnace test and a complete collapse would occur if no safety cut-off criterion is applied. This also seems to be the reason for limiting the test cut-off to a deflection of span/20.

It is only recently, that fire tests have been conducted on compartments of whole structures. Full-scale testing is extremely expensive; with the consequence that there will never be a large volume of documented results and current results will be used to verify numerical models on which future developments in design will be based. At present, Eurocode 3 Part 1-2 [10], Cl. 3.4.1-4, allows for the use of advanced calculation models, but their design procedures are still in terms of isolated members and fire resistance is mainly determined for real or simulated furnace test.

3.4.5 Loadings

Eurocode 1 Part 2-2 [30] presents rules for calculating design actions (loadings) in fire, which allows for the low probability of a major fire event coinciding with high load intensities. In Eurocode 3 Part 1-2 [10], for the fire event, the permanent characteristic actions (dead loading) are used unfactored ($\gamma_{GA} = 1.0$) while the principal characteristic variable action (imposed loading) is factored down by a combination factor $\Psi_{1.1}$ whose value lies between 0.5 and 0.9 depending on the building usage. The reduction factor can be expressed as follows:

$$\eta_{fi} = \frac{E_{fi.d.t}}{R_d} \qquad (3.27)$$

(loading in fire as a proportion of ambient-temperature design resistance), which is relevant when global structural analysis is used, or

$$\eta_{fi} = \frac{E_{fi.d.t}}{E_d} \qquad (3.28)$$

(loading in fire as a proportion of ambient-temperature factored design load). This is conservative and employed in the design of individual members, when only the principal variable action is used together with the permanent action. This may be defined in terms of the characteristic loads and their factors as follows:

$$\eta_{fi} = \frac{\gamma_{GA}.G_k + \psi_{1.1}Q_{k.1}}{\gamma_G.G_k + \gamma_{G.1}.G_{k.1}} \quad (3.29)$$

3.4.6 Basic Principles of fire resistant design

Fire resistant design of structural steel members is the calculation of the fire resistance time of the members, when subjected to the standard fire curve, before it would fail. It needs to be within specified time limits, as dictated in relevant national building regulations, for example Eurocode 1 Part 2-2, section 2 [30]. This may be expressed in three alternative forms:

- The fire resistance time should exceed the requirement for the building usage and type. When loaded to the design load level and subjected to a nominal fire temperature curve:

  $t_{fi.d} \geq t_{fi.requ}$ (3.30)

  where $t_{fi.d}$ is the design standard fire resistance time of a member and $t_{fi.requ}$ is the standard fire resistance nominal time required.
- The load-bearing resistance of the member should exceed the design loading when it has been heated for the required time in the nominal fire:

  $R_{fi.d.t} \geq E_{fi.d.t}$ (3.31)

  where $R_{fi.d.t}$ is the design load-bearing resistance time of a member and $E_{fi.d.t}$ is the design effect of actions on a member at a given time.

- The critical temperature of a member loaded to the design level should exceed the design temperature associated with the required exposure to the nominal fire:

  $\theta_{cr.d} \geq \theta_d$ (3.32)

  where $\theta_{cr.d}$ is the critical design temperature of a member and θ_d is the design temperature of a member.

3.4.7 Cross section classification

In fire design, compression members and beams carrying a concrete slab on the compression flange are classified as for ambient-temperature design, because of low strain levels which are developed in the compression flanges at failure. Similarly, this also applies to class 3 and 4 members, for which the strains are also low. For other members, the limiting proportion value of ε is decreased as temperature rises, adversely affecting section classification. Therefore, the

limiting proportions of members in classes 1 or 2 are modified to an effective width/thickness ratio:

$$\left[\frac{b}{t}\right]_{eff} = \frac{b}{t}\sqrt{\left[\left(\frac{f_y}{235}\right)\left(\frac{k_{y.\theta}}{k_{E.\theta}}\right)\right]} \qquad (3.33)$$

where

b/t = actual width/thickness

f_y = steel yield strength

$k_{y.\theta}$ = yield strength reduction factor for steel at temperature θ

$k_{E.\theta}$ = elastic modulus reduction factor for steel at temperature θ.

One needs to note that this effect may cause the classification of a member to change as the temperature changes and imply that section classification becomes an iterative process.

3.4.8 Critical temperature

The temperature at which a member fails under a given loading is the critical temperature. This can be calculated for all types of members in Eurocode 3 Part 1-2 [10] from the degree of utilisation μ_o of the member in the fire design situation. Equation (3.34) is plotted in Fig. 3.14 and defines the critical temperature:

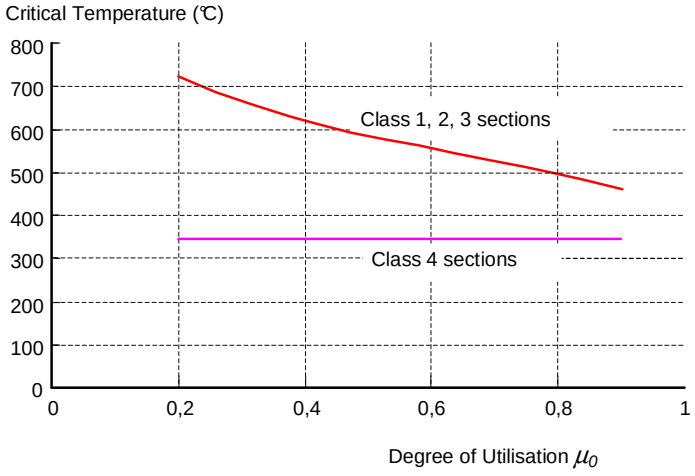

Figure 3.14 Critical temperature, related to degree of utilisation [10].

$$\theta_{cr} = 39.191n\left[\frac{1}{0.9674\mu_0^{3.833}} - 1\right] + 482 \qquad (3.34)$$

This equation applies to all classes of members except the very slender class 4 sections, for which a single conservative value of 350 ^{0} C is specified.

The degree of utilisation μ_o is basically the design loading in a fire situation as a proportion of the design resistance at ambient-temperature (or at time t = 0), but using the material partial safety factors which apply in fire design.

$$\mu_0 = \frac{E_{fi.d}}{R_{fi.d.0}} \tag{3.35}$$

A simple conservative version can be used for tension members and restrained beams, where lateral-torsional buckling is not possible, as follows:

$$\mu_0 = \eta_{fi}\left[\frac{\gamma_{M.fi}}{\gamma_{M1}}\right] \tag{3.36}$$

3.4.9 Resistance of tension members

For a tension member under uniform cross-sectional temperature θ the design resistance in fire is determined by using the reduction factor $k_{y.\theta}$ on yield strength at elevated temperature and an adjustment for the relative material safety factors in normal design and fire design:

$$N_{fi.\theta.Rd} = k_{y.\theta}.N_{Rd}.\left[\frac{\gamma_{M1}}{\gamma_{M.f_i}}\right] \tag{3.37}$$

so that the degree of utilisation is

$$\mu_0 = \frac{N_{fi.d}}{N_{fi.20.RD}} = \frac{N_{fi.d}}{N_{RD}}\left[\frac{\gamma_{M.fi}}{\gamma_{M1}}\right] \tag{3.38}$$

3.4.10 Resistance of restrained beams

For the moment of resistance in fire for class 1 and 2 sections with uniform cross-sectional temperature θ is calculated from the normal plastic resistance moment for strength design by using the reduction factor $k_{y.\theta}$ on yield strength at elevated temperature. An adjustment for the relative material safety factors in normal design and fire design is applied as follows:

$$M_{fi.\theta.RD} = k_{y.\theta}.M_{RD}.\left[\frac{\gamma_{M1}}{\gamma_{M.fi}}\right] \tag{3.39}$$

For a class 3 section the same expression applies but with the elastic moment of resistance used for M_{Rd}. In the case of beams supporting concrete slabs, the design moment of resistance is calculated by dividing the cross-section into uniform strips and reducing the strength of each strip according to its temperature. The moment of resistance is then obtained by summation

across the section. Alternatively it may be determined by the use of empirical adaptation factors κ_1 and κ_2 to obtain the moment of resistance at time t as:

$$M_{fi.t.RD} = \frac{M_{fi.\theta.RD}}{k_1.k_2} \tag{3.40}$$

where κ_1 is the factor non-uniform cross-sectional temperature and κ_2 is the factor for temperature reduction towards the supports of a statically indeterminate beam. The values of these two factors are specified in Eurocode 3 Part 1-2 [10]; κ_1 is specified as 0.7 for slabs supported on the top flange and κ_2 is 0.85 for indeterminate beams (specified in Eurocode 3 [9] the UK), while the default values is 1.0.

Shear resistance follows the same concept for tension and bending and the expression is as follows:

$$V_{fi.t.RD} = k_{y.\theta.\max} V_{RD} \left[\frac{\gamma_{M1}}{\gamma_{M.fi}} \right] \frac{1}{k_1.k_2} \tag{3.41}$$

3.4.11 Lateral-torsional buckling

If the compression flange of a member is not continuously restrained, the lateral-torsional buckling moment is determined for class 1 and 2 sections using the formula from Eurocode 3 Part 1-1 [39], with minor amendment for the fire situation:

$$M_{b.fi.t.RD} = W_{p1.y}.k_{y.\theta.com}.f_y \left[\frac{\chi_{LT.fi}}{1.2} \right] \frac{1}{\gamma_{M.fi}} \tag{3.42}$$

where

$\chi_{LT.fi}$ = lateral-torsional buckling reduction factor in fire design situation

$k_{y.\theta.com}$ = yield strength reduction factor at the maximum compression flange temperature at time t

The factor 1.2 is an empirical correction factor for a number of effects. The lateral-torsional buckling reduction factor $\chi_{LT.fi}$ is determined as in ambient-temperature design, except that the normalized slenderness used is adapted to the elevated temperature steel properties:

$$\chi_{Lt.\theta.com} = \overline{\chi}_{LT}\sqrt{\frac{k_{y.\theta.com}}{k_{E.\theta.com}}} \quad (3.43)$$

Where

$K_{E.\theta.com}$ = elastic modulus reduction factor at the maximum compression flange temperature at time t

It must be noted that lateral-torsional buckling only needs to be considered if $\overline{\chi}_{LT.\theta.com}$ exceeds 0.4 for lower slenderness only the bending resistance is necessary.

3.4.12 Resistance of compression members

The design buckling resistance of columns of class 1, 2 and 3 is determined by allowing for a reduction in strength and an increase in normalized slenderness at elevated temperatures. The design buckling resistance $N_{b.fi.t.Rd}$ at time t for a compression member is given by:

$$N_{b.fi.t.Rd} = \chi_{fi} A k_{y.\theta} / \gamma_{M.fi} \quad (3.44)$$

where χ_{fi} is the reduction factor for flexural buckling in the fire design situation and $k_{y.\theta}$ is the reduction factor for the yield strength of steel at the steel temperature θ_a reached at time t.

3.5 Theory of structural steel behaviour under fire conditions

3.5.1 Introduction

A significant amount of research has been conducted in order to understand the complex interactions of the different structural mechanisms that take place when structures are subjected to fire conditions. One result of this was the paper produced by A.S. Usmani et al. [40] on which most of the discussion in this section is based.

3.5.2 Thermal Expansion

The following relationship governs structures subjected to fire conditions:

$$\varepsilon_{total} = \varepsilon_{thermal} + \varepsilon_{mechanical} \quad (3.45)$$

where $\varepsilon_{thermal}$ equal to the thermal strain and $\varepsilon_{mechanical}$ equal to the mechanical strain and with

$$\varepsilon_{mechanical} \rightarrow \sigma \text{ and } \varepsilon_{total} \rightarrow \delta \tag{3.46}$$

which implies that total strains govern the deformed shape of a structure δ and that the stress in the structure σ depends only on the mechanical strains. An increase in temperature results in thermal strains in most structural materials and is given by

$$\varepsilon_T = \alpha \Delta T \tag{3.47}$$

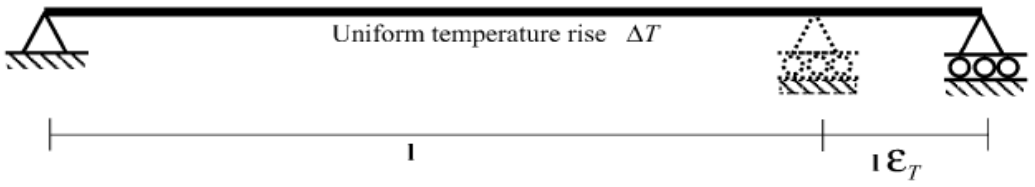

Fig. 3.15. Uniform heating of a simply supported beam [40]

Figure 3.15 shows a simply supported beam with no axial restraint and subjected to a uniform temperature, ΔT. This beam will simply experience an increase in length of $\ell \propto \Delta T$. The beam will not develop any mechanical strain and therefore the total strain (ε_t) will be equal to thermal strain (ε_T). Therefore no stresses will be generated in this beam.

3.5.3 Rigid lateral restraints to thermal expansion

The total strain (ε_t) in an axially restraint beam is equal to zero because the thermal expansion is balanced out by the equal and opposite contraction caused by the restraining force P as shown in figure 3.16. The above scenario applies to a beam subjected to a uniform temperature increase, ΔT.

$$P = EA\varepsilon_m = -EA\varepsilon_T = -EA\alpha\Delta T$$

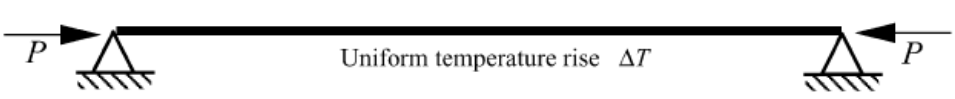

Fig. 3.16. Axially restrained beam subjected to uniform temperature [40]

The beam will respond in the following two ways, if the temperature is increased indefinitely and will be dependent on the slenderness of the beam:

- In a stocky beam the yield stress (σ_y) will be attained and will continue to yield without an increase in the stress if the beam material has an elastic-plastic stress-strain relationship. The yield temperature increment is given by

$$\Delta T_y = \frac{\Delta_y}{E\alpha} \tag{3.48}$$

- A slender beam will exceed the Euler buckling load before the material reaches its yield stress. The critical buckling temperature in equation 3.49 can be obtained by equating the Euler buckling load to the restraining force P.
-

$$\Delta T_{cr} = \frac{\Pi^2}{\alpha}\left(\frac{r}{l}\right)^2 = \frac{\Pi^2}{\alpha\lambda^2} \tag{3.49}$$

Where r is the radius of gyration, λ is the slenderness ratio l/r and l is the effective length.

If the temperature of the beam is increased further, then the following will happen to a beam that consists of an elastic material which has no thermal degradation of it's properties: the increase in thermal expansion strains will be absorbed in the outward deflection (δ) of the beam as the restraining force P remains constant (Fig 3.17).

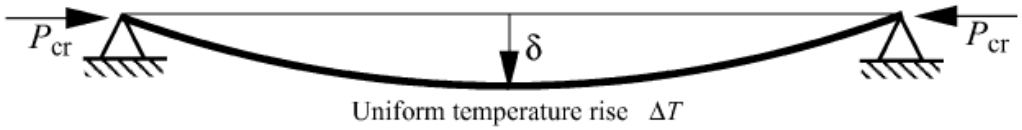

Fig. 3.17. Buckling of an axially restrained beam subjected to uniform heating [40]

3.5.4 Finite lateral restraints to thermal expansion

Figure 3.18 shows a beam that is axially restrained by a translational spring of stiffness K_t. In this case, the compressive axial stress is given by

$$\sigma = \frac{E \propto \Delta T}{\left(1 + EA/k_t L\right.} \tag{3.50}$$

And the critical buckling temperature is given by:

$$\Delta T_{cr} = \frac{\Pi^2}{\alpha \lambda^2}\left(1 + \frac{EA}{k_t L}\right) \tag{3.51}$$

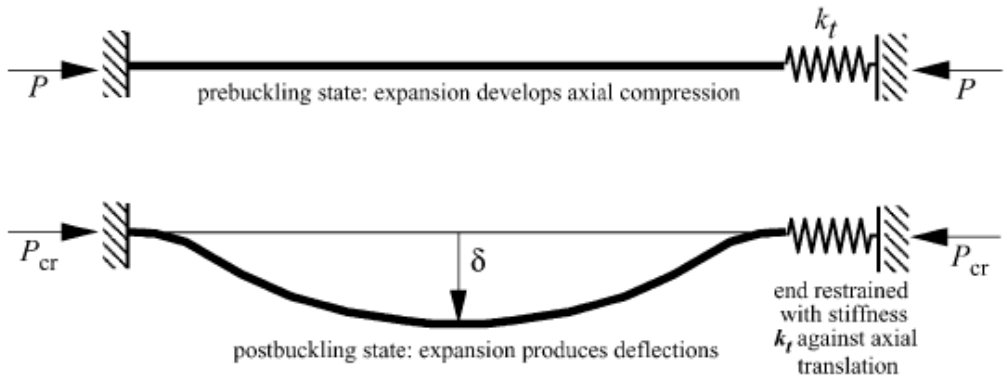

Fig. 3.18. Heating of beam with finite axial restraint [40]

3.5.5 Thermal Bowing

Concrete slabs that are supported by steel beams on the ceiling of a compartment, have a significant effect on the behaviour of the steel beams. The steel beams and concrete slabs are subjected to very high temperature gradients due to the slow rate of heat transfer to concrete. The surfaces of the members on the outside of the compartment will be much cooler than the surfaces of the members on the inside of the compartment as these surfaces are directly exposed to the fire. Therefore, the inner surfaces will expand more than the outer surfaces. This will cause bending in these members and is referred to as thermal bowing. The thermal gradient $T_{,y}$ over the depth is

$$T_{,y} = \frac{T_2 - T_1}{d} \tag{3.52}$$

A uniform curvature ϕ is caused along the length as a result of the thermal gradient,

$$\phi = \alpha T_{,y} \tag{3.53}$$

The curvature induces a contraction strain, and can be computed from Fig 3.19 as:

$$\varepsilon\phi = 1 - \frac{\sin\left(\ell \phi / 2\right)}{\ell \phi / 2} \tag{3.54}$$

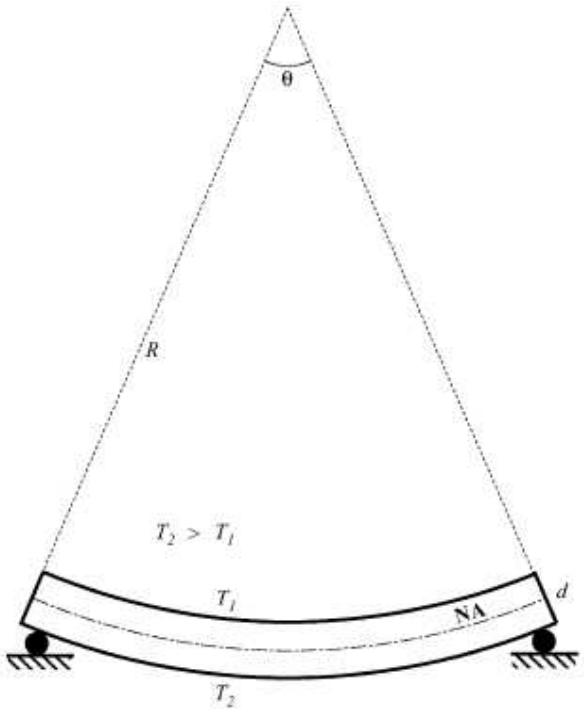

Fig. 3.19. Simply supported beam subjected to uniform thermal gradient [40]

If a uniform thermal gradient $T,_y$ is applied to an axially restraint beam as shown in figure 3.20, then tension will be induced in the beam. If a uniform temperature gradient is applied to a fix ended beam, an equal and opposite curvature is induced by the support moments which cancel out the thermal curvature at midspan. The beam remains straight with a constant moment $M = EI\phi$ along its length as can be seen in figure 3.21.

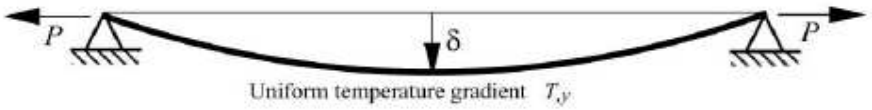

Fig. 3.20. Laterally restrained beam subjected to a uniform thermal gradient [40]

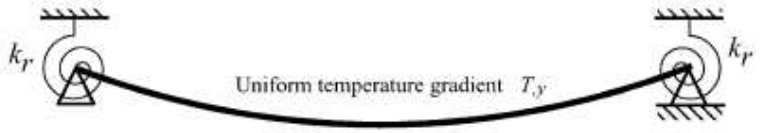

Fig. 3.21. Beam with finite rotational restraint with a uniform thermal gradient [40]

A beam that is restrained rotationally at the supports by rotational springs of stiffness is shown in figure 3.22. Perfect internal and rotational restraints are not easily achieved in real structures and therefore have finite capacities only. Therefore, the restraining moment in the springs due to a uniform thermal gradient $T,_y$ can be expressed as

$$M_k = \frac{E\alpha T,_y}{(1+2EI/k_t l)} \tag{3.55}$$

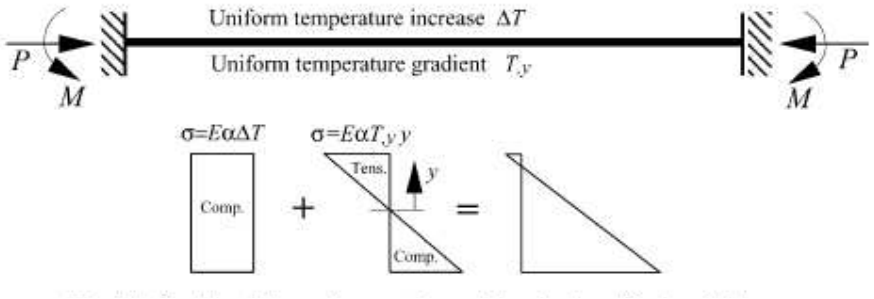

Fig. 3.22. Combined thermal expansion and bowing in a fix ended beam [40]

3.5.6 Deflections

A slender beam that is axially restrained and is subjected to uniform heating will buckle at low elastic strains. The beam will deflect outwards if there is any further expansion and the midspan deflections can be estimated by

$$\delta = \frac{2\ell}{\Pi}\sqrt{\varepsilon_r + \varepsilon_T^2/2} \tag{3.56}$$

This is an approximation of a sine curve length $l(1+\varepsilon_T)$ where ε_T is the thermal expansion strain $(\propto \Delta T)$.

If this beam is subjected to a uniform thermal gradient, only bowing will result and is governed by the flexure-tension interaction. The deflections are limited by the $P-\delta$ moments which restrain the curvature caused by the thermal gradients. The deflections can be determined from

$$\delta = \frac{2\ell}{\Pi}\sqrt{\varepsilon_t + \varepsilon_t^2/2} \tag{3.57}$$

Where ε_t is the tensile strains produced in the beam and is given by

$$\varepsilon_t = \frac{P}{EA} \tag{3.58}$$

The tensile force P_t can be calculated from the following equation:

$$P_t = \left(\sqrt{\frac{1}{2}\left(\frac{\prod \delta}{l}\right)^2 + 1} - 1 \right) EA \tag{3.59}$$

The equation for the tensile force is obtained by substituting Eq (3.58) into Eq (3.57).

The uniform curvature ϕ for a simply supported beam is

$$\frac{d^2 y}{dx^2} = \phi \tag{3.60}$$

A tensile force P will be generated in a laterally restrained beam and will cause a movement P_y over the beam length. Therefore

$$\frac{d^2 y}{dx^2} = \phi + \frac{P_y}{EI} \tag{3.61}$$

Or

$$\frac{d^2 y}{dx^2} - k^2 y = \phi \tag{3.62}$$

where

$$k = \sqrt{\frac{P}{EI}} \tag{3.63}$$

Therefore, the deflection of the beam in figure 3.20 can be expressed as follows:

$$y(x) = \frac{\phi}{k^2}\left(\frac{\cosh k\ell - 1}{\sinh k\ell} \sinh k\alpha - \cosh kn + 1 \right) \tag{3.64}$$

3.5.7 Thermal expansion and thermal bowing combined

The beam in figure 3.22 is restrained rotationally and laterally at both ends and is subjected to both a mean temperature rise and a thermal gradient through its depth. This beam will experience a uniform compressive stress due to the restraint to expansion and will experience a uniform moment due to the thermal gradient.

The top of the beam will experience either significant compression or tension while the bottom of the beam will experience very high compressive stresses. These compressive stresses cause local buckling in the lower flanges. Local buckling causes a hinge at interior support which is considered as fixed and thus relieves the hopping moment. This support now only provides lateral restraint.

In the previous section restrained expansion caused compression and bowing caused tension. These two effects are dependent on an average equivalent temperature rise ΔT and an average

equivalent thermal gradient $T_{,y}$. The effective strain E_{eff} for combinations of thermal expansion and bowing can be defined as follows:

$$\varepsilon_{eff} = \varepsilon_T - \varepsilon_\phi \tag{3.65}$$

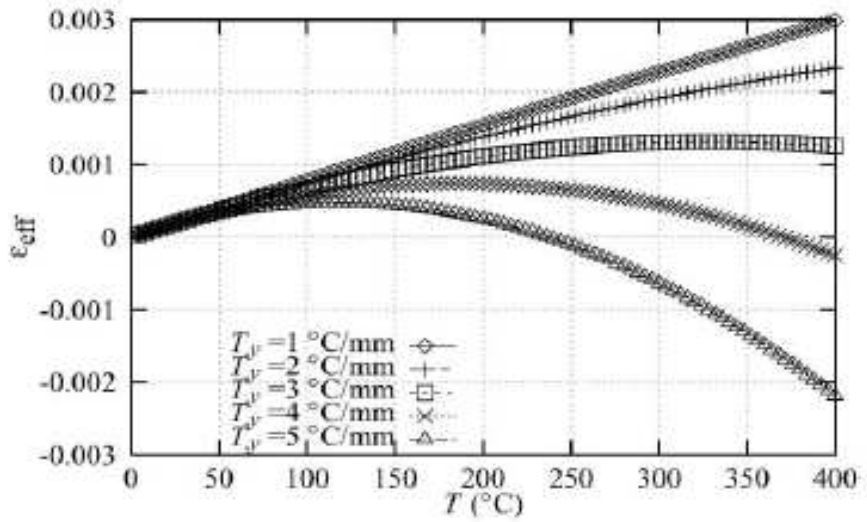

Fig. 3.23. Effective expansion strains [40]

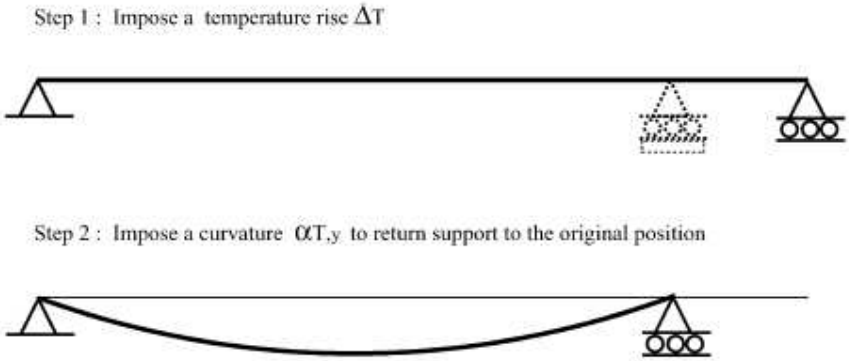

Fig. 3.24. Case 1: Zero stress [40]

Positive values of E_{eff} mean that compression is dominant while negative values imply that tension is dominant. Figure 3.23 shows a plot of effective strain E_{eff} against various thermal gradients $T_{,y}$. While the temperature is increased from zero to 400 three cases of stress in a beam will be discussed as follows:

i) Case 1: Zero stress in the beam $(\varepsilon_{eff} = 0)$

- All the thermal strains are converted in displacements as shown in figure 3.24.

- Deflections are caused by thermal bowing in order to absorb the excessive length generated by thermal expansion.

The deflection can be defined as:

$$Y_m = \frac{2\ell}{\prod}\sqrt{\varepsilon_T + \frac{\varepsilon_T^2}{2}} \tag{3.66}$$

ii) Case 2: Thermal expansion dominant $(\varepsilon_{eff} \rangle 0)$

Pre-and post-buckling phases are produced when $\varepsilon_T >> \varepsilon_\phi$. A small part of pre-bucking deflections ($\overline{Y}_m$) generated by elastic bending while a larger part are generate from the deflections imposed by curvature ($Y_m(\phi)$).

$$Y_m = \frac{Y_0}{1 - \left(\Delta T \big/ \Delta T_{cr}\right)} + Y_m(\phi) \tag{3.67}$$

Y_0 is the initial elastic deflection before heating due to the imposed loads on the beam and ($Y_m(\phi)$) is the additional deflection due to thermal bowing given by

$$Y_m(\phi) = \frac{2\ell}{\prod}\sqrt{\varepsilon_\phi + \frac{\varepsilon_\phi^2}{2}} \tag{3.68}$$

The critical buckling temperature (ΔT_{cr}) is increased because the thermal gradient delays the buckling event. The critical buckling temperature is now given by

$$\Delta T_{cr} = \frac{1}{\propto}\left(\frac{\prod^2}{\lambda^2} + \varepsilon_\phi\right) \tag{3.69}$$

Typical variation in buckling temperature with a change in gradient for a beam of slenderness ratio l/r equal to 70 is given in figure 3.25.

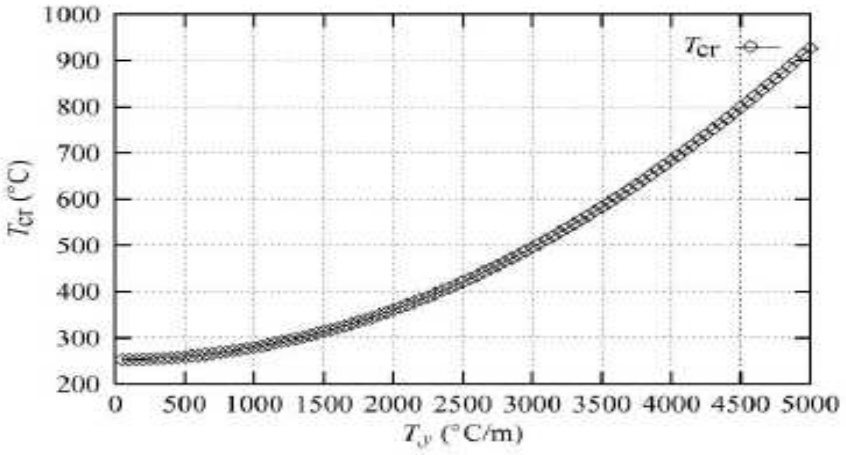

Fig. 3.25. Critical buckling temperatures vs. thermal gradient [40]

The post-buckling deflections will continue to increase due to the additional expansion strains ε_T^+ and is given by

$$Y_m^+ = \frac{2\ell}{\prod}\sqrt{\varepsilon_T^+ + \frac{\varepsilon_T^{+2}}{2}} \tag{3.70}$$

iii) Case 3: Thermal bowing dominant $(\varepsilon_{eff} \langle 0)$

Deflection resulting from the bowing of the excess length generated through expansion can be defined as follows:

$$(Y_m)_1 = \frac{2\ell}{\prod}\sqrt{\varepsilon_T + \frac{\varepsilon_T^2}{2}} \tag{3.71}$$

The tension force (P_{eff}) resulting from the excess contraction strain (E_{eff}) produces a tensile strain given by

$$\varepsilon_t = \frac{P_{eff}}{EA} \tag{3.72}$$

This will produce further deflections which can be defined as

$$(Y_m)_2 = \frac{2\ell}{\prod}\sqrt{\varepsilon_t + \frac{\varepsilon_t^2}{2}} \qquad (3.73)$$

3.6 Conclusions

The standard fire resistance test focuses mainly on the fire resistance time of isolated members forming part of complete steel framed buildings. This focus should rather be shifted to the design of these buildings to withstand these fire temperatures, thus minimizing loss of life and damage to property. Current analytical techniques for estimating the heating rates of isolated members are purely empirical and predictive. Individual members of steel framed buildings subjected to fire conditions experience a slower heating rate than predicted by the standard fire resistance test.

Members that are exposed to fire conditions and forming part of complete frames experience axial and rotational restraint which may increase or decrease their failure strength. Members in a fire compartment experience expansion and induce lateral deflections and moments in columns. Temperature gradients along the length and across the cross section of steel members influence the level and type of stress experienced by these members.

A number of authors have developed numerous analytical and design techniques over the past two decades. The computational results obtained from these techniques were in most cases compared to the results obtained from experiments conducted. These experiments yielded conclusions as follows:

i) The effective length of columns varied from values below unity to unity representing fixed ended and pin ended boundary conditions.
ii) The failure of columns at elevated temperature is only dependent on the axial load applied and not on the connection stiffness and the applied moment.
iii) The restraining effect of frame continuity reduces the limiting temperature of frames.
iv) Frames subjected to fire conditions experience a loss of strength and is reflected in an elastic buckling analysis.

Classical formulae from the Eurocode standards are presented for the estimation the steel heating rates, the analysis and the design of steel members. From the literature review and the above summary, it is clear that these formulae are rather conservative. The fundamental theory behind structural steel behaviour under fire conditions is presented in this chapter.

3.7 Problem definition

Although a lot of research has been conducted, over the past two decades, about the effects of heat on steel structures, it is evident that there are matters that still require further investigation. The following are of concern:

i) The effects of heat on the behaviour of structural steel members

The behaviour of structural steel members subjected to heat need to be assessed in terms of their deformations, stress developments and overall strength.

ii) The effect of boundary conditions on isolated steel members

The behaviour of isolated steel members with different support conditions i.e. pinned or fixed, must be studied in terms of deformations, stress developments and overall strength for different heating regimes.

iii) The effect of different heating regimes on complete frames

The behaviour of members of complete frames that are subjected to heat must be studied in terms of deformations, stress developments and overall strength. Initially, all members of a frame will be subjected to a uniform temperature increase and then individual members forming part of a frame will be subjected to either a uniform or gradient temperature increase.

4. Investigation of fire behaviour of structural steel members and frames

4.1 Introduction

A finite element analysis software package, namely ADINA [7] was employed to investigate the effects of temperature on structural steel elements and one-dimensional frames. This software was developed by Bathe [7] Professor of Mechanical Engineering, Massachusetts Institute of Technology.

The objectives of this chapter are to demonstrate the effects of temperature on some or all of the members in terms of the stress and deformations developments, and the reduction of strength in simple structural steel members to complex one-dimensional structural steel frames. The models vary from simple members, for example, individual beams and columns to more complex frames, for example, portal frames and multi storey frames.

In order to achieve the above mentioned objectives, this chapter will discuss the following issues:

- FE background
- FE models investigated under which the support conditions, the global degrees of freedom and the applied temperature loadings are discussed.
- Element groups
- Material models under which the application of the gradient temperature on members is explained.
- Model verification
- Discussion of results

4.2 FE Background

The development of finite element method began in the 1940's with the structural engineering work of Hrennikof [41] in 1941. Tremendous advancements occurred in its application to solve complicated engineering problems since the early 1950's. In short the general steps of the finite element method are as follows;

- Discretization and selection of element types
- Selection of a displacement function
- Defining the strain/displacement and stress/strain relationship

- Deriving the element stiffness matrices and equations
- Assemblage of the element equations to obtain the global equations and the introduction of boundary conditions
- Solving the unknown degrees of freedom
- Solving for the element strains and stresses
- Interpreting the results.

4.3 Modelling using ADINA

4.3.1 FE Models Investigation

The models that were set up in the finite element program are listed below and in table 4.1.

1. Pinned support Beam at varying uniform temperatures, refer to figure 4.7.
2. Pinned support Beam with a varying gradient temperature along its length, refer to figure 4.8
3. Fixed support beam at varying uniform temperature, refer to figure 4.9.
4. Fixed support beam at varying gradient temperature along its length, refer to figure 4.10.
5. Column: one end fixed the other end free to move in y-direction only at varying uniform temperature, refer to figure 4.11.
6. Column: same support conditions at varying gradient temperature along its length refer to figure 4.12.
7. Portal Frame at varying uniform beam and column temperatures, refer to figure 4.13.
8. Portal Frame at varying uniform beam temperatures, refer to figure 4.14.
9. Portal Frame at varying uniform column temperatures, refer to figure 4.15.
10. Portal Frame at varying gradient beam temperatures, refer to figure 4.16.
11. Portal Frame at varying gradient column temperatures along its length, refer to figure 4.17.
12. Multi-storey Frame at varying uniform beam and column temperature in fire compartment, refer to figure 4.18.
13. Multi-storey Frame at varying uniform beam temperatures, refer to figure 4.19.

Table 4.1: Summary details of models investigated

No.	Model	Section sizes (kg/m)	Support conditions	Loading			Length (m)	
				UDL (kN/m)	Point load (kN)	Temperature load (°C)	Beam	Column
1	Simply Support Beam	356x171x51:I-Beam	Simple	15	N/A	Various uniform temperatures 20 ° C - 1000 ° C	6m	N/A
2	Simply Support Beam	356x171x51:I-Beam	Simple	15	N/A	Gradient temperature along the beam length 95 ° C - 952 ° C	6m	N/A
3	Fixed Support Beam	356x171x51:I-Beam	Fixed	15	N/A	Various uniform temperatures 20 ° C - 1000 ° C	6m	N/A
4	Fixed Support Beam	356x171x51:I-Beam	Fixed	15	N/A	Gradient temperature along the beam length 95 ° C - 952 ° C	6m	N/A
5	Column	254x254x73:H-Column	Lower end: fixed Upper end: vertically unrestrained	N/A	1079 kN at top of Column 10.79 kN at mid height-horizontal	Various uniform temperatures 20 ° C - 1000 ° C	N/A	4m
6	Column	254x254x73:H-Column	Lower end: fixed Upper end: vertically unrestrained	N/A	1079 kN at top of Column 10.79 kN at mid height-horizontal	Gradient temperature along the column length-as in beam 95 ° C - 952 ° C	N/A	4m
7	Portal Frame	305x165x41: I-Beam 203x203x52:H-Column	Both Supports Fixed	25.4	500 kN on top of each Column	Various uniform temperatures apllied to all members in the compartment (20 ºC - 1000 ºC)	5.7m	3.5m
8	Portal Frame	305x165x41: I-Beam 203x203x52:H-Column	Both Supports Fixed	25.4	500 kN on top of each Column	Various uniform temperatures applied to the beam only 20 ° C - 1000 ° C	5.7m	3.5m
9	Portal Frame	305x165x41: I-Beam 203x203x52:H-Column	Both Supports Fixed	25.4	500 kN on top of each Column	The column at various gradient temperatures along it's length 95 ºC - 952 ºC(see Table 4.4)	5.7m	3.5m
10	Portal Frame	305x165x41: I-Beam 203x203x52:H-Column	Both Supports Fixed	25.4	500 kN on top of each Column	Various gradient temperatures applied to the beam length RHS Col. at ambient temp. LHS Col. -a third of top length at 7% of beam edge temp.	5.7m	3.5m
11	Portal Frame	305x165x41: I-Beam 203x203x52:H-Column	Both Supports Fixed	25.4	500 kN on top of each Column	Various uniform temperatures applied to the LHS column only 20 ° C - 1000 ° C	5.7m	3.5m
12	Multi Storey Frame	305x165x41: I-Beam 203x203x52:H-Column	All Supports Fixed	25.4	75.5 kN on top of external columns 151 kN on top of internal columns	Various uniform temperatures applied to the beam and the columns of the lower LHS compartment (20 ºC - 1000 ºC)	3 bays at 5.5m each	3 floors at 3.5m high
13	Multi Storey Frame	305x165x41: I-Beam 203x203x52:H-Column	All Supports Fixed	25.4	75.5 kN on top of external columns 151 kN on top of internal columns	Various uniform temperatures applied to the beam only of the lower LHS compartment (20 ºC - 1000 ºC)	3 bays at 5.5m each	3 floors at 3.5m high

The load ratio R for beams is given by

$$R = \frac{M_f}{M_c} \tag{4.1}$$

where M_f is the applied moment and M_c is the moment capacity. The load ratio R for columns is given by

$$R = \frac{F_f}{A_g P_c} + \frac{M_{fx}}{M_b} + \frac{M_{fy}}{P_c Z_y} \tag{4.2}$$

where F_f is the axial load at the fire limit state, A_g is the gross area, P_c is the compressive stress, P_y is the design strength of steel, Z_y is the elastic modulus about the minor axis, M_{fx} and M_{fy} are the maximum moments about the major and minor axes, respectively and M_b is the buckling resistance moment. The load ratio (R) on the isolated beam members were kept low at 0.2 in order to prevent the beam from collapsing at low temperatures. The load ratio for the beams of the portal and multi-storey frames were approximately 0.5 while the load ratio for the columns of these frames were at approximately 0.3 and 0.1, respectively. These values were chosen so that the frames still have sufficient capacity for the additional range of temperature loads.

The master degrees of freedom (MODF) are the global degrees of the complete model and allow the modeller to specify the directions in which the model is allowed to move and rotate. The supports can be fixed for some or all of these movements or rotations. Table 4.2 gives a summary of the master degrees of freedom and the support fixity details for all the models. X, y and z indicates the axes directions as shown in figure 4.1. θ_x, θ_y and θ_z are the x-, y- and z-rotations about the respective axes as shown in figure 4.1.

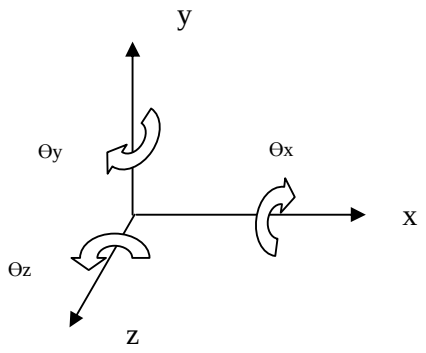

Fig. 4.1: Positive axes used for all models

Table 4.2: Summary of master degrees of freedom (MODF) and support fixity detail for each model

Model		Degrees of freedom					
		X	Y	Z	θ_x	θ_y	θ_z
Pinned Beam	Support A Support B MODF	X X X	X X F	X X X	X X X	X X X	F F F
Fixed Beam	Support A Support B MODF	X X X	X X F	X X X	X X X	X X X	X X F
Beam-column	Support A Support B MODF	X X F	X F F	X X X	X X X	X X X	X F F
Portal Frame	Supports MODF	X F	X F	X X	X X	X X	X F
Multi-storey Frame	Supports MODF	X F	X F	X X	X X	X X	X F
X	fixed for the degree of freedom						
F	free to move for the degree of freedom						

4.3.2 Element Groups

The software ADINA [7] allows the use of various element types viz. truss elements, 2D and 3D elements, shell elements, beam elements with limitation to the type of material models that can be applied with each specific element group.

For the current models, the hermitian beam was utilized which allows the input of the physical dimensions of the I-beam profile. When creating the element group, ADINA [7] prompts for the material properties/model to be associated with this type of section. Basically, all types of sections are available for use with this program for example, U-beams, L-beams.

4.3.3 Material Models

The software offers various material models, for example, bilinear and multi-linear plastic materials, isotropic elastic and orthotropic elastic materials and so on. Since Adina does not allow non-linear material models to be used with hermitian beams; the isotropic elastic material model was used. The only drawback of this was that while it is possible to perform a temperature

analysis, it was not possible to utilize the temperature model effectively in terms of temperature gradients across the cross-sectional profile and along the length of the member. Consequently, values of Young's modulus (E) and the coefficient of thermal expansion (α) had to be entered for each material model used to represent the complete steel members or section length of members at various temperatures. The variance of the modulus of elasticity, taken from the M.B. Wong et al. [26] is given below in equation 4.1:

$$\frac{E(T)}{E(20)} = 1.0 + \frac{T}{2000 \ln\left[\frac{T}{1100}\right]} \quad 0^{o}C < T \le 600^{o}C$$
$$= \frac{690\left(1 - \frac{T}{1100}\right)}{T - 53.5} \quad 600^{o}C < T \le 1000^{o}C \qquad (4.1)$$

where E (20) is the modulus of elasticity of steel at ambient temperature, that is, at 20˚C while E (T) is the modulus of elasticity of steel at a given temperature. The coefficient of thermal expansion, α, of steel increases with temperature and can be defined by the linear functions [25] in equation 4.2.

$$\alpha(T) = (11.4 + 0.01T) * 10^{-6} / {}^{o}C \qquad (4.2)$$

The gradient of temperature along the length of a beam and column were based upon temperature models in ADINA[7]. The beam temperature and the portal temperature distribution are shown in figures 4.2 and 4.3, respectively. These models were based on emissivity values of 0.5 to 0.85 for
0 ˚C to 1000 ˚C and 199.5 to 13.3GPa for values of E in the temperature range of 0˚C to 1000˚C (Table 4.2).

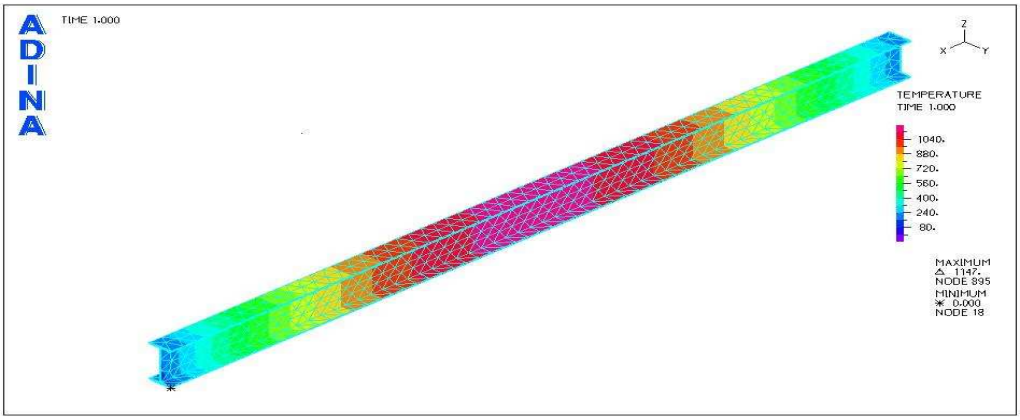

Fig. 4.2 ADINA model of beam temperature distribution

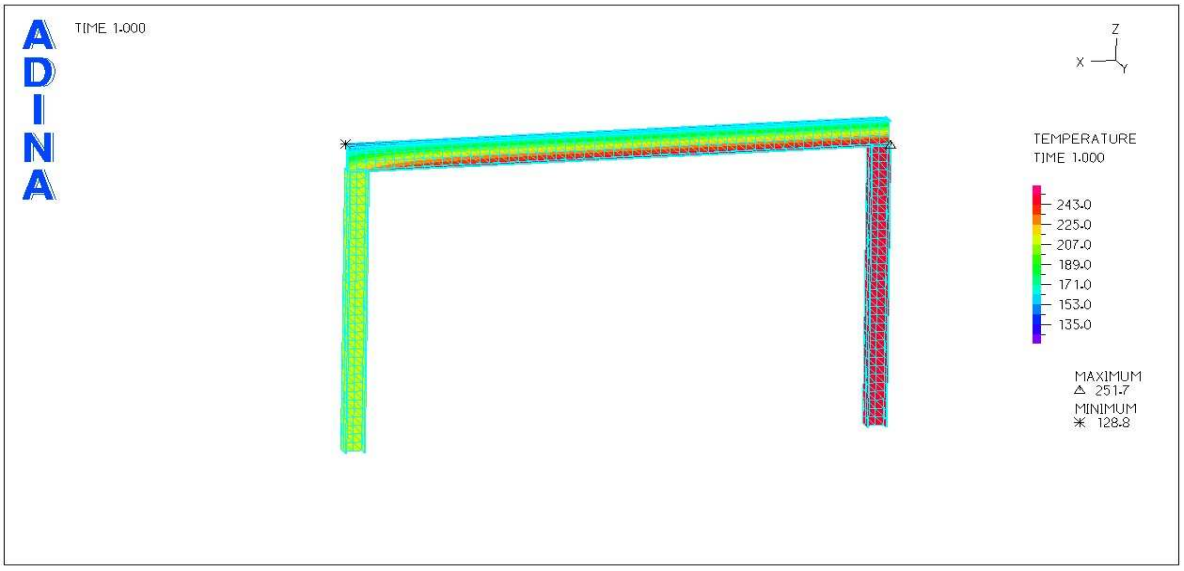

Fig. 4.3 ADINA model of Portal frame temperature distribution

Table 4.3: Relationship between T, E & α (Equations 4.1 and 4.2)

Temperature	E-Values 10^6(kN/m^2)	α-Values 10^{-6}/ ^{0}C
20	199.5	11.6
100	195.8	12.4
200	188.3	13.4
300	176.9	14.4
400	160.5	15.4
500	136.6	16.4
600	101	17.4
700	77.6	18.4
800	50.4	19.4
900	29.6	20.4
1000	13.3	21.4

Figure 4.4 shows the temperature gradient applied along the beam length. A temperature is applied at midspan of the beam, that is, at point 3. The temperature at point two is obtained by reducing the temperature at point 3 by 11% and the temperature at point 1 is obtained by reducing the temperature at point 2 by 38%. The same principle is applied to point 0 which is obtained by reducing the temperature at point 1 by 51%. Therefore the total temperature gradient is equivalent to 87% from the point 3 at midspan to point 0 at the support end of the beam.

The temperature T3, for the length L3, was calculated as the average of the temperatures at points 2 and 3. The applied temperatures and the calculated temperatures (T1 to T3) for the lengths L1 to L3 are listed in Table 4.3. The values for the Young's modulus (E) and the coefficient of thermal expansion (α) were obtained from Table 4.2 and intermediate values were obtained by interpolation.

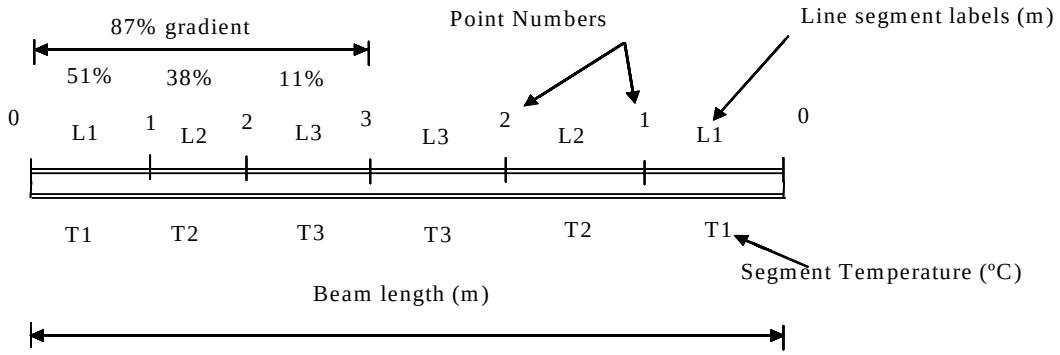

Figure 4.4: Temperature gradient along the beam length

For the column models the actual column length was divided into the same number of segments (6) as for the beams and therefore the same temperature gradient was applied as for the beam models.

Table 4.4: Derivation of applied gradient temperature along the beam length and the temperature at the 1/4 top length of the column. (Read in conjunction with figure 4.4)

Applied temperature at Point 3 (º C)	Variance	Point 2 (º C)	Point 1 (º C)	Point 0 (º C)	T3 (º C) Temp 2-3	T3 (º C) Temp 1-2	T3 (º C) Temp 0-1	Top 1/4 Length of column 7% of temperature of L1
100	87	90	57	13	95	74	35	22.45
200	174	181	115	26	190	148	70	24.9
300	261	271	172	39	286	222	106	27.42
400	348	362	229	52	381	296	141	29.87
500	435	452	287	65	476	370	176	32.32
600	522	543	344	78	571	443	211	34.77
700	609	633	402	91	667	517	246	37.22
800	696	723	459	104	762	591	281	39.67
900	783	814	516	117	857	665	317	42.19
1000	870	904	574	130	952	739	352	44.64

For the portal frame models, the column lengths were divided into 3 segments. The temperature of the top third (1/3) length was modelled at 7% of the beam length L1 plus 20˚C (ambient temperature) and are shown in Table 4.3. This distribution is only applicable for the portal frame beam at various gradient temperatures, that is, model 10.

The portal frame with the column at various gradient temperatures, that is, model 9, the temperature gradients applied to the column are shown in Table 4.4 and in Figure 4.3.

A static and linearized buckling analysis was performed for every temperature step for each of the models investigated.

4.3.4 Model verification

The verification model was taken from M.B. Wong et al. [26] and can be seen in fig. 4.5. A linearized buckling analysis was performed and the marginal difference (2 to 3 %) was rather a constant value lower than predicted by the unit load factor method (Figure 4.6). This difference can be ascribed to differences in the models e.g. the stiffness of the joints, grade of steel etc.

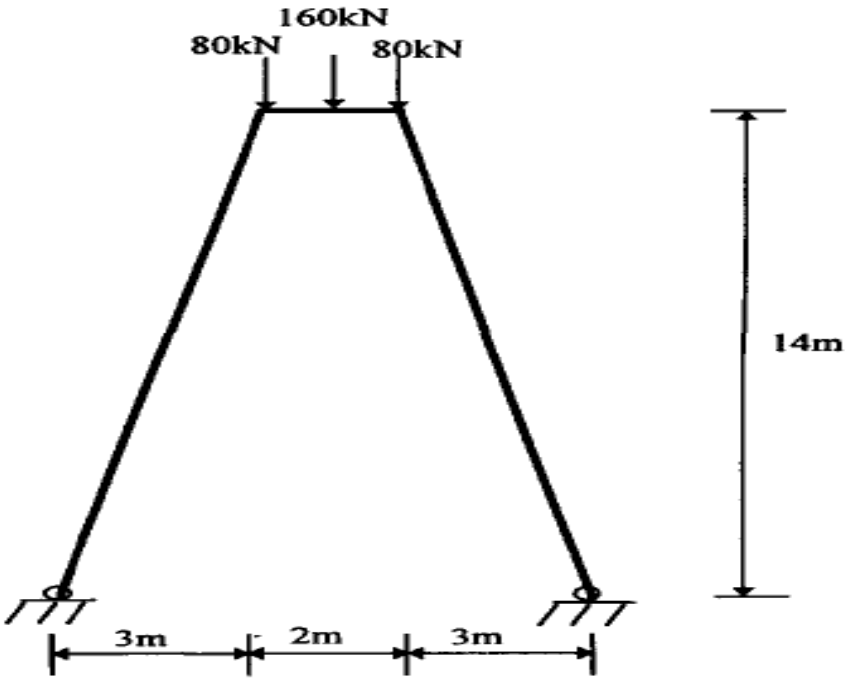

Fig. 4.5 Frame model used as verification model taken M.B.Wong et al. [26]

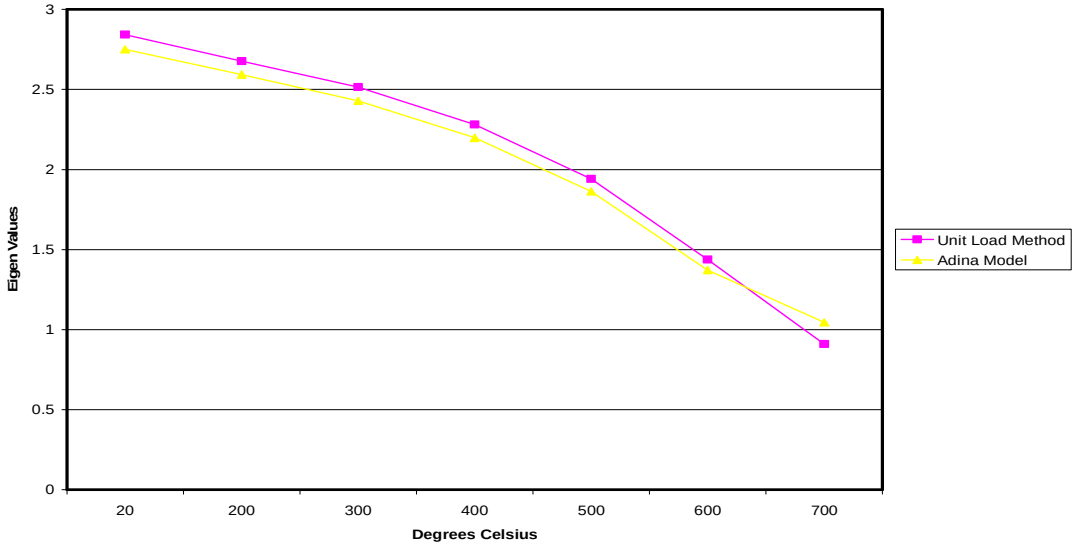

Fig. 4.6: Buckling values for the frame from the unit load method versus the ADINA model.

The results obtained for the bending moments of model 5, a beam-column subjected to uniform temperatures, an axial load of 1079 kN and a horizontal load of 10.79 kN at mid height, compared identical to the results obtained for a similar model by J.Y. Richard Liew et al. [42]. The bending moment of the beam-column (5.4 kNm) remained constant throughout the uniform temperature increases. The x-deflection of model 5 in this current research is 0.32 mm at 600 ˚C. The x-deflections predicted by the model of J.Y. Richard Liew et al. [42] is well below 0.5 mm up to approximately 550 ˚C and then rapidly increases to 7.87 mm at 603 ˚C. The current research model therefore compares well to the model of J.Y. Richard Liew et al. [42] in terms of x-deflections up to 550 ˚C but at higher temperatures (for example at 600 ˚C) predicts approximately 96 % lower x-deflections. This can be ascribed to factors such as the actual degree of stiffness applied to fixed supports, the type of elements used, the actual material model used and also the actual fineness of the mesh employed.

4.4 Discussion of results

4.4.1 Simply Supported Beam Model

4.4.1.1 Model 1: Uniform heats applied to the beam

It was considered necessary to model a simply supported beam as this type of member is one of the fundamental members of larger structures. The beam is a 356 x171 x 51 kg/m section subjected to a 15 kN/m uniformly distributed load (Figure 4.7).

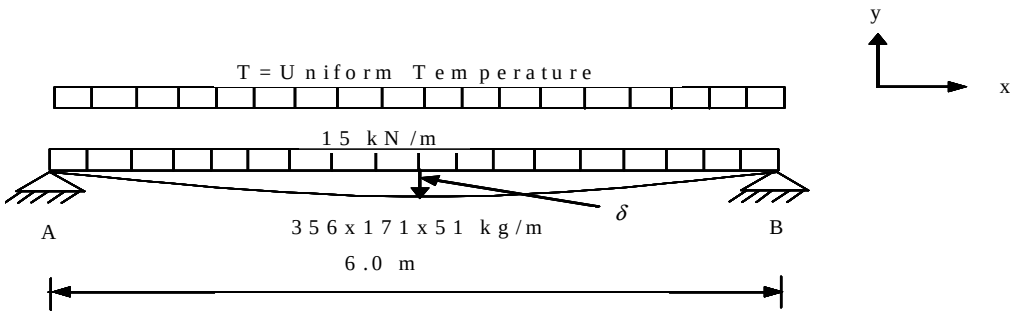

Figure 4.7: Model 1: Simply supported beam with various uniform temperature along the beam length

The beam was modelled as line segments and the elastic hermitian beam properties were assigned to this line. The elastic hermitian beam cross sections available in the program are I-, L-, and U-sections. The actual cross section dimensional properties were entered for the beam section modelled. The material model used was an isotropic linear elastic material with values of

Young's modulus and the coefficient of thermal expansion entered which corresponded to the appropriate temperatures applied to the various segments. The supports were allowed to rotate about the z-axis only. A uniformly distributed load was applied along the beam length and a uniform temperature was applied to the beam cross section. The bending moment distribution remained unchanged throughout all the temperature ranges at a value of 67.5 kNm (Figure 4.9).

In figure 4.8, it can be seen that the deflection gradually increases as the temperature increases uniformly to reach a peak value of approximately 140 mm at a temperature of 1000 ˚C. The limit deflection (L/300 = 6000/300 = 20 mm) as given SANS 0100-1[43] is clearly exceeded at about 650 ˚C. However, when studying the buckling strength of the beam, it can be observed that the beam collapses at 450 ˚C with a residual strength of 6.25% of its strength at ambient temperature (Figure 4.10). The results for the beam moments and the y-deflections for this model are shown in table 4.5, respectively.

Table 4.5: Summary of the results for model 1 (simply supported beam)

		Values at 20 ºC and percentage increase of values from ambient		Values at 200 ºC and percentage increase of values from ambient		Values at 400 ºC and percentage increase of values from ambient		Values at 600 ºC and percentage increase of values from ambient		Values at 800 ºC and percentage increase of values from ambient		Values at 1000 ºC and percentage increase of values from ambient	
		Value at Ambient(20 ºC)	% Increase of value from ambient	Value at 200 ºC	% Increase of value from ambient	Value at 400 ºC	% Increase of value from ambient	Value at 600 ºC	% Increase of value from ambient	Value at 800 ºC	% Increase of value from ambient	Value at 1000 ºC	% Increase of value from ambient
Moments (kNm)	Support A	0.00	0.00	0.00	0.00	0.00	0.00	0.00	0.00	0.00	0.00	0.00	0.00
	Mid span	67.50	0.00	67.50	0.00	67.50	0.00	67.50	0.00	67.50	0.00	67.50	0.00
	Support B	0.00	0.00	0.00	0.00	0.00	0.00	0.00	0.00	0.00	0.00	0.00	0.00
Y-Deflections (mm)	Support A	0.00	0.00	0.00	0.00	0.00	0.00	0.00	0.00	0.00	0.00	0.00	0.00
	Mid span	-1.80	0.00	-9.70	538.89	-11.30	627.78	-18.00	1000.00	-36.08	2004.44	-136.43	7579.44
	Support B	0.00	0.00	0.00	0.00	0.00	0.00	0.00	0.00	0.00	0.00	0.00	0.00

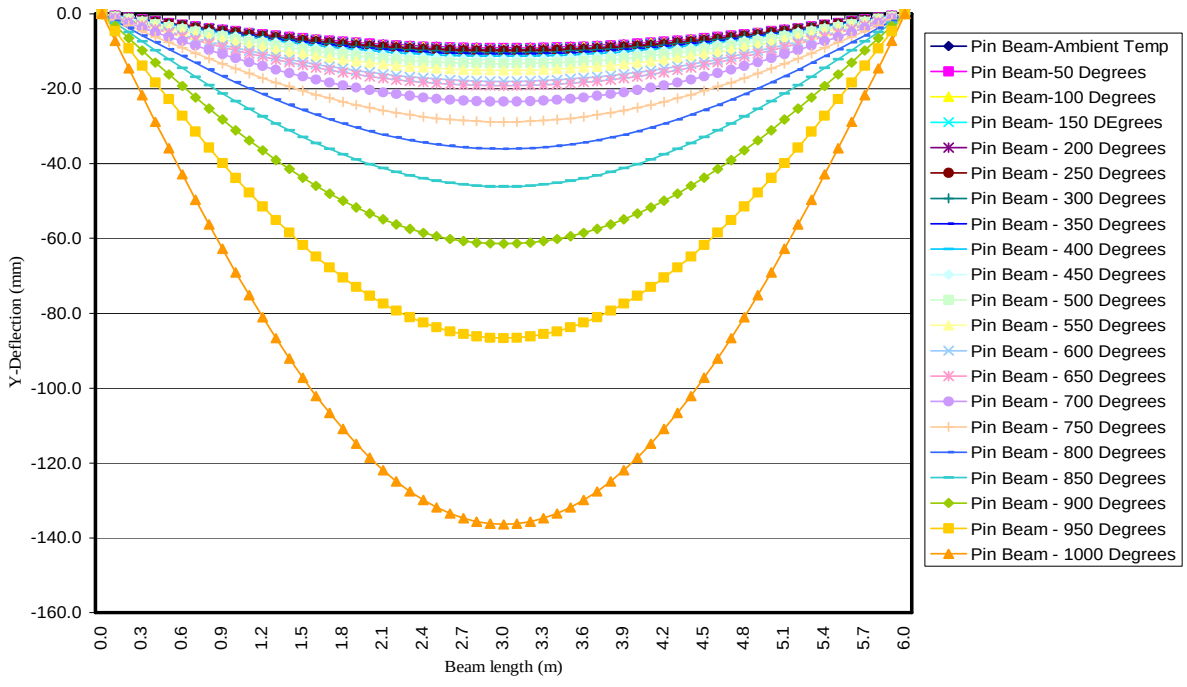

Figure 4.8: Pinned beam Y-deflections at uniform temperatures

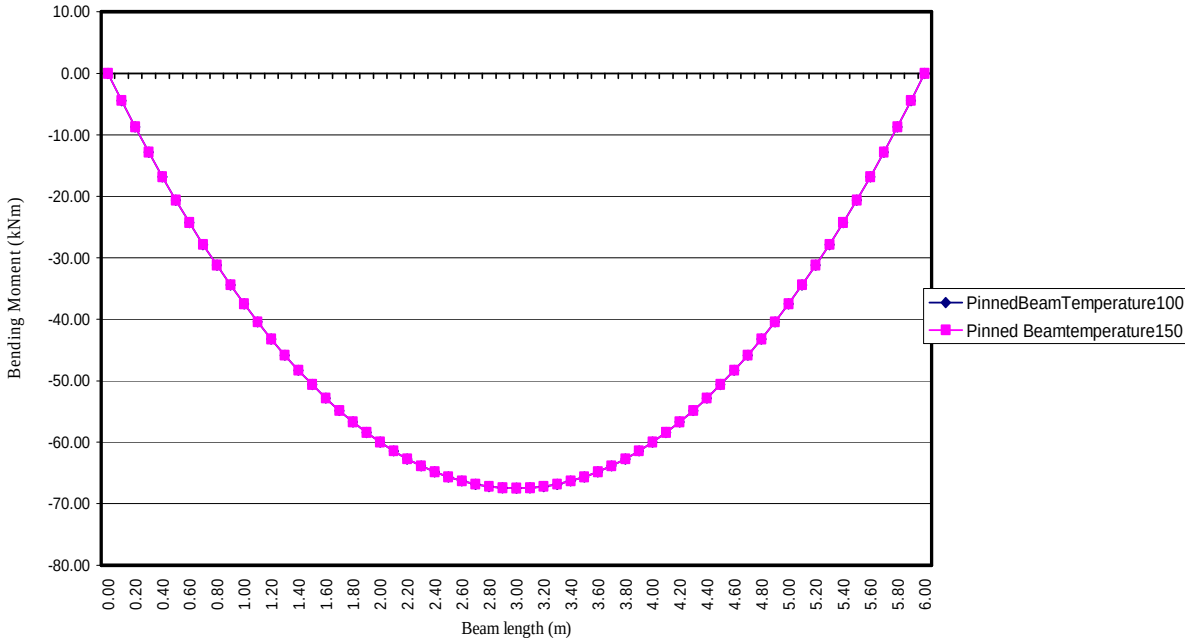

Figure 4.9: Pinned beam moments at uniform temperatures

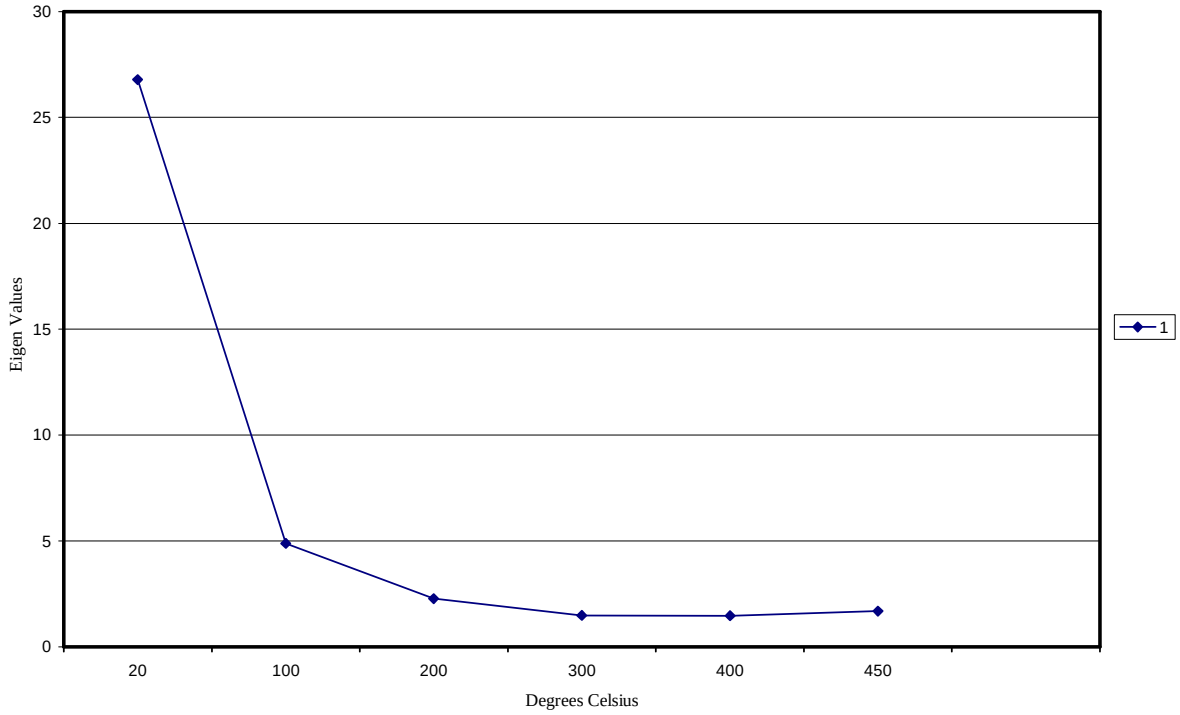

Figure 4.10: Eigen buckling values for the pinned beam at uniform temperatures

4.4.1.2 Model 2: Various gradient heats applied along the beam length

The same beam was modelled once again; the exact line segments, hermitian beam elements, material models and static loads were applied. Only this time a temperature gradient was applied along the beam (Figure 4.11).

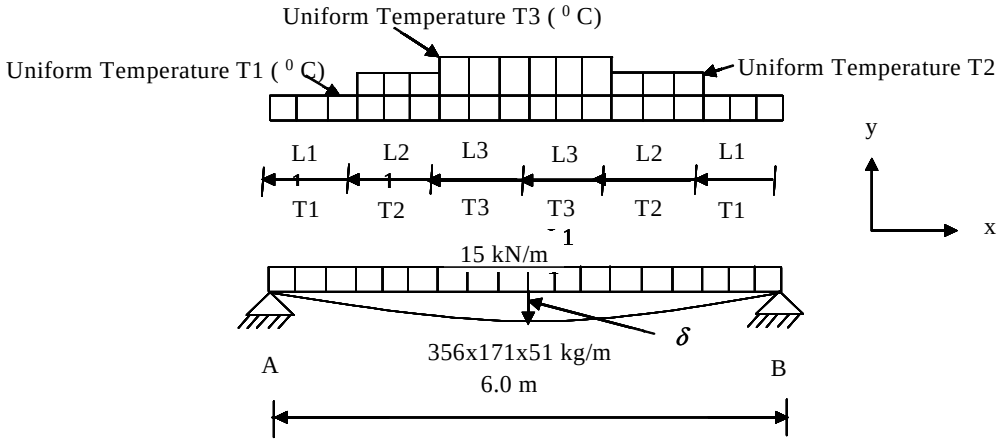

Figure 4.11: Model 2: simply supported beam with various temperature gradients along the beam length

The deflection behaviour for the beam can be seen in figure 4.12 up to a temperature of 571 ˚C, which corresponds to the strength deterioration curve of figure 4.13. The reduced strength of the beam is at 5.8 % of the ambient frame strength. It should also be noted that for both beams, the buckling strength increases after approximately 330 ˚C and 476 ˚C, respectively, (Figures 4.10 and 4.13). Also, it was observed that beams that were subjected to gradient temperatures, deteriorated at a slower rate. The beam moment profile is shown in figure 4.9. The beam moments and the y-deflections for this model is shown in table 4.6, respectively.

Table 4.6: Summary of the results for model 2 (simply supported beam)

		Values at 20 °C and percentage increase of values from ambient		Values at 95 °C and percentage increase of values from ambient		Values at 190 °C and percentage increase of values from ambient		Values at 286 °C and percentage increase of values from ambient		Values at 381 °C and percentage increase of values from ambient		Values at 476 °C and percentage increase of values from ambient		Values at 571 °C and percentage increase of values from ambient		Values at 667 °C and percentage increase of values from ambient		Values at 762 °C and percentage increase of values from ambient		Values at 857 °C and percentage increase of values from ambient		Values at 952 °C and percentage increase of values from ambient	
		Value at Ambient(20 °C)	% Increase of value from ambient	Value at 95 °C	% Increase of value from ambient	Value at 190 °C	% Increase of value from ambient	Value at 286 °C	% Increase of value from ambient	Value at 381 °C	% Increase of value from ambient	Value at 476 °C	% Increase of value from ambient	Value at 571 °C	% Increase of value from ambient	Value at 667 °C	% Increase of value from ambient	Value at 762 °C	% Increase of value from ambient	Value at 857 °C	% Increase of value from ambient	Value at 952 °C	% Increase of value from ambient
Moments (kNm)	Support A	0.00	0.00	0.00	0.00	0.00	0.00	0.00	0.00	0.00	0.00	0.00	0.00	0.00	0.00	0.00	0.00	0.00	0.00	0.00	0.00	0.00	0.00
	Mid span	67.50	0.00	67.50	0.00	67.50	0.00	67.50	0.00	67.50	0.00	67.50	0.00	67.50	0.00	67.50	0.00	67.50	0.00	67.50	0.00	67.50	0.00
	Support B	0.00	0.00	0.00	0.00	0.00	0.00	0.00	0.00	0.00	0.00	0.00	0.00	0.00	0.00	0.00	0.00	0.00	0.00	0.00	0.00	0.00	0.00
Y-Deflections (mm)	Support A	0.00	0.00	0.00	0.00	0.00	0.00	0.00	0.00	0.00	0.00	0.00	0.00	0.00	0.00	N/A	N/A	N/A	N/A	N/A	N/A	N/A	N/A
	Mid span	-1.80	0.00	-9.25	513.89	-9.54	530.00	-10.00	555.56	-11.30	627.78	-12.00	666.67	-14.55	808.33	N/A	N/A	N/A	N/A	N/A	N/A	N/A	N/A
	Support B	0.00	0.00	0.00	0.00	0.00	0.00	0.00	0.00	0.00	0.00	0.00	0.00	0.00	0.00	N/A	N/A	N/A	N/A	N/A	N/A	N/A	N/A

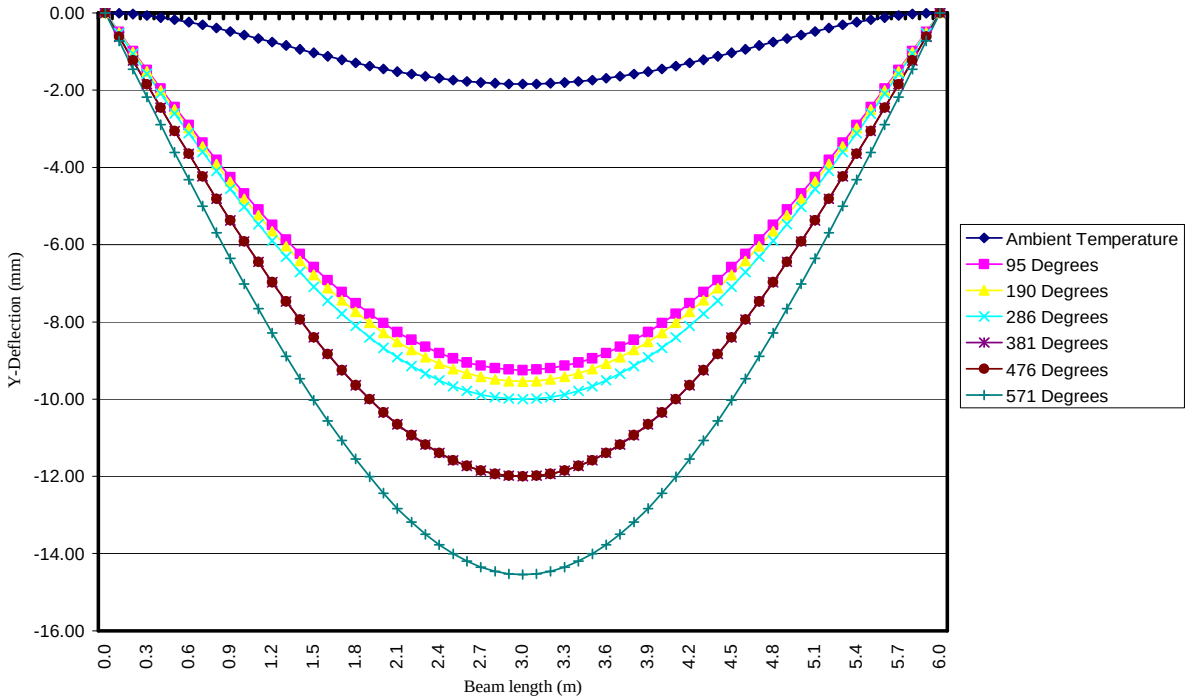

Figure 4.12: Pinned beam Y-deflections at gradient temperatures along the length

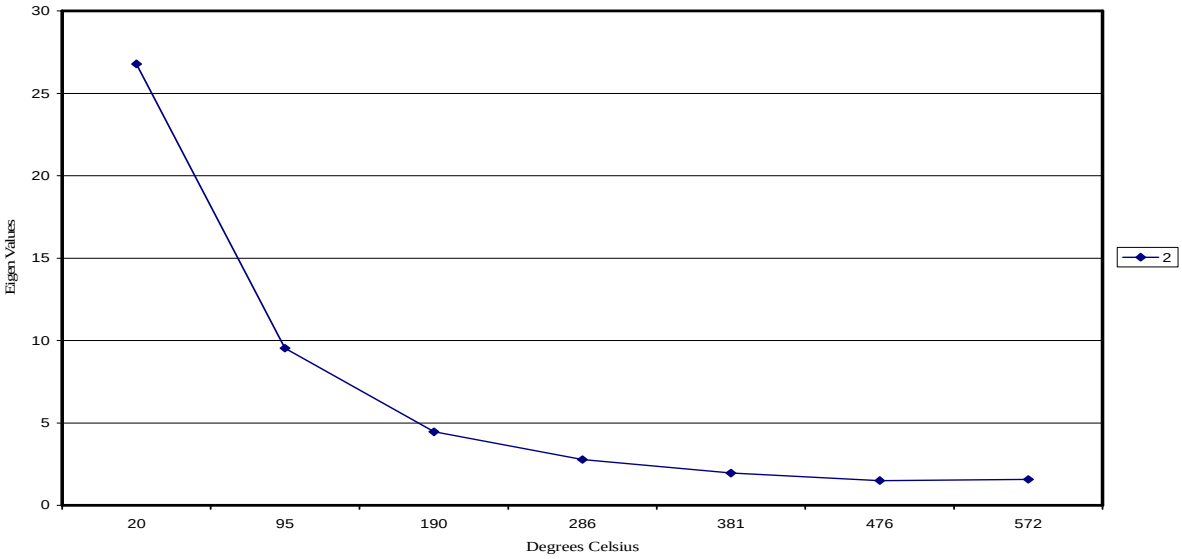

Figure 4.13: Eigen buckling values for the pinned beam at gradient temperatures

4.4.2 Fixed Support Beam

4.4.2.1 Model 3: Uniform heats applied to the beam

This time a beam was modelled with both supports fixed. The beam was modelled as line segments and the hermitian beam element group was used to model the 356 x 171x 51 kg/m section. The same isotropic linear elastic material model was used with the values of Young's

modulus and the coefficient of thermal expansion corresponding to the applied various temperatures of the beam segments. The same static loading of 15 kN/m was applied with a uniform cross sectional temperature applied throughout the beam length (Figure 4.14).

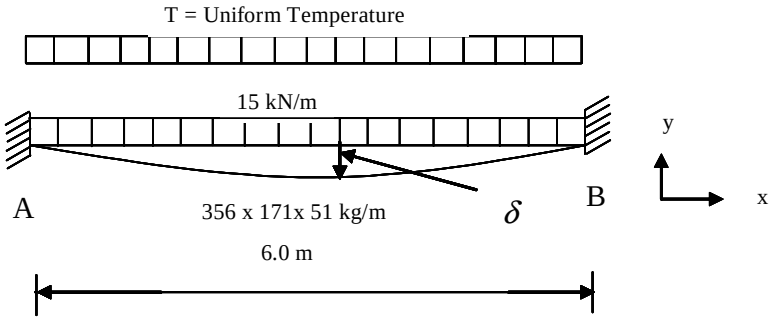

Figure 4.14: Model 3: Fixed supported beam with various uniform temperatures along the beam length

Table 4.7: Summary for the results of model 3 (fixed support beam)

		Values at 20 ºC and percentage increase of values from ambient		Values at 200 ºC and percentage increase of values from ambient		Values at 400 ºC and percentage increase of values from ambient		Values at 600 ºC and percentage increase of values from ambient		Values at 800 ºC and percentage increase of values from ambient		Values at 1000 ºC and percentage increase of values from ambient	
		Value at Ambient(20 ºC)	% Increase of value from ambient	Value at 200 ºC	% Increase of value from ambient	Value at 400 ºC	% Increase of value from ambient	Value at 600 ºC	% Increase of value from ambient	Value at 800 ºC	% Increase of value from ambient	Value at 1000 ºC	% Increase of value from ambient
Moments (kNm)	Support A	45.00	0.00	45.00	0.00	45.00	0.00	0.00	0.00	45.00	0.00	45.00	0.00
	Mid span	-22.50	0.00	-22.50	0.00	-22.50	0.00	0.00	0.00	-22.50	0.00	-22.50	0.00
	Support B	45.00	0.00	45.00	0.00	45.00	0.00	0.00	0.00	45.00	0.00	45.00	0.00
Y-Deflections (mm)	Support A	0.00	0.00	0.00	0.00	0.00	0.00	0.00	0.00	0.00	0.00	0.00	0.00
	Mid span	-1.80	0.00	-1.93	107.22	-2.27	126.11	-3.60	200.00	-7.22	401.11	-27.35	1519.44
	Support B	0.00	0.00	0.00	0.00	0.00	0.00	0.00	0.00	0.00	0.00	0.00	0.00

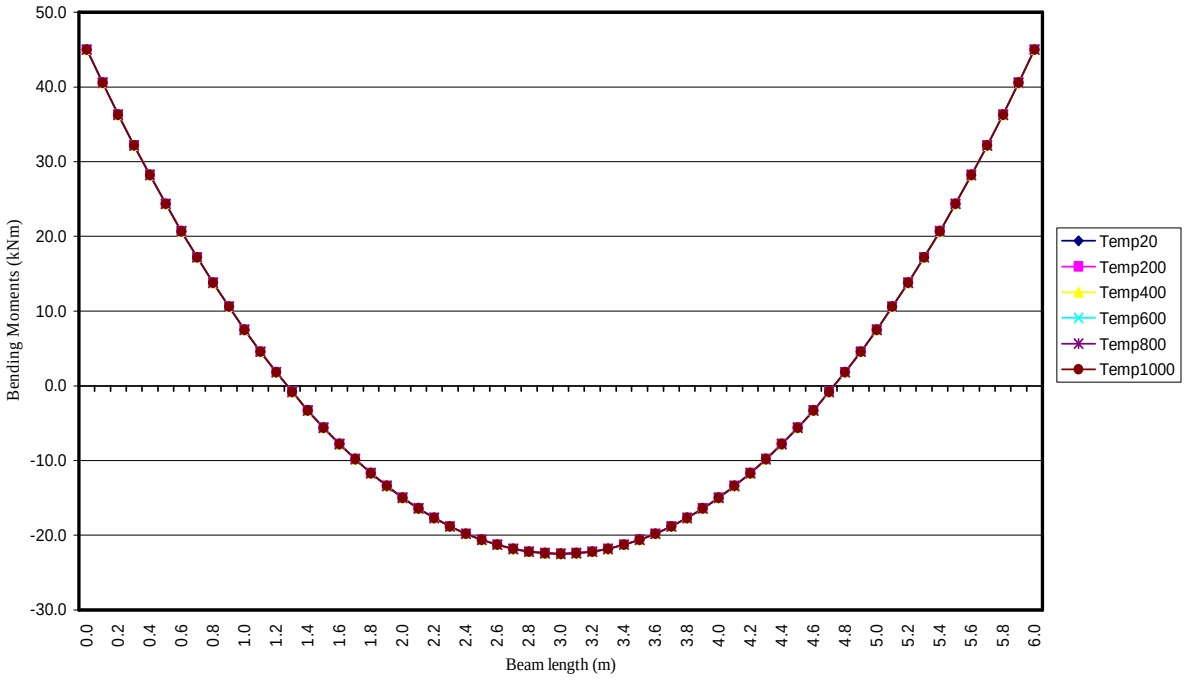

Figure 4.15: Fixed beam moments at uniform temperatures

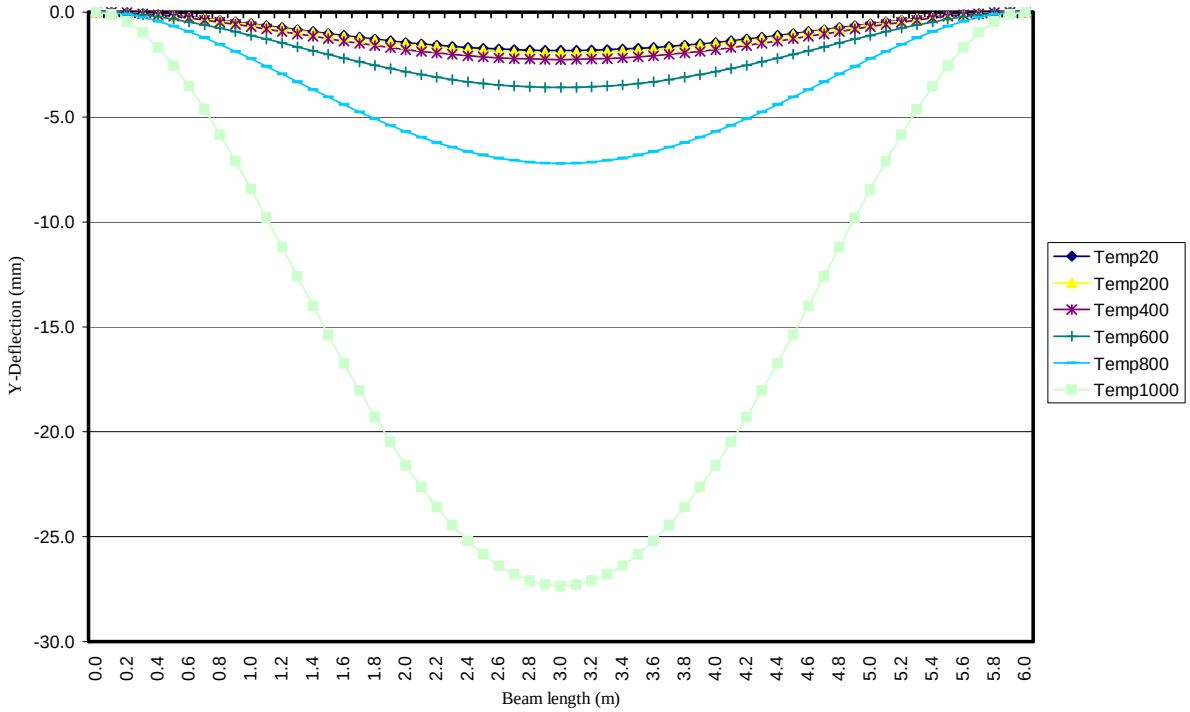

Figure 4.16: Fixed beam Y-deflections at uniform temperatures

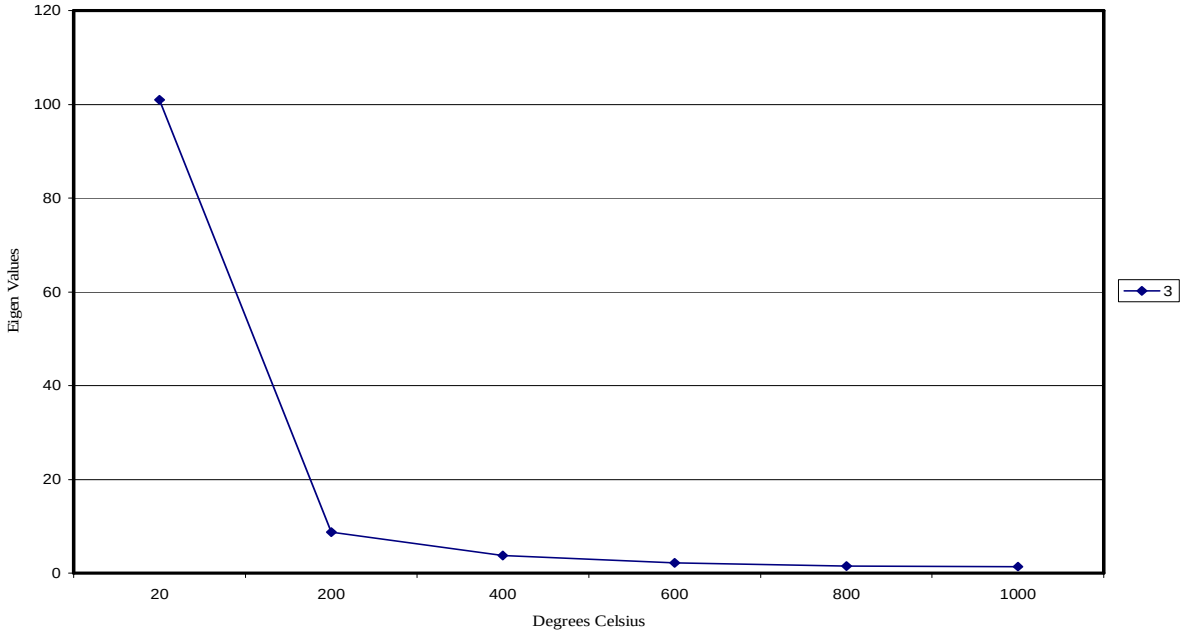

Figure 4.17: Eigen buckling values for the fixed beam at uniform temperature increases

As the temperature is increased uniformly, the bending moment remains constant at -22.50 and 45.00 kNm at the mid span and supports of the beam, respectively (Figure 4.15 and Table 4.7). The vertical deflection at midspan is very small with increasing temperature up to about 800 ˚C and then suddenly jumps to a total increase of 1489% at 1000 ˚C (Table 4.7). In figure 4.16, it

can be seen that the beam exceeds the serviceability limit of 20 mm. Figure 4.17 shows that when the beam is at 1000 ˚C, it has approximately 1.4% of its ambient temperature strength. Table 4.7 gives the beam moments and the y-deflections for this model, respectively.

4.4.2.2 Model 4: Gradient heats applied along the beam length

The same fixed support beam was modelled (Figure 4.18), but this time with a varying gradient temperature along the beam length but with a constant cross sectional temperature. The same beam was modelled as line segments and the hermitian beam element group was used to model the 356 x 171 x 51 kg/m section. The same isotropic linear elastic material model was used with the values of Young's modulus and the coefficient of thermal expansion corresponding to the applied various temperatures of the beam segments, as before.

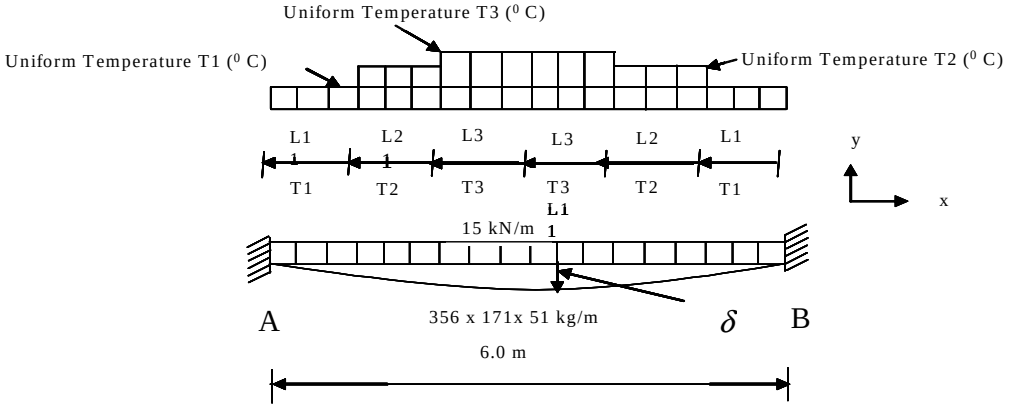

Figure 4.18: Model 4: Fixed supported beam with various gradient temperatures along the beam length

Table 4.8: Summary of the results for model 4 (fixed support beam) subjected to gradient temperatures

		Values at 20 ℃ and percentage increase of values from ambient		Values at 95 ℃ and percentage increase of values from ambient		Values at 190 ℃ and percentage increase of values from ambient		Values at 286 ℃ and percentage increase of values from ambient		Values at 381 ℃ and percentage increase of values from ambient		Values at 476 ℃ and percentage increase of values from ambient		Values at 571 ℃ and percentage increase of values from ambient		Values at 667 ℃ and percentage increase of values from ambient		Values at 762 ℃ and percentage increase of values from ambient		Values at 857 ℃ and percentage increase of values from ambient		Values at 952 ℃ and percentage increase of values from ambient	
		Value at Ambient(20 ℃)	% Increase of value from ambient	Value at 95 ℃	% Increase of value from ambient	Value at 190 ℃	% Increase of value from ambient	Value at 286 ℃	% Increase of value from ambient	Value at 381 ℃	% Increase of value from ambient	Value at 476 ℃	% Increase of value from ambient	Value at 571 ℃	% Increase of value from ambient	Value at 667 ℃	% Increase of value from ambient	Value at 762 ℃	% Increase of value from ambient	Value at 857 ℃	% Increase of value from ambient	Value at 952 ℃	% Increase of value from ambient
Moments (kNm)	Support A	45.00	0.00	45.11	100.24	45.33	100.73	45.67	101.49	46.22	102.71	47.11	104.69	48.69	108.20	50.23	111.62	52.61	116.91	55.15	122.56	57.91	128.69
	Mid span	-22.50	0.00	-22.39	99.51	-22.17	98.53	-21.83	97.02	-21.28	94.58	-20.39	90.62	-18.81	83.60	-17.27	76.76	-14.89	66.18	-12.35	54.89	-9.59	42.62
	Support B	45.00	0.00	45.11	100.24	45.33	100.73	45.67	101.49	46.22	102.71	47.11	104.69	48.69	108.20	50.23	100.00	52.61	116.91	55.15	122.56	57.91	128.69
Y-Deflections (mm)	Support A	0.00	0.00	0.00	0.00	0.00	0.00	0.00	0.00	0.00	0.00	0.00	0.00	0.00	0.00	0.00	0.00	0.00	0.00	0.00	100.00	0.00	0.00
	Mid span	-1.80	0.00	-1.80	0.00	-1.90	105.56	-1.90	105.56	-2.00	111.11	-2.15	119.44	-2.39	132.78	-2.66	147.78	-3.12	173.33	-3.71	206.11	-4.64	257.78
	Support B	0.00	0.00	0.00	0.00	0.00	0.00	0.00	0.00	0.00	0.00	0.00	0.00	0.00	0.00	0.00	0.00	0.00	0.00	0.00	100.00	0.00	0.00

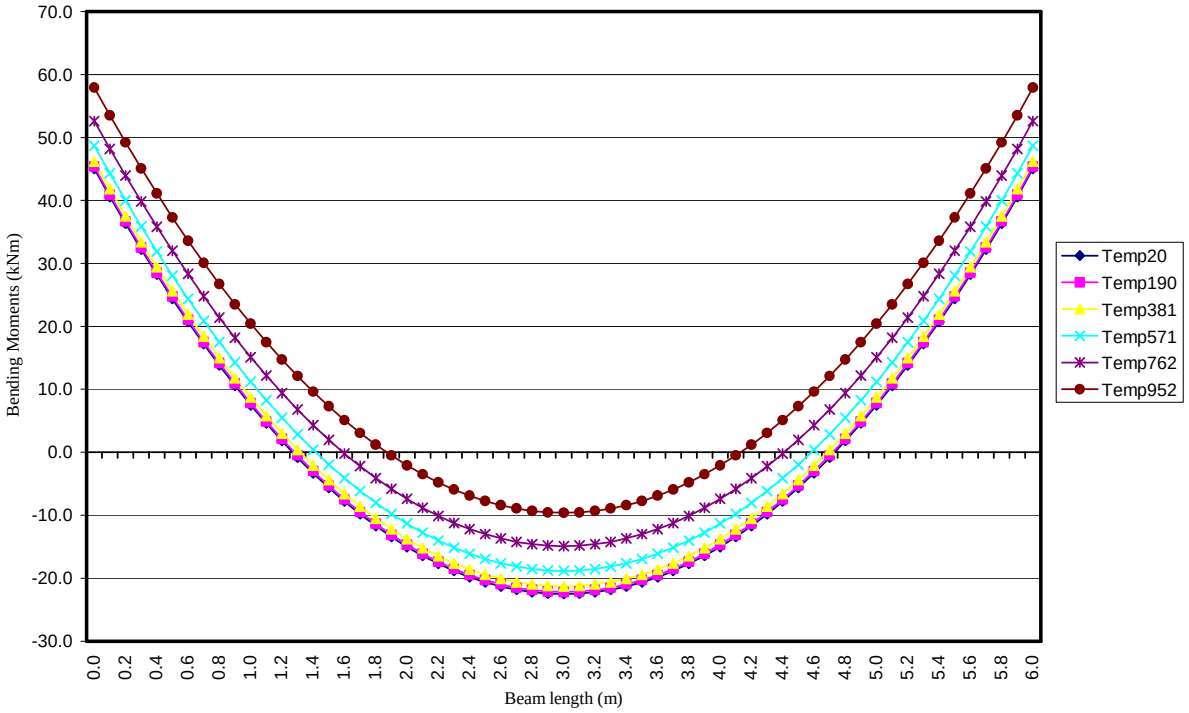

Figure 4.19: Fixed beam moments at gradient temperatures along the beam length

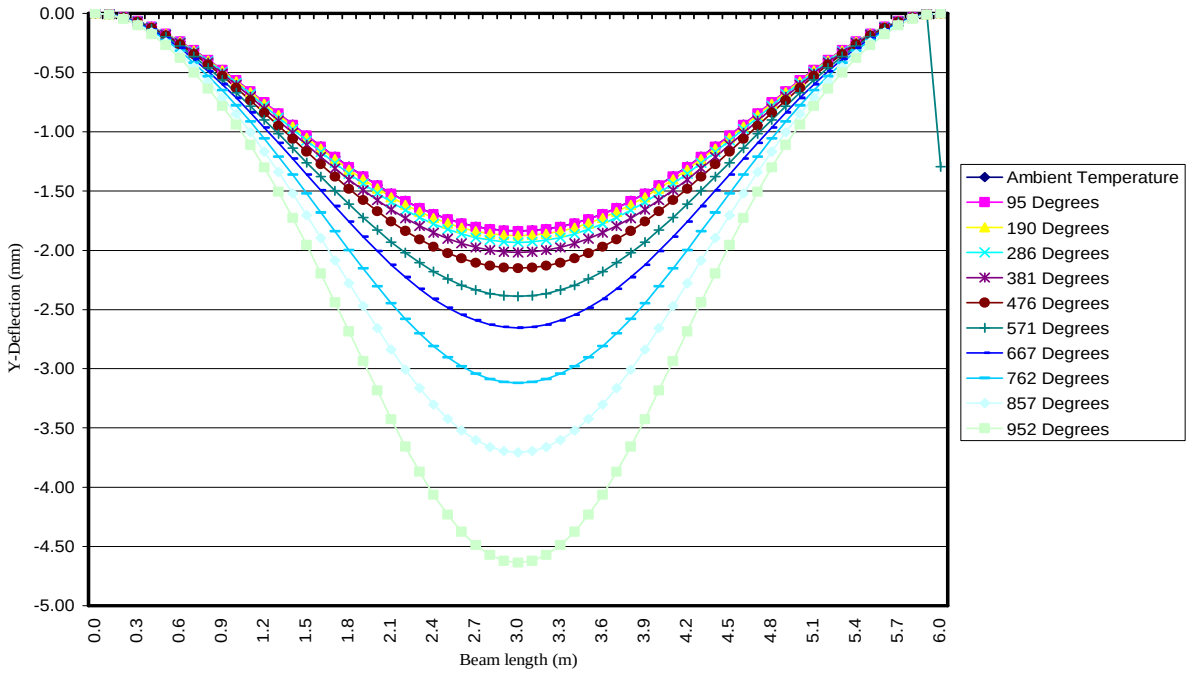

Figure 4.20: Fix beam Y-deflections at gradient temperatures along the length

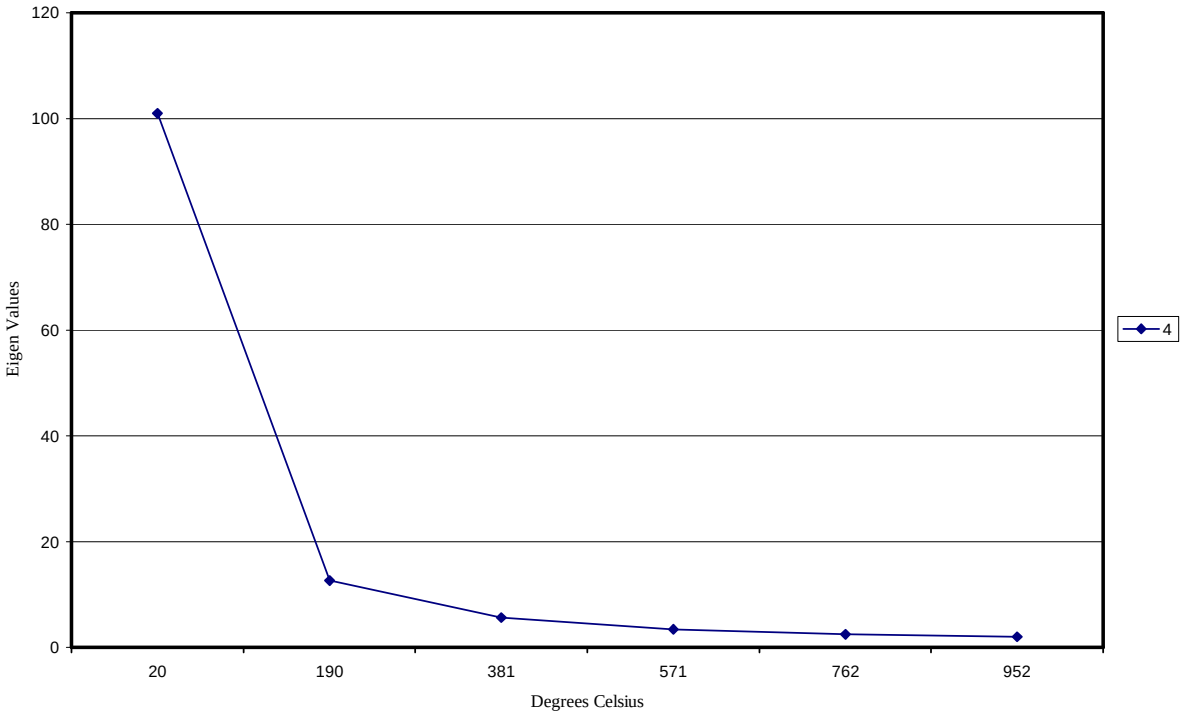

Figure 4.21: Eigen buckling values for the fixed beam at gradient temperature increases

It can be seen in figure 4.19 that the mid span moment is distributed to the supports as the temperature increases. Distribution in this context implies that more of the moment is absorbed by the stiffer end supports of the beam which is at a lower temperature than the weaker mid span section of the beam. The decrease of moments in the mid span is approximately 43 % and the increase at the supports is approximately 128 % (Figure 4.19 and Table 4.8). Figure 4.20 and table 4.8 show that the vertical deflection increased by approximately 258 %. It can be seen from figure 4.21 that the beam still has 2% of its strength remaining, which is about 0.6% more than for the uniformly heated beam. Table 4.8 gives a summary of the beam moments and the y-deflections for this model, respectively.

4.4.3 Beam-column

4.4.3.1 Model 5: Uniform heats applied to beam-column

A column composed of a 254 x 254 x 73 kg/m H-Section was modelled as fixed at the base and the top was only allowed to move vertically (figure 4.22). A vertical load of 1079 kN was applied to the top of the column and a horizontal load of 10.79 kN (0.01P) at mid-height as shown in figure 4.22. The column was modelled as line segments and the hermitian beam element group properties were assigned to the line segments to model the 254 x 254 x 73 kg/m H-section. The linear elastic material model was used to represent the structural steel and the

appropriate values for the Young's modulus and the coefficient of thermal expansion, corresponding to the applied various temperatures of the beam segments, were assigned.

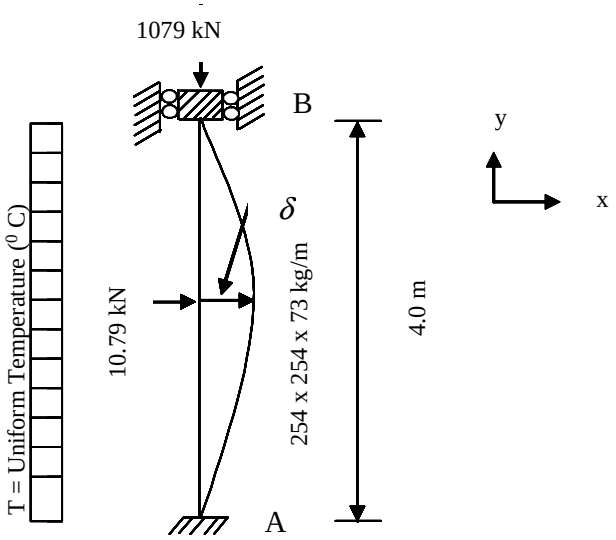

Figure 4.22: Model 5: Beam-column fixed at base and allowed to move vertically at the top only with various uniform temperatures applied along the beam-column length

For the uniformly heated column at varying uniform temperatures, the bending moment remained constant at values of -5.40 kNm and 5.40 kNm at the mid height and supports of the column, respectively. The vertical deflection was also negligible. The x-deflection was the only other notable variable with an increase of 1506% of ambient temperature deflection (Figure 4.23 and Table 4.9). Figure 4.24 show the column possesses only 1.09 % of its ambient temperature strength at 1000 ˚C. Table 4.9 gives a summary of the output values for the column moments and the x-deflections for this model, respectively.

Table 4.9: Summary of the results for model 5 (top support of beam-column free to move vertically) subjected to uniform temperatures

		Values at 20 ºC and percentage increase of values from ambient		Values at 200 ºC and percentage increase of values from ambient		Values at 400 ºC and percentage increase of values from ambient		Values at 600 ºC and percentage increase of values from ambient		Values at 800 ºC and percentage increase of values from ambient		Values at 1000 ºC and percentage increase of values from ambient	
		Value at Ambient(20 ºC)	% Increase of value from ambient	Value at 200 ºC	% Increase of value from ambient	Value at 400 ºC	% Increase of value from ambient	Value at 600 ºC	% Increase of value from ambient	Value at 800 ºC	% Increase of value from ambient	Value at 1000 ºC	% Increase of value from ambient
Moments (kNm)	Support A	5.40	0.00	5.40	0.00	5.40	0.00	5.40	0.00	5.40	0.00	5.40	0.00
	Mid span	-5.40	0.00	-5.40	0.00	-5.40	0.00	-5.40	0.00	-5.40	0.00	-5.40	0.00
	Support B	5.40	0.00	5.40	0.00	5.40	0.00	5.40	0.00	5.40	0.00	5.40	0.00
X-Deflections (mm)	Support A	0.00	0.00	0.00	0.00	0.00	0.00	0.00	0.00	0.00	0.00	0.00	0.00
	Mid span	0.16	0.00	0.17	106.25	0.20	125.00	0.32	200.00	0.64	400.00	2.41	1506.25
	Support B	0.00	0.00	0.00	0.00	0.00	0.00	0.00	0.00	0.00	0.00	0.00	0.00

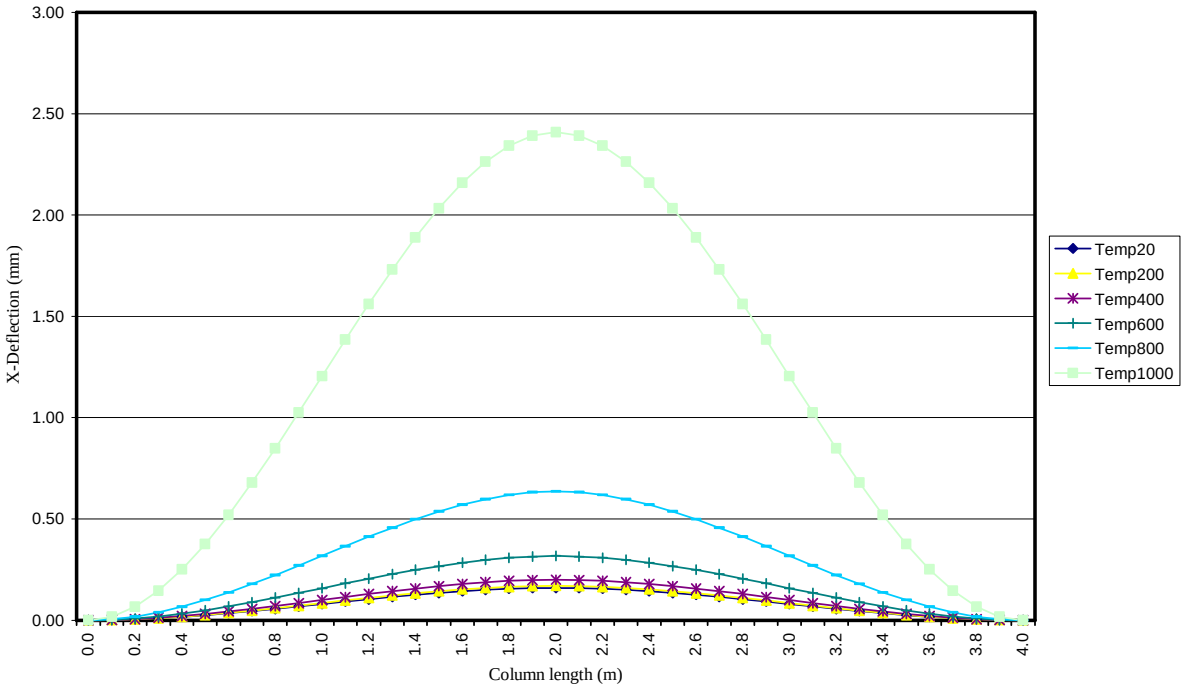

Figure 4.23: Beam-column X-deflections for varying uniform temperature [Beam-column Y-deflection-negligible; Beam-column X-moment-constant]

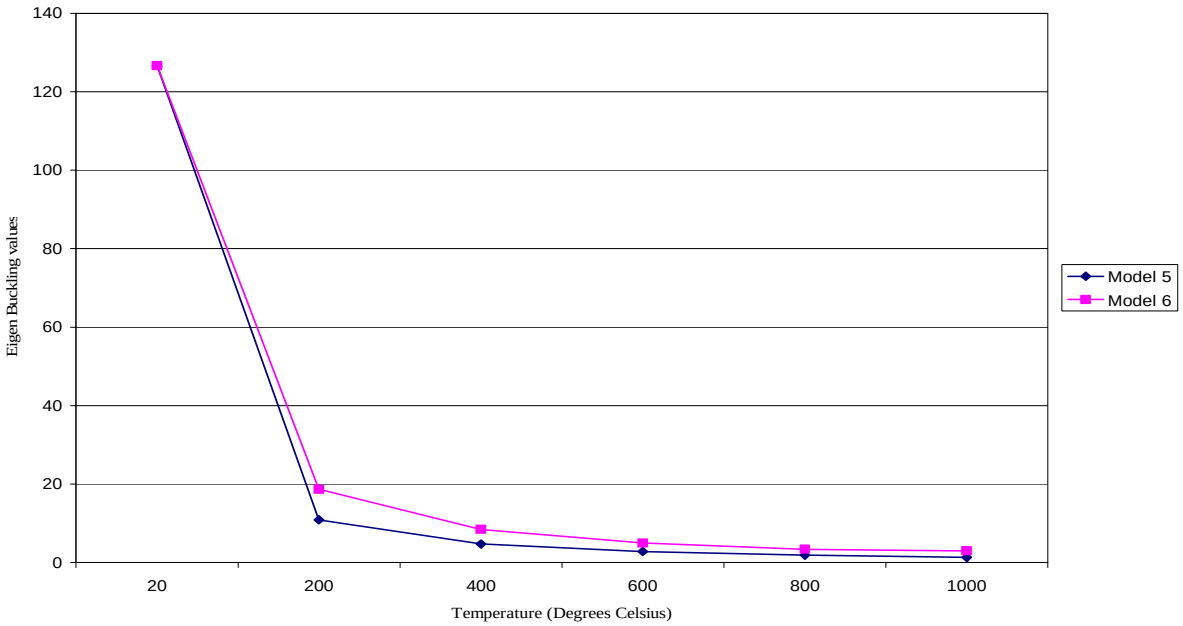

Figure 4.24: Beam-column Eigen buckling values

4.4.3.2 Model 6: Gradient heat applied along the beam-column length

A similar beam-column as in model 5, with the same support conditions and static loads (Figure 4.25) was used for this model. The column was modelled as line segments and the hermitian beam element group was used to model the 254 x 254 x 73 kg/m H-section.

The same isotropic linear elastic material model was used with the values of Young's modulus and the coefficient of thermal expansion corresponding to the applied various gradient temperatures of the beam segments (Figure 4.25).

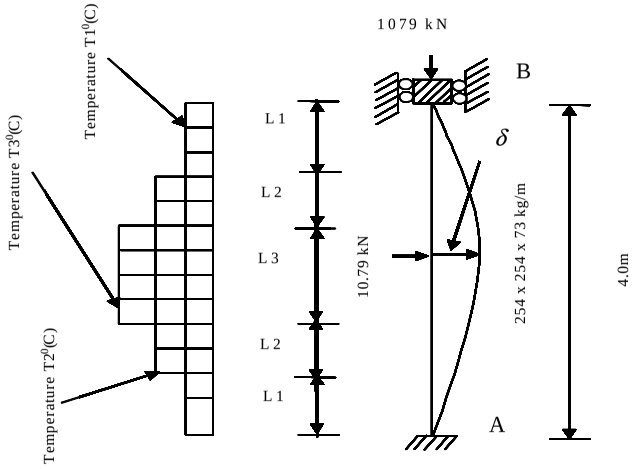

Figure 4.25: Model 6: Beam-column fixed at base and allowed to move vertically at the top only with various gradient temperatures applied along the beam-column length

The column at gradient temperature distributes its moments from the mid span section of the beam to the supports (Figure 4.26). This distribution amounts to a 141 % increase of the moments at the supports and a reduction 42 % in the mid span moments (Figure 4.26 and Table 4.10). The y-deflection seemed increased to a maximum of just over 4mm (Figure 4.27). The y-deflection values in table 4.10 are given at 1m from the base or the top of the column and not at mid span. The x-deflection increased by 288 % and is considerably lower than for the uniformly heated column, as can be seen in figure 4.28 and in table 4.10.

Table 4.10: Summary of the results for model 6 (top support of beam-column free to move vertically) subjected to gradient temperatures

		Values at 20 °C and percentage increase of values from ambient		Values at 95 °C and percentage increase of values from ambient		Values at 190 °C and percentage increase of values from ambient		Values at 286 °C and percentage increase of values from ambient		Values at 381 °C and percentage increase of values from ambient		Values at 476 °C and percentage increase of values from ambient		Values at 571 °C and percentage increase of values from ambient		Values at 667 °C and percentage increase of values from ambient		Values at 762 °C and percentage increase of values from ambient		Values at 857 °C and percentage increase of values from ambient		Values at 952 °C and percentage increase of values from ambient	
		Value at Ambient(20 °C)	% Increase of value from ambient	Value at 95 °C	% Increase of value from ambient	Value at 190 °C	% Increase of value from ambient	Value at 286 °C	% Increase of value from ambient	Value at 381 °C	% Increase of value from ambient	Value at 476 °C	% Increase of value from ambient	Value at 571 °C	% Increase of value from ambient	Value at 667 °C	% Increase of value from ambient	Value at 762 °C	% Increase of value from ambient	Value at 857 °C	% Increase of value from ambient	Value at 952 °C	% Increase of value from ambient
Moments (kNm)	Support A	5.40	0.00		0.00	5.40	0.00		0.00	5.60	103.70		0.00	5.90	109.26		0.00	6.60	122.22		0.00	7.60	140.74
	Mid span	-5.40	0.00		0.00	-5.30	98.15		0.00	-5.20	96.30		0.00	-4.80	88.89		0.00	-4.20	77.78		0.00	-3.10	57.41
	Support B	5.40	0.00		0.00	5.40	0.00		0.00	5.60	103.70		0.00	5.90	109.26		100.00	6.60	122.22		0.00	7.60	140.74
Y-Deflections (mm)	Support A	0.00	0.00		0.00	0.00	0.00		0.00	0.00	0.00	0.00	0.00	0.00	0.00	0.00	0.00	0.00	0.00	0.00	0.00	0.00	0.00
	Mid span	0.10	0.00		0.00	-0.53	-630.00		0.00	-1.10	-1200.00	0.00	0.00	-1.40	-1500.00	0.00	0.00	-0.60	-700.00	0.00	0.00	2.00	1900.00
	Support B	0.00	0.00		0.00	0.00	0.00		0.00	0.00	0.00	0.00	0.00	0.00	0.00	0.00	0.00	0.00	0.00	0.00	0.00	0.00	0.00
X-Deflections (mm)	Support A	0.00	0.00		0.00	0.00	100.00		0.00	0.00	100.00	0.00	0.00	0.00	0.00	0.00	0.00	0.00	0.00	0.00	0.00	0.00	0.00
	Mid span	0.16	0.00		0.00	0.17	106.25		0.00	0.18	112.50	0.00	0.00	0.21	131.25	0.00	0.00	0.29	181.25	0.00	0.00	0.46	287.50
	Support B	0.00	0.00		0.00	0.00	100.00		0.00	0.00	100.00	0.00	0.00	0.00	0.00	0.00	0.00	0.00	0.00	0.00	0.00	0.00	0.00

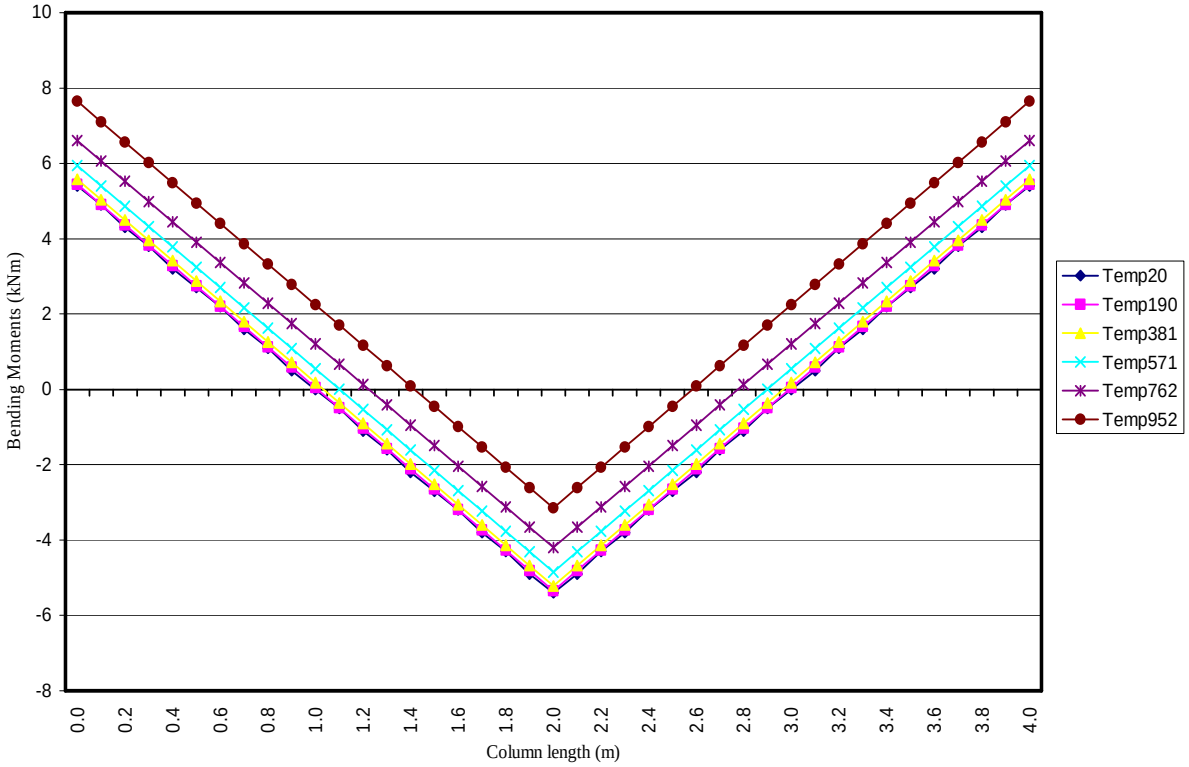

Figure 4.26: Beam-column moments at gradient temperatures along the length

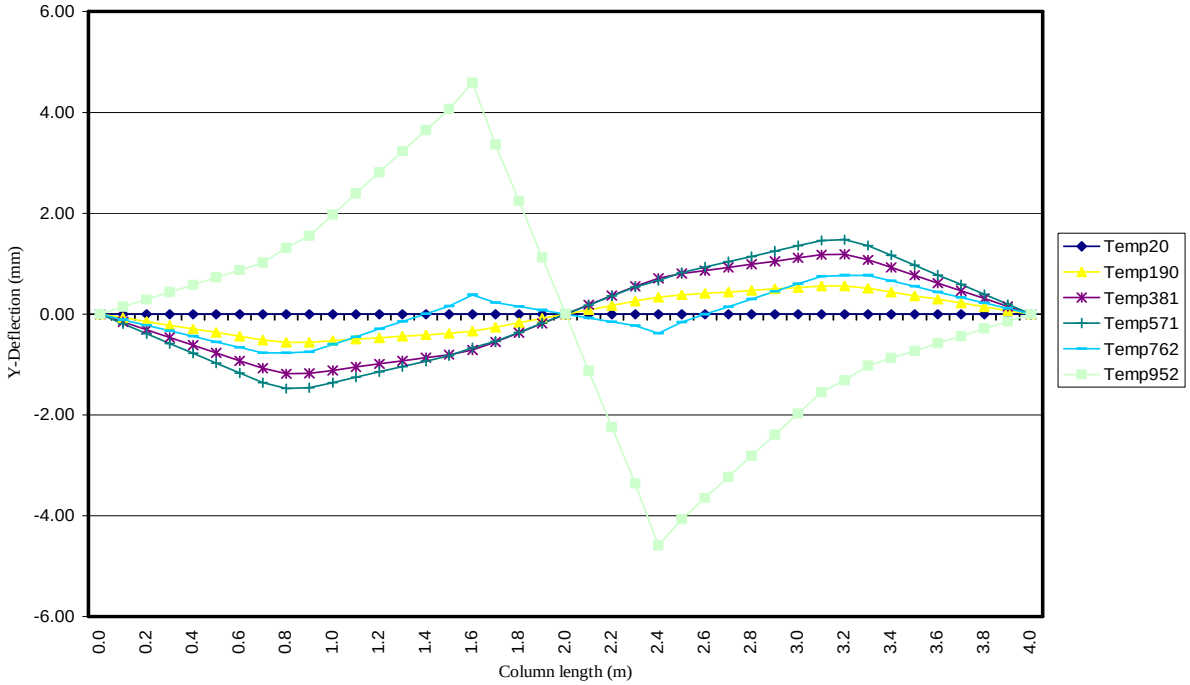

Figure 4.27: Beam-column Y-deflections at gradient temperatures along the length

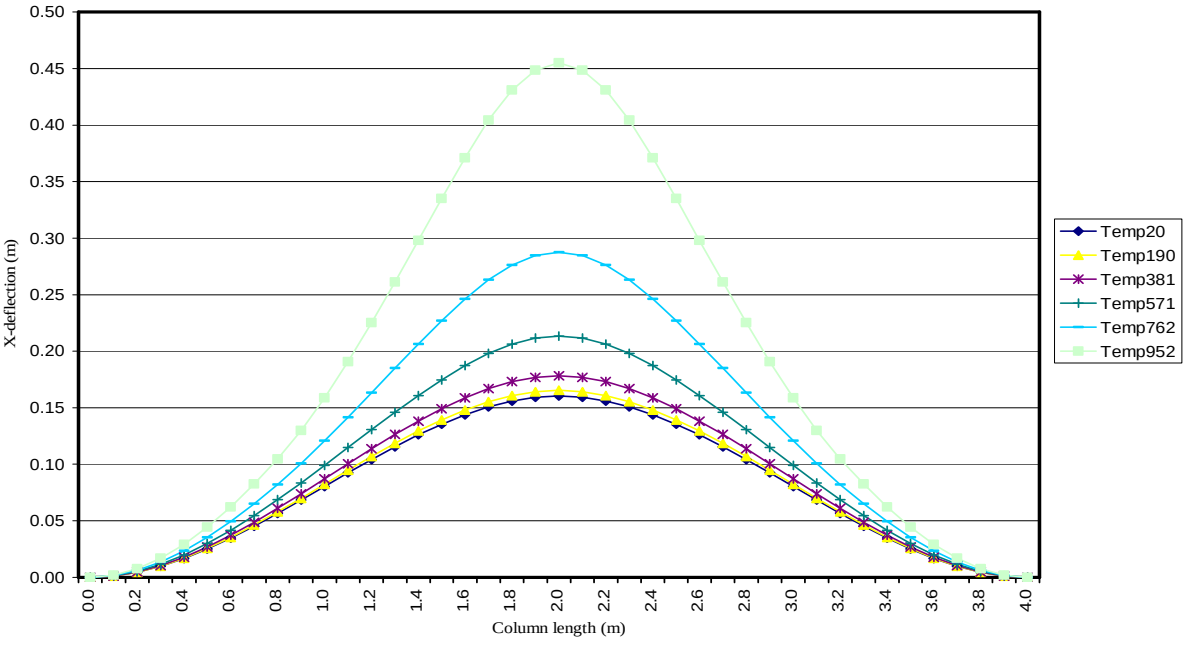

Figure 4.28: Beam-column X-deflections at gradient temperatures along the length

4.4.4 Portal Frames

4.4.4.1 Model 7: All members heated uniformly

The portal beam is loaded with a UDL of 25 kN/m and two axial loads of 500 kN on each column. The beam is a 305 x 165 x 41 kg/m I- Beam and column a 203 x 203 x 52 H- section (Figure 4.29).

The frame was generated as line diagrams for the columns and beams. The hermitian beam element group was assigned to the line segments in order to generate the 305 x 165 x 41 kg/m and 203 x 203 x 52 kg/m beam and column sections, respectively. An isotropic linear elastic material model was generated for the beam or column line segments sharing the same material and cross sectional properties. In this case, it was only necessary to generate two material models and two element groups.

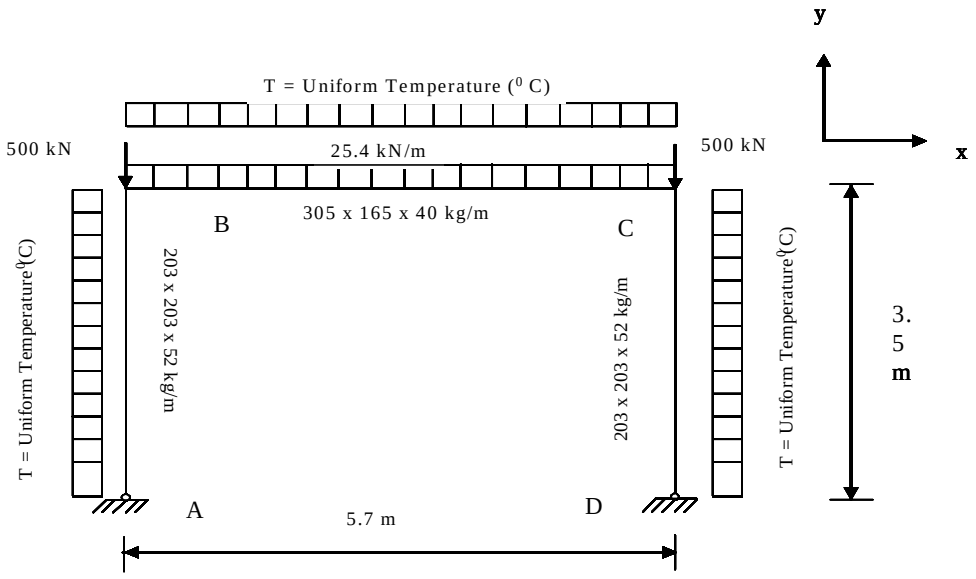

Figure 4.29: Model 7: Portal frame: all members at various uniform temperatures

The values of Young's modulus and the coefficient of thermal expansion corresponding to the applied various uniform temperatures of the beam and column line segments were assigned to the appropriate corresponding material model (Figure 4.29).

The temperature of the beam and the columns were increased constantly in increments of 100 ^{o} C. It can be seen that the moments in the beam are distributed away from the mid span toward the rigid connections between the beam and column (Figure 4.30 and Table 4.11).

As expected, the beam experiences an axial expansion (Figure 4.31) and results in a moment in the columns (Figure 4.32 and Table 4.11). It can be seen how the column reacts to the axial thrust of the beam in figure 4.33. It first forms a half sine curve, resisting both axial and horizontal load and is eventually forced outwards by the horizontal axial thrust of the beam.

Studying the x-deflection curve in figure 4.33, it can be seen that the deflection in mid span is counteracted by the stiffer section of the column-beam connection (table 4.11) which possesses more strength due to the fact that it is at a lower temperature. In figure 4.34, it can be seen how the buckling strength of the frame decreases with temperature to approximately 9.44% at 960 ˚C. The results for model 7 is given in table 4.11 which gives output values for the beam moments, x-deflections, y-deflections and column moments.

At 1000 ˚C, the bending moment in the beam has a load ratio of R = 80/169 = 0.47 and limiting temperature of 659 ˚C as per BS 5950 Part 8:1990. The design temperature would be 767 ˚C for a resistance period of 30 min. If the limiting temperature is less than the design temperature, a beam will require fire protection as per BS 5950 Part 8:1990. It can therefore be seen, that the frame beam does not comply with this criteria and fire protection is required. However, it must be noted that the frame beam has been subjected to a temperature of 1000 ˚C at a load ratio (R) of 0.47, which exceeds the design temperature of 767 ˚C by 233 ˚C. The y-deflection at 600 ˚C is approximately at the deflection limit of 19 mm (L/300) and is exceeded by approximately 360 ˚C. This may cause irreversible deformation but the beam however has not collapsed.

Table 4.11: Summary of the results for model 7 (supports fixed in all directions) subjected to uniform temperatures

		Values at 20 ºC and percentage increase of values from ambient		Values at 200 ºC and percentage increase of values from ambient		Values at 400 ºC and percentage increase of values from ambient		Values at 600 ºC and percentage increase of values from ambient		Values at 800 ºC and percentage increase of values from ambient		Values at 1000 ºC and percentage increase of values from ambient	
		Value at Ambient(20 ºC)	% Increase of value from ambient	Value at 200 ºC	% Increase of value from ambient	Value at 400 ºC	% Increase of value from ambient	Value at 600 ºC	% Increase of value from ambient	Value at 800 ºC	% Increase of value from ambient	Value at 1000 ºC	% Increase of value from ambient
Beam Moments (kNm)	Connection B	46.44	0.00	55.49	119.49	59.48	128.08	69.17	148.94	76.05	163.76	77.43	166.73
	Mid span	-59.60	0.00	-47.84	80.27	-43.84	73.56	-34.13	57.27	-27.25	45.72	-25.87	43.41
	Connection C	46.35	0.00	55.41	119.55	59.48	128.33	69.15	149.19	76.05	164.08	77.41	167.01
Column Moments (kNm)	Support A	-23.93	0.00	-43.31	180.99	-56.89	237.74	-47.71	199.37	-32.44	135.56	-35.96	150.27
	Mid span	11.25	0.00	6.41	56.98	3.01	26.76	5.31	47.20	9.12	81.07	8.32	73.96
	Connection B	46.44	0.00	56.12	120.84	62.90	135.44	58.32	125.58	50.69	109.15	52.60	113.26
Beam Y-Deflections (mm)	Connection B	-1.10	0.00	6.51	-691.82	15.34	-1494.55	33.40	-3136.36	48.25	-4486.36	51.89	-4717.27
	Mid span	-10.91	0.00	-1.41	12.92	7.46	-168.38	25.66	-335.20	25.87	-337.12	-76.09	697.43
	Connection C	-1.10	0.00	6.51	-691.82	15.34	-1494.55	33.40	-3136.36	48.25	-4486.36	51.89	-4717.27
Column X-Deflections (mm)	Support A	0.00	0.00	0.00	0.00	0.00	0.00	0.00	0.00	0.00	0.00	0.00	0.00
	Mid span	1.78	0.00	4.33	243.26	7.69	432.02	14.13	793.82	30.11	1691.57	30.42	1708.99
	Connection B	0.28	0.00	6.59	2353.57	14.13	5046.43	23.27	8310.71	30.65	10946.43	88.56	31628.57

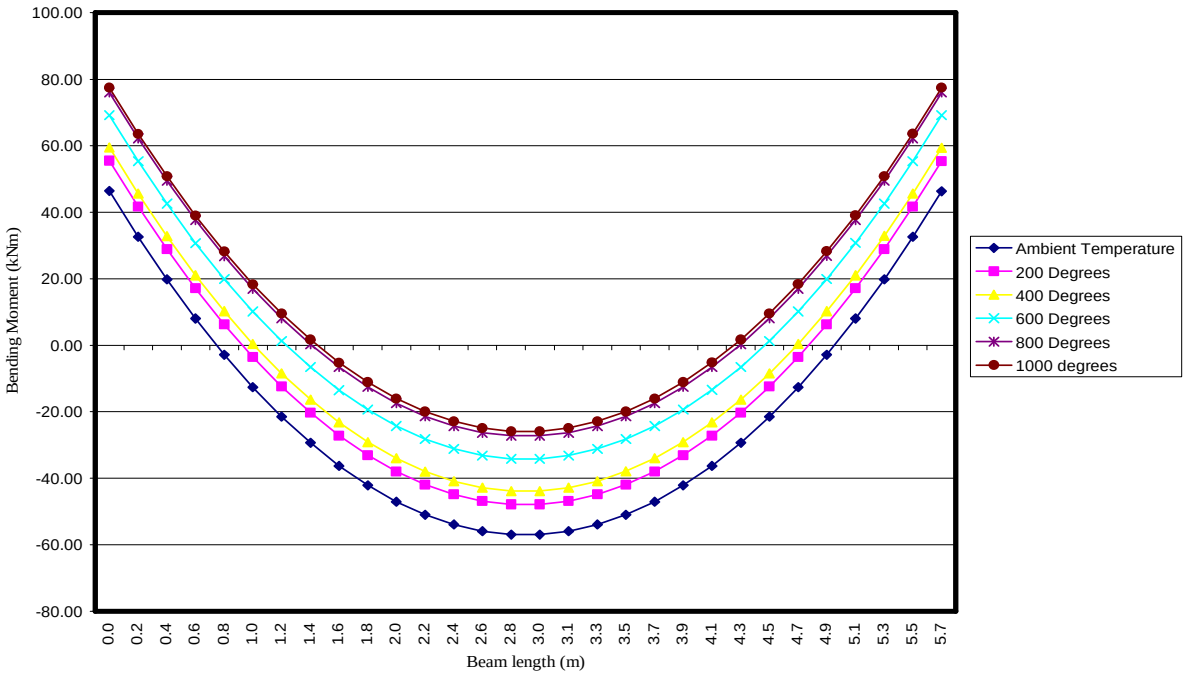

Figure 4.30: Portal beam moments for the portal beam & columns at uniform temperatures

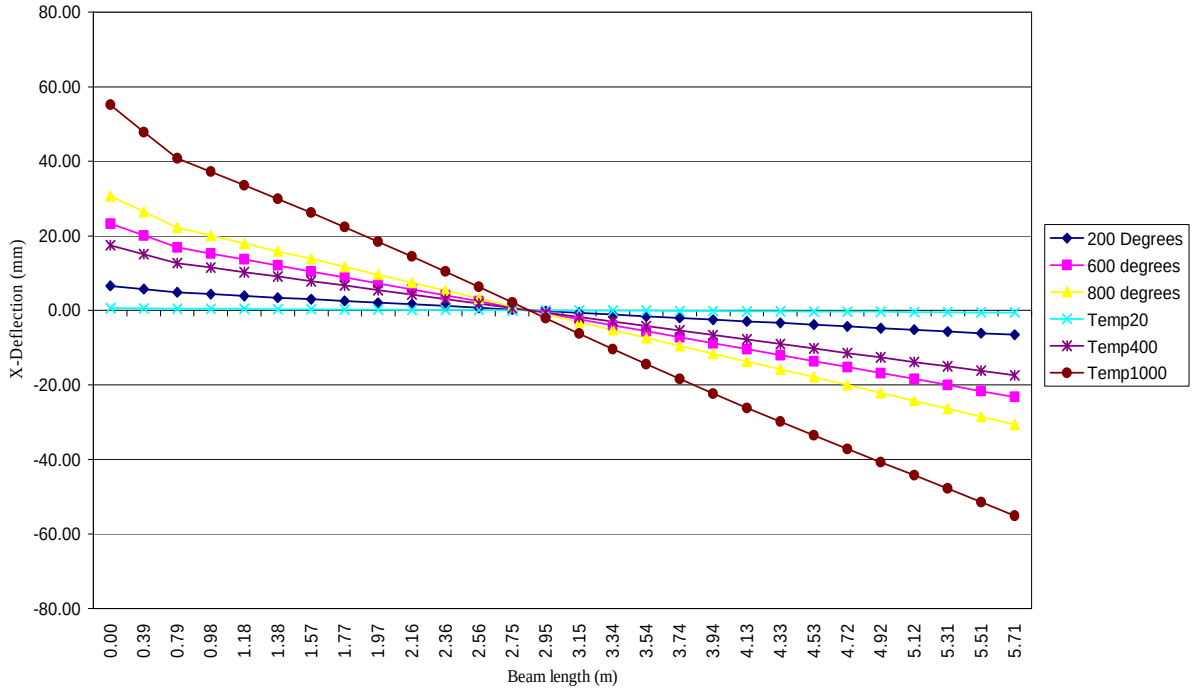

Figure 4.31: Portal beam X-deflections for the portal beam & columns at uniform temperatures

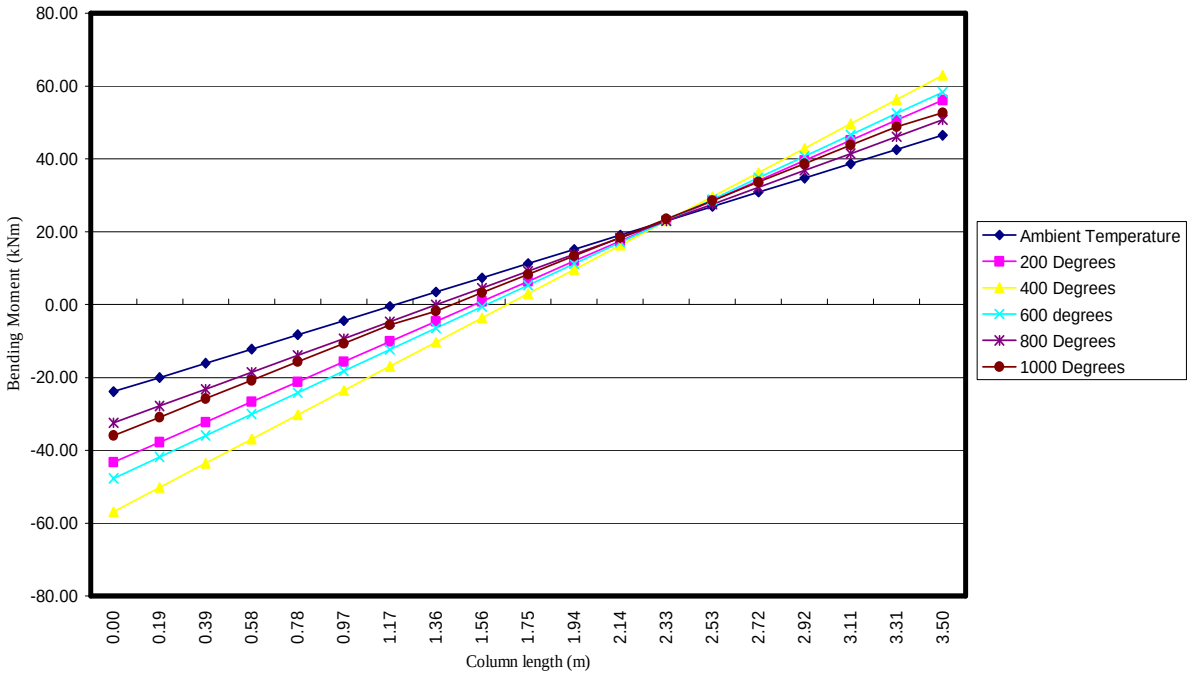

Figure 4.32: Portal column moments for the portal beam & columns at uniform temperatures

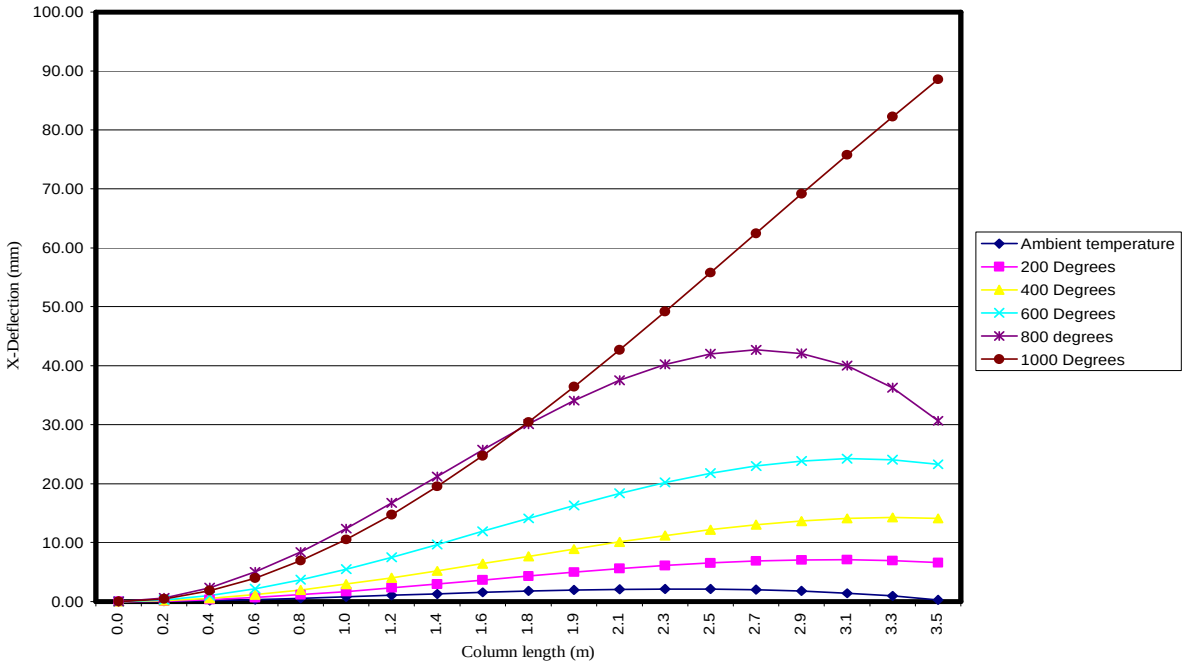

Figure 4.33: Portal column X-deflections for the portal beam & columns at uniform temperatures

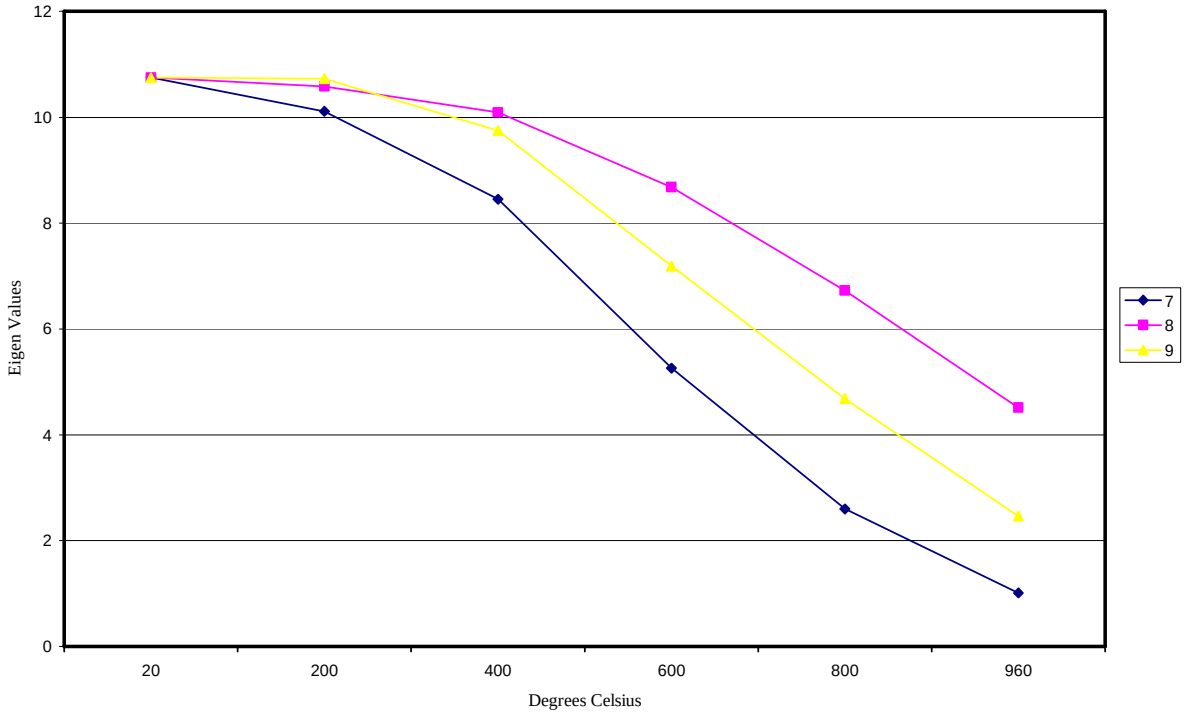

Figure 4.34: Eigen buckling values for the portal frame models 7, 8 & 9

4.4.4.2 Model 8: Only the beam heated uniformly

The same portal frame, as in model 7, was modelled with the same line segments for the beam and the columns, but with only the beam temperature varied uniformly (Figure 4.35). The exact same material models with the values of Young's modulus and the coefficient of thermal expansion corresponding to the applied various uniform temperatures of the beam and column line segments were assigned to the appropriate corresponding material model. In this case it was again only necessary to generate two material models and two element groups (Figure 4.35). The beam and column sections used were 305 x 165 x 41 kg/m and 203 x 203 x 52 kg/m, respectively, and the exact static loads were applied as before (Table 4.1). The supports of the frame were fixed in all degrees of freedom and the beam-column connections were modelled as fixed connections.

Again, when looking at figure 4.36, it can be noted that the distribution of moments away from mid span causing a maximum increase of 80 % at the supports at 800 ˚C (Table 4.12). At this point the moments at the supports suddenly starts decreasing and the mid span moments start to increase at approximately 800 ˚C. It can be assumed that there is a redistribution of the loads to prevent failure as the moment capacity at the connection is reached. The reverse increase in moments is approximately equal to 20 % (Table 4.12).

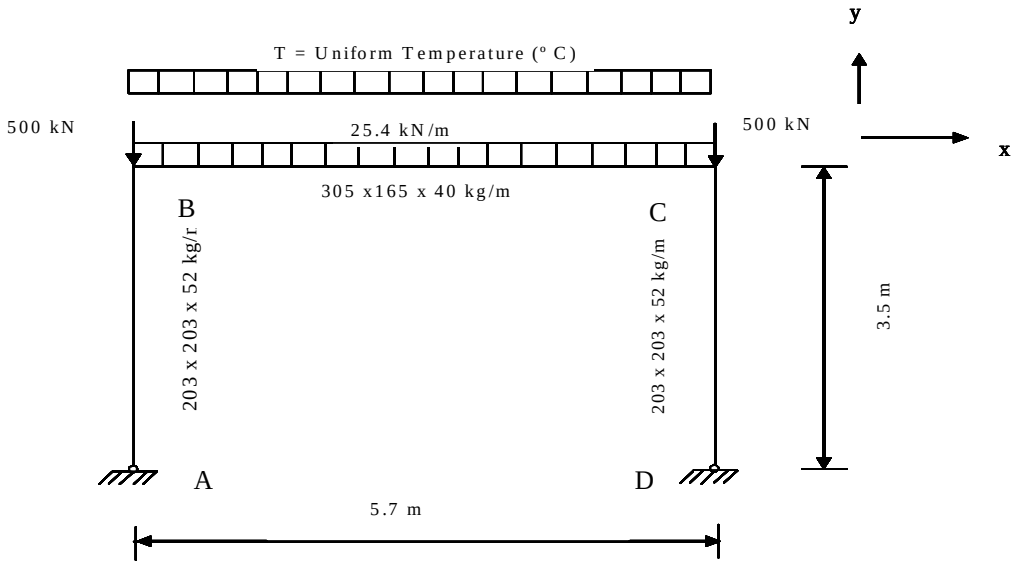

Figure 4.35: Model 8: Portal beam at various uniform temperatures

The column is however subjected to large moments caused by the horizontal thrust of the expanding beam. The column however, also redistributes the moments within itself so that it can be observed that a rather larger moment is developed in the base of the column (Figure 4.37) with an increase of 741 % as shown in table 4.12 for model 8. It can also be seen that the column deflection exceeds the L/300 serviceability deflection limit. Here L/300 = 11.67 mm, whereas the maximum deflection of the column is at 57.8 mm, equalling to an approximate increase of 11115 % due to temperature (Figure 4.38 and Table 4.12).

Once again, it can be seen that the beam y-deflection is reduced as the beam heats up. It can be taken that the cooler and stiffer joints are reducing the mid span deflections. However, at about 1000 ˚C the deflection in mid span increases dramatically to close to 40 mm, and exceeds the L/300 serviceability limit of 190 mm (Figure 4.39 and Table 4.12). The reverse percentage deflection increase is equal to 350 %, (Table 4.12).

By studying the buckling analysis, it can be seen that the strength of the portal frame at 1000 ˚ C is still at 42 % (figure 4.34) while the strength for the complete portal frame heated uniformly is only at 9.44%. The beam x-deflection is shown in figure 4.40 and ties up with the column deflection of 57.8 mm. The expansion of an unrestrained beam [40] is given by

$$\text{Expansion} = \alpha L T \qquad (4.3)$$

Where α the coefficient of expansion, L is the length of the beam and T is the difference between the temperatures of the heated member and the temperature of the member at room temperature, that is, 20 ˚ C.

The estimated thermal expansion from eqn 4.3, for this beam is 121.98 mm which is approximately twice the actual deflection shown in figure 4.40. Based on this observation, it can be assumed that the columns have played a major part in restraining the expansion of the beam. The output values for the beam moments, x-deflections, y-deflections and column moments are summarized in table 4.12.

Table 4.12: Summary of the results for model 8 (supports fixed in all directions) with beam subjected to uniform temperatures

		Values at 20 °C and percentage increase of values from ambient		Values at 100 °C and percentage increase of values from ambient		Values at 200 °C and percentage increase of values from ambient		Values at 300 °C and percentage increase of values from ambient		Values at 400 °C and percentage increase of values from ambient		Values at 500 °C and percentage increase of values from ambient		Values at 600 °C and percentage increase of values from ambient		Values at 700 °C and percentage increase of values from ambient		Values at 800 °C and percentage increase of values from ambient		Values at 900 °C and percentage increase of values from ambient		Values at 1000 °C and percentage increase of values from ambient	
		Value at Ambient(20 °C)	% Increase of value from ambient	Value at 100 °C	% Increase of value from ambient	Value at 200 °C	% Increase of value from ambient	Value at 300 °C	% Increase of value from ambient	Value at 400 °C	% Increase of value from ambient	Value at 500 °C	% Increase of value from ambient	Value at 600 °C	% Increase of value from ambient	Value at 700 °C	% Increase of value from ambient	Value at 800 °C	% Increase of value from ambient	Value at 900 °C	% Increase of value from ambient	Value at 1000 °C	% Increase of value from ambient
Beam moments (kNm)	Connection B	47.20	0.00	0.00	0.00	59.10	125.21	0.00	0.00	74.30	157.42	0.00	0.00	84.80	179.66		0.00	85.50	181.14		0.00	75.90	160.81
	Mid span	-56.00	0.00	0.00	0.00	-44.00	78.57	0.00	0.00	-28.90	51.61	0.00	0.00	-18.40	32.86		0.00	-17.70	31.61		0.00	-27.30	48.75
	Connection C	47.00	0.00	0.00	0.00	59.10	125.74	0.00	0.00	74.20	157.87	0.00	0.00	84.70	180.21		100.00	85.40	181.70		0.00	75.80	161.28
Column moment (kNm)	Support A	-24.93	0.00		0.00	-48.70	195.35		0.00	-81.24	325.87	0.00	100.00	-117.00	469.31	0.00	0.00	-152.90	613.32	0.00	0.00	-184.50	740.07
	Mid span	9.14	0.00		0.00	2.20	24.07		0.00	-7.80	-185.34	0.00	0.00	-21.70	-337.42	0.00	0.00	-40.40	-542.01	0.00	0.00	-61.50	-772.87
	Connection B	47.23	0.00		0.00	59.10	125.13		0.00	74.27	157.25	0.00	100.00	84.80	179.55	0.00	0.00	85.50	181.03	0.00	0.00	75.90	160.70
Beam Y-Deflections (mm)	Connection B	-1.10	0.00		0.00	-1.40	127.27		0.00	-1.31	119.09	0.00	100.00	-1.20	109.09	0.00	0.00	-1.10	100.00	0.00	0.00	-1.00	90.91
	Mid span	-10.91	0.00		0.00	-8.40	76.99		0.00	-4.88	44.73	0.00	0.00	-1.80	16.50	0.00	0.00	-1.60	14.67	0.00	0.00	-38.20	350.14
	Connection C	-1.10	0.00		0.00	-1.40	127.27		0.00	-1.31	119.09	0.00	100.00	-1.20	109.09	0.00	0.00	-1.10	100.00	0.00	0.00	-1.00	90.91
Column X-Deflections (mm)	Support A	0.00	0.00		0.00	0.00	0.00		0.00	0.00	0.00	0.00	0.00	0.00	0.00	0.00	0.00	0.00	0.00	0.00	0.00	0.00	100.00
	Mid span	-1.79	0.00		0.00	-4.19	234.08		0.00	-7.49	418.44	0.00	0.00	-11.25	628.49	0.00	0.00	-15.22	850.28	0.00	0.00	-18.93	1057.54
	Connection B	-0.52	0.00		0.00	-7.54	1450.00		0.00	-17.40	3346.15	0.00	100.00	-29.43	5659.62	0.00	0.00	-43.46	8357.69	0.00	0.00	-57.80	11115.38

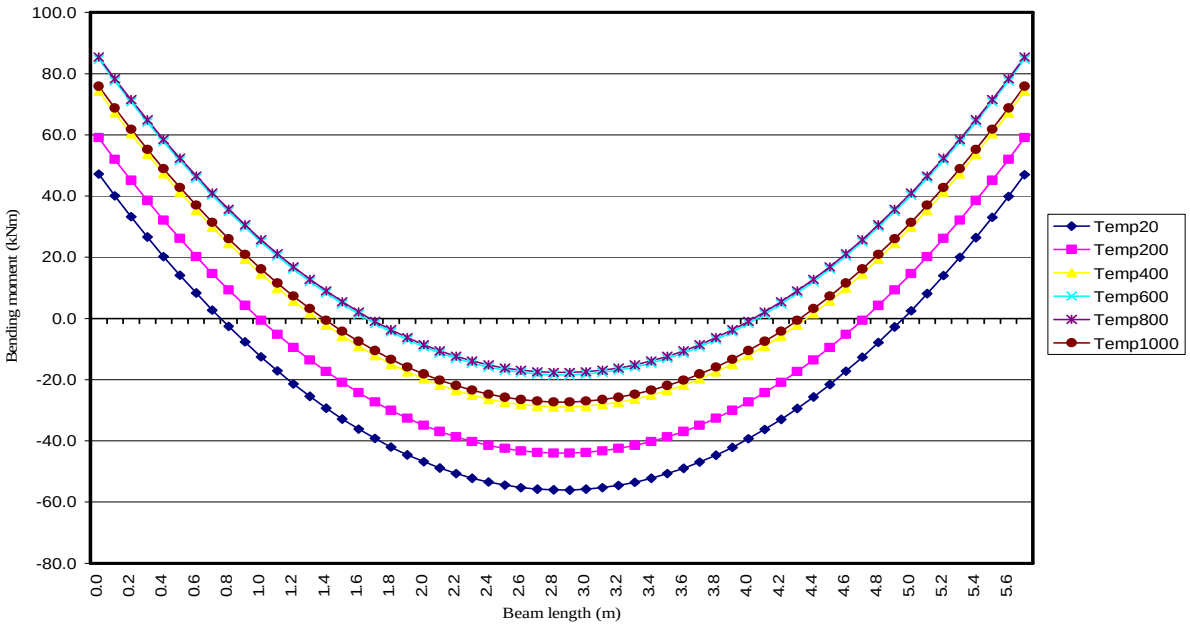

Figure 4.36: Portal beam moments for the portal beam at uniform temperatures

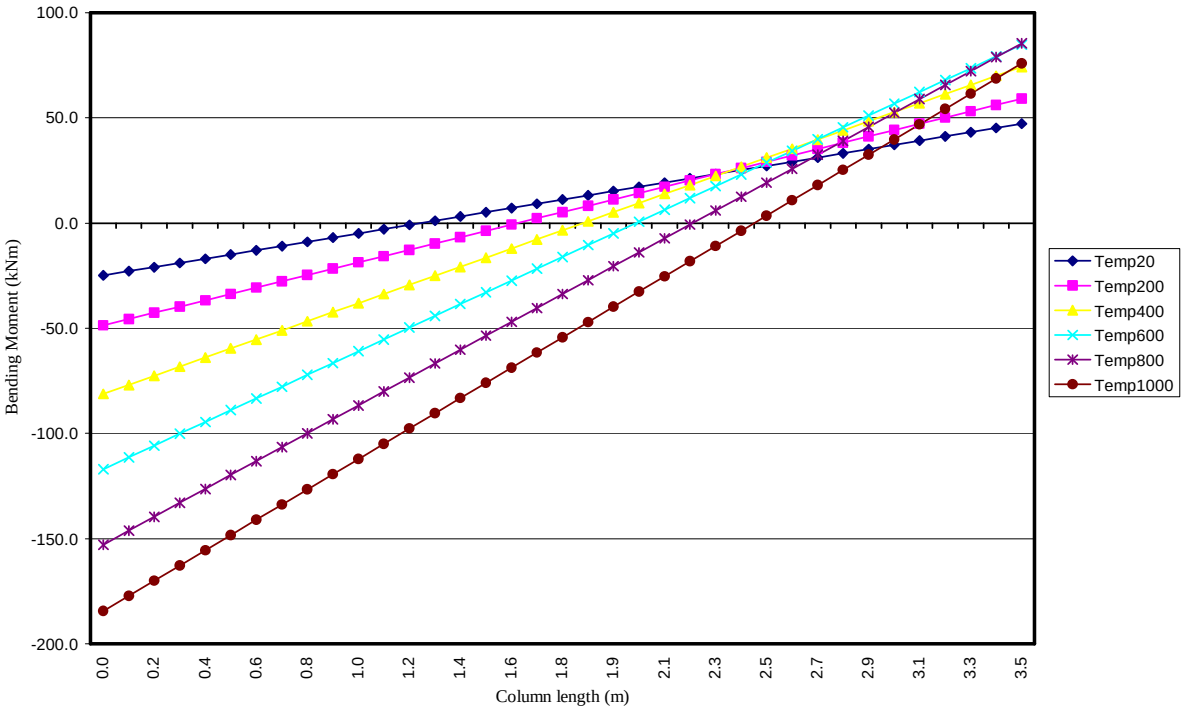

Figure 4.37: Portal column moments for the portal beam at uniform temperatures

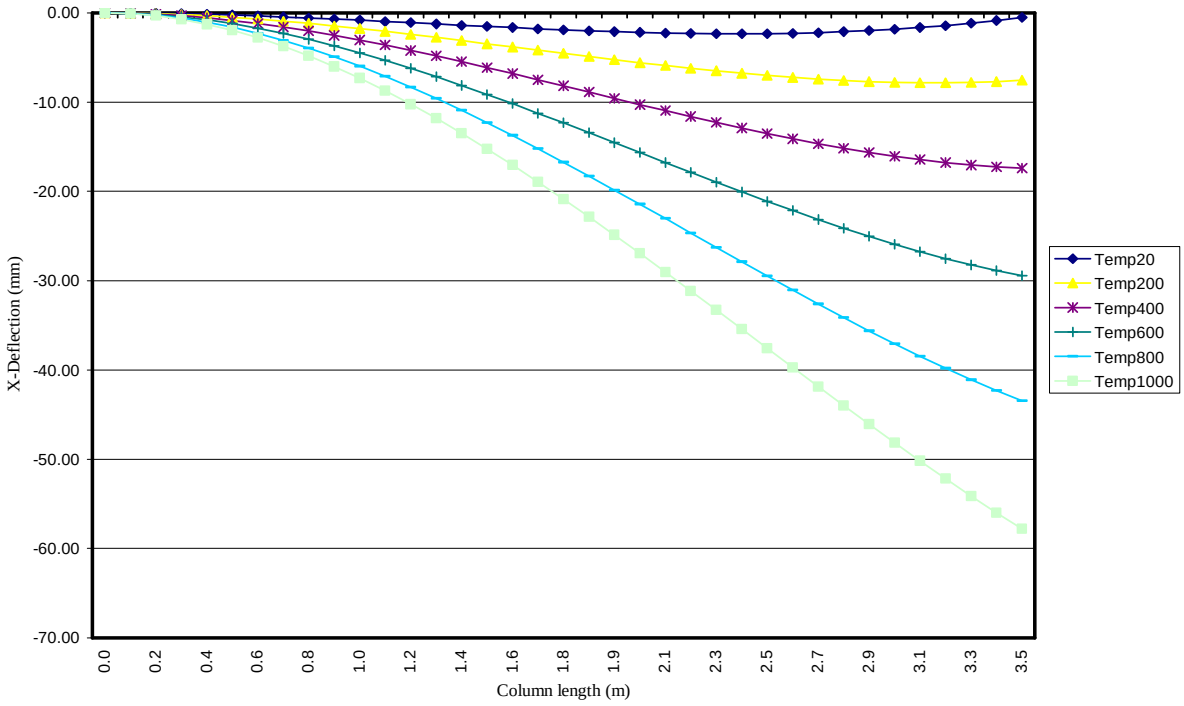

Figure 4.38: Portal column X-deflections for the portal beam at uniform temperatures

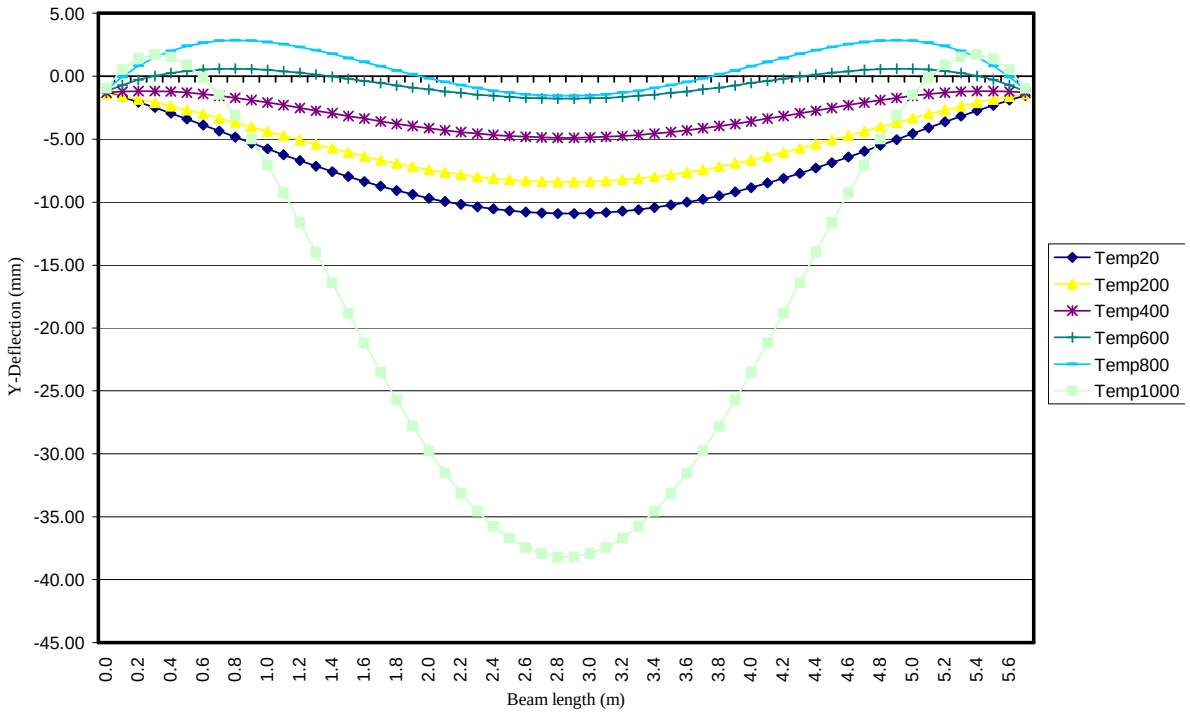

Figure 4.39: Portal beam Y-deflections for the portal beam at uniform temperatures

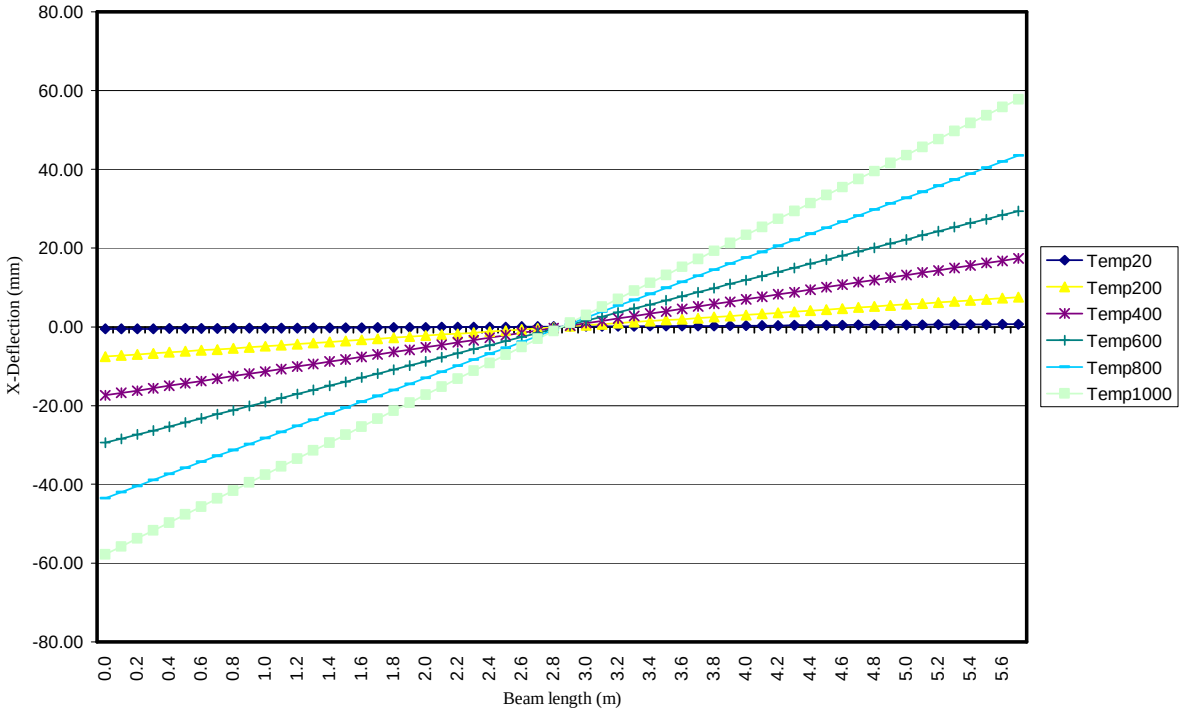

Figure 4.40: Portal beam X-deflections for the portal beam at uniform temperatures

4.4.4.3 Model 9: Column heated at various uniform temperatures

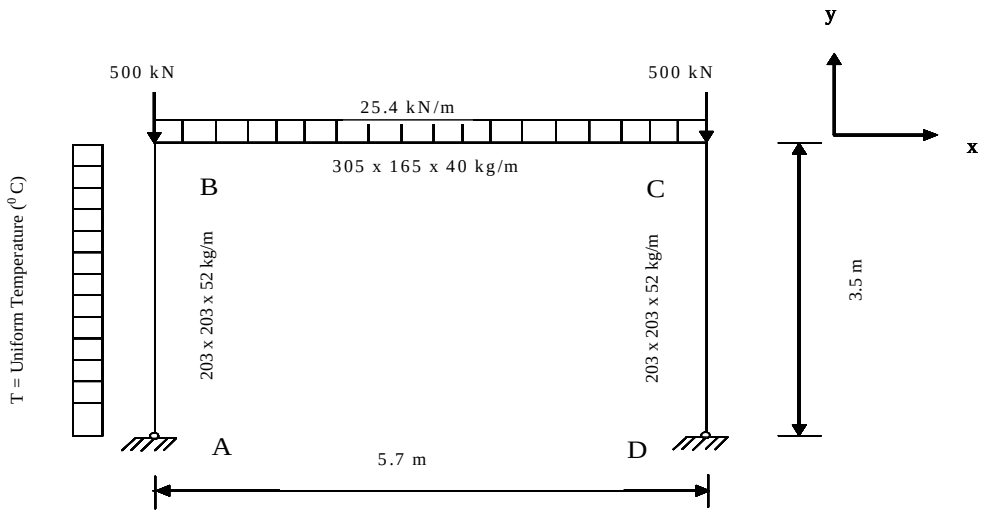

Figure 4.41: Model 9: Portal column at various uniform temperatures

In this case, the same portal frame was modelled with line segments for the columns and the beam. The hermitian beam elements were used to generate the 203 x 203 x 52 kg/m columns and the 305 x 165 x 41 kg/m beam (Figure 4.41). In total three element groups were generated as well as three isotropic linear elastic material models.

The values of Young's modulus and the coefficient of thermal expansion corresponding to the applied various uniform temperatures of the column line segments were assigned to the appropriate corresponding material model. In this case the column temperature was varied uniformly. The same portal frame with the same static loads and boundary conditions, beam sections, and so on, was used (Figure 4.41).

The beam moments, obtained from a static analysis, increased at mid span by 161 % and reduced at the right hand side (RHS) support by 76 % and 69 % at the left hand side support (Figure 4.42 and Table 4.13). It can be noted that the left hand side (LHS) support moment initially increased by 10 % up to 400 ˚C before being reduced to 31 %. This is a notable behaviour pattern, because so far there was distribution to the supports away from the mid span regions. There may be various explanations for this behaviour. One explanation may be that the heated column has a reduced moment capacity but still have sufficient axial capacity. The beam cannot redistribute its moments as it is not subjected to heat as is the case in models 7 and 8. The beam therefore behaves similar to a simply supported beam.

The other scenario could be that the vertically expanding column causes curvature in the beam member resulting in an increase in moments in the mid span of the beam. This additional

curvature causes a reduction in curvature at the supports, resulting in reduced moments at the beam-column connections.

In figure 4.43, it can be seen that the column expands vertically by the same amount that the beam deflects in the y- direction. The deflection at 0.0 meters, that is, LHS support, increases by -4815 % (upwards) while the deflection increases by 139 % (downwards) at the other end (Figure 4.43 and Table 4.13).

Furthermore, figure 4.44 shows that the column moment at the top reduces by 68 % and that the base moments reduced by 71 % (Table 4.13).

The column x-deflection, shown in figure 4.45 exhibits a notable pattern. It forms a half sine curve that later develops into a form that is about a 75% of a full sine curve. The column x-deflection at mid span has increased by – 540 % (outwards in the negative x-direction) while it increased by + 127 % (inwards in the positive x-direction) at the top (Figure 4.45 and Table 4.13).

The beam x-deflection is shown in figure 4.46 and it can be seen that the left hand side (LHS) of the graph goes from a positive to a negative deflection.

Table 4.13: Summary of the results for model 9 (supports fixed in all directions): LHS column subjected to uniform temperatures

		Values at 20 ºC and percentage increase of values from ambient		Values at 200 ºC and percentage increase of values from ambient		Values at 400 ºC and percentage increase of values from ambient		Values at 600 ºC and percentage increase of values from ambient		Values at 800 ºC and percentage increase of values from ambient		Values at 1000 ºC and percentage increase of values from ambient	
		Value at Ambient(20 ºC)	% Increase of value from ambient	Value at 200 ºC	% Increase of value from ambient	Value at 400 ºC	% Increase of value from ambient	Value at 600 ºC	% Increase of value from ambient	Value at 800 ºC	% Increase of value from ambient	Value at 1000 ºC	% Increase of value from ambient
Beam Moments (kNm)	Connection B	47.20	0.00	49.40	104.66	51.80	109.75	47.60	100.85	36.50	77.33	14.60	30.93
	Mid span	-56.00	0.00	-57.60	102.86	-58.90	105.18	-64.30	114.82	-74.30	132.68	-90.20	161.07
	Connection C	47.00	0.00	41.80	88.94	36.60	77.87	29.90	63.62	20.90	44.47	11.40	24.26
Column Moments (kNm)	Support A	-24.90	0.00	-19.40	77.91	-16.20	65.06	-15.41	61.89	-13.98	56.14	-7.17	28.80
	Mid span	9.10	0.00	15.00	164.84	17.80	195.60	16.09	176.81	11.27	123.85	3.70	40.66
	Connection B	45.20	0.00	49.40	109.29	51.80	114.60	47.60	105.31	36.53	80.82	14.57	32.23
Beam Y-Deflections (mm)	Connection B	-1.10	0.00	7.75	-804.55	19.64	-1885.45	33.50	-3145.45	48.22	-4483.64	51.87	-4815.45
	Mid span	-10.91	0.00	-6.69	61.32	-1.09	9.99	4.53	-141.52	9.46	-186.71	7.48	-168.56
	Connection C	-1.10	0.00	-1.53	139.09	-1.53	139.09	-1.53	139.09	-1.53	139.09	-1.53	139.09
Column X-Deflections (mm)	Support A	0.00	0.00	0.00	0.00	0.00	0.00	0.00	0.00	0.00	0.00	0.00	0.00
	Mid span	-1.79	0.00	1.24	-169.27	0.89	-149.72	1.43	-179.89	3.26	-282.12	7.88	-540.22
	Connection B	-0.52	0.00	-2.20	423.08	-4.76	915.38	-6.54	1257.69	-6.70	1288.46	-0.66	126.92

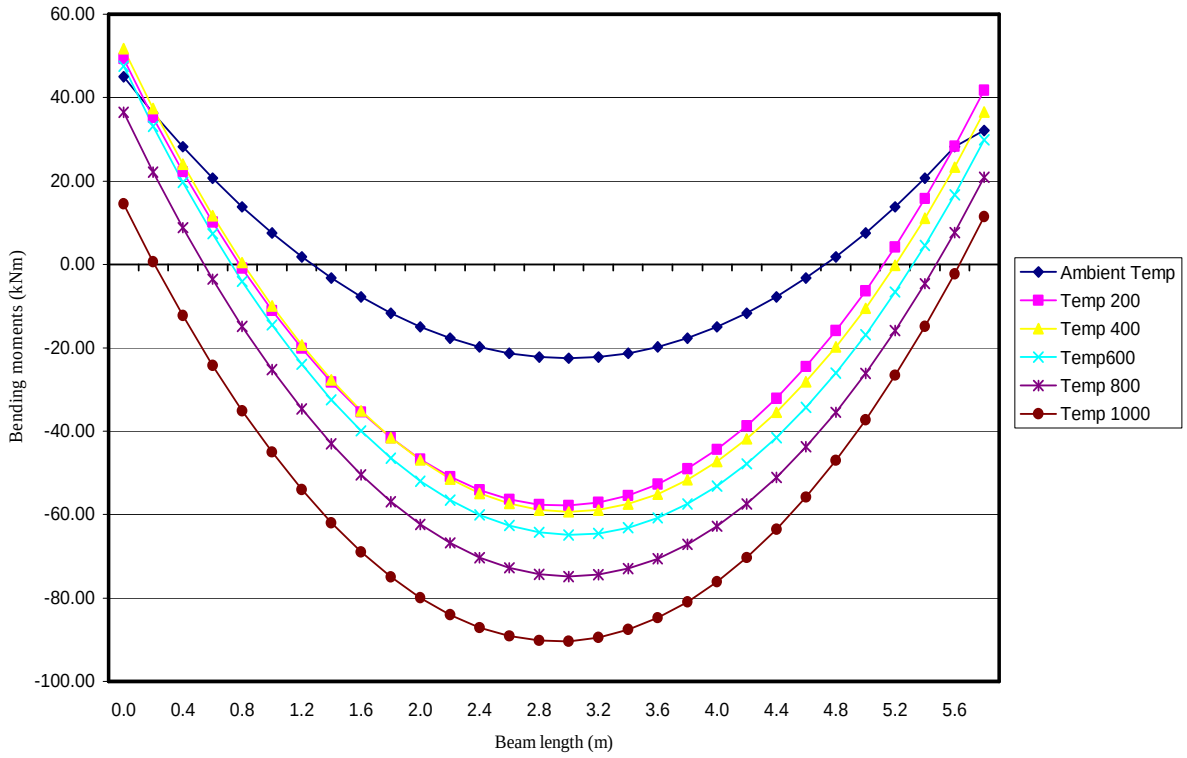

Figure 4.42: Portal beam moments for varying uniform LHS column temperatures

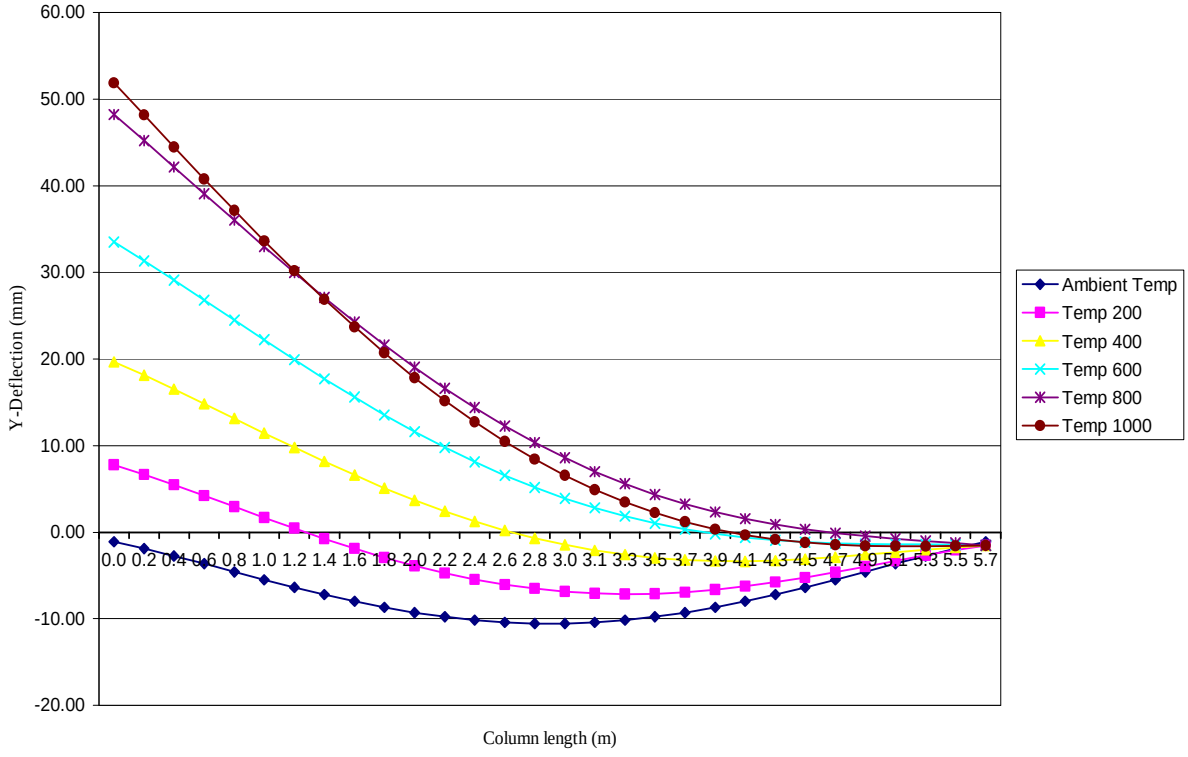

Figure 4.43: Portal beam Y-deflections for uniform LHS column temperatures

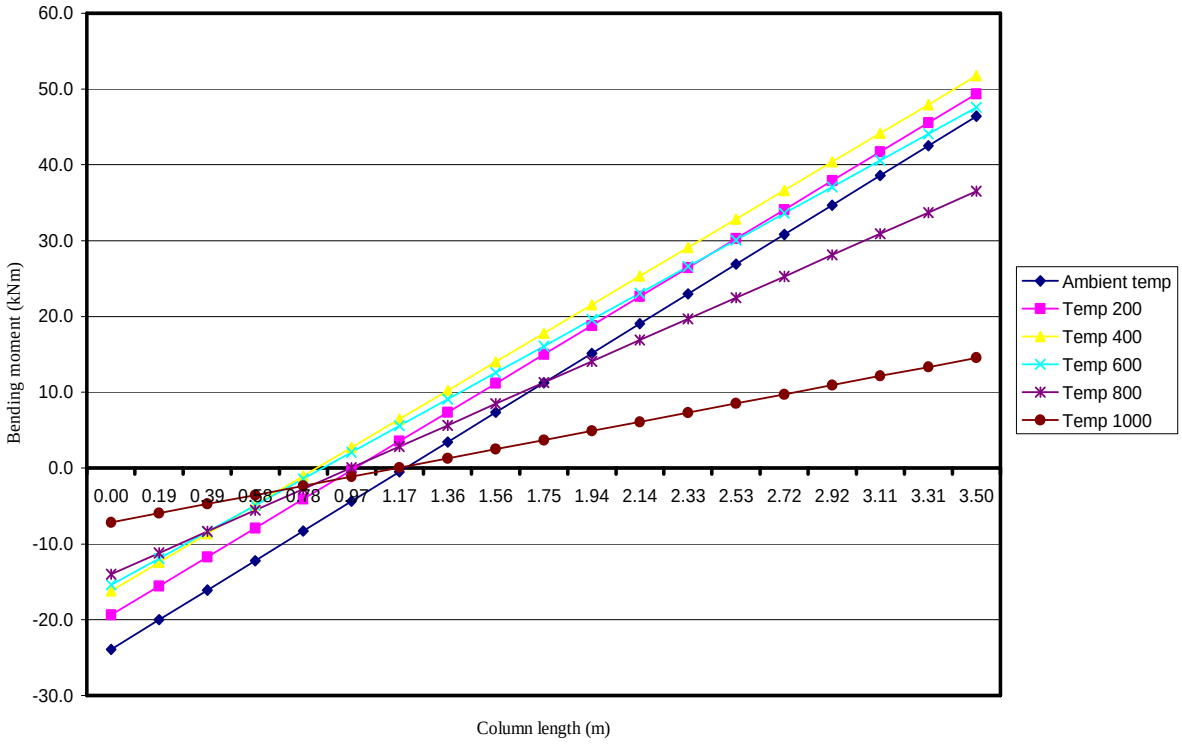

Figure 4.44: Portal column moments for uniform LHS column temperatures

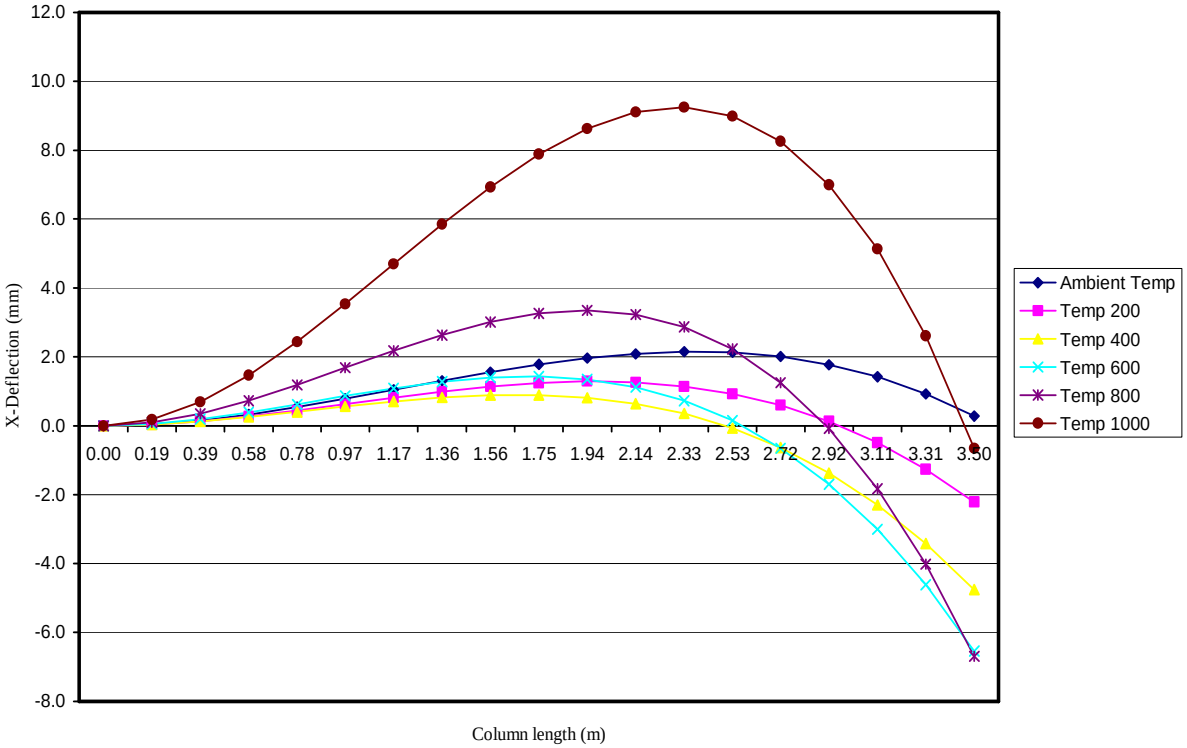

Figure 4.45: Portal column X-deflections for the LHS column at uniform temperatures

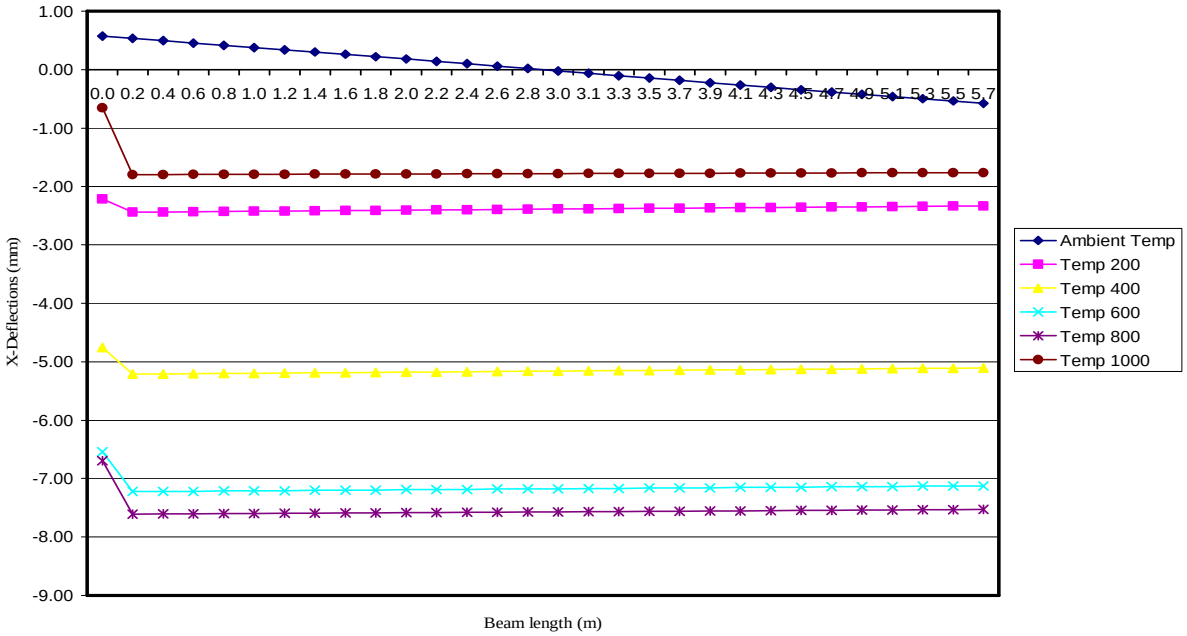

Figure 4.46: Portal beam X-deflections for the LHS column at uniform temperatures

4.4.4.4 Model 10: Various gradient heats applied along the beam length

The study on the portal frame is extended further by applying a temperature gradient along the beam only and keeping the columns constant except for allowing heat distribution of 7% to a third length of the LHS column top length (Figure 4.47). Table 4.14 lists the actual temperatures applied to the top third (1/3) length of the column.

The portal frame was modelled with line segments for the columns and the beam. The beam was modelled with six line segments and the LHS column was modelled with two segments while the RHS column was modelled with a single line segment. The hermitian beam elements were used to generate the 203 x 203 x 52 kg/m columns and the 305 x 165 x 41 kg/m beam (Figure 4.47).

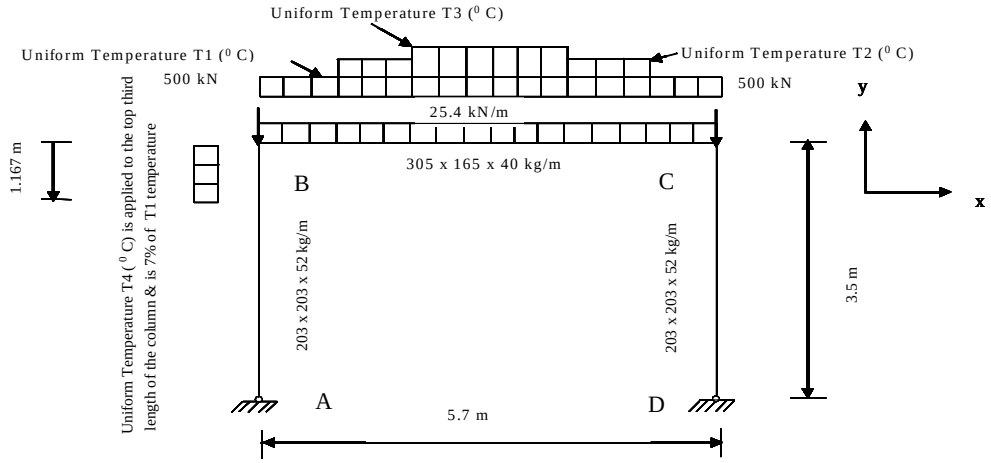

Figure 4.47: Model 10: Portal beam with temperature gradients along the beam length

Overall, five element groups were generated as well as five isotropic linear elastic material models. The values of Young's modulus and the coefficient of thermal expansion corresponding to the applied various uniform temperatures of the beam and column line segments were assigned to the appropriate corresponding material model. It can be seen in figure 4.47 that the same portal frame as model 9 was used with the same static loading; the supports are fixed as well.

It can once again be seen, that the mid span moments of the beam are reduced by 90 % and the support moments are increased by approximately 200 % (Figure 4.48). As can be seen in table 4.14, the magnitude of these values can have a negative impact on the structural integrity of the frame (Figure 4.48).

The column moments are once again increased by the axial thrust of the beam (approximately 210 % at the top and 567 % at the base of the column). The moments for this model are shown in table 4.14 and will impact negatively on the structural integrity of the frame (Figure 4.49). Figure 4.50 indicates the extent of the column x-deflection or lateral deflection. The percentage deflection increase is approximately 7340 % from ambient (Table 4.14).

Figure 4.51 shows that the beam mid span has a downwards deflection at low temperatures but changes to an upwards deflection at temperatures above approximately 800 º C. This indicates a reverse bowing effect. The reverse deflection percentage of 127 % is a notable value and can influence the durability of the frame and the actual development is seen in table 4.14. The beam x-deflection (Figure 4.52) also increased by approximately 7340 % due to temperature increase. The temperature gradient however has reduced both the beam and column deflections compared to the deflections of the portal frames in models 7 and 8 in which the beams were subjected to uniform temperature increases (Tables 4.11, 4.12 and 4.14).

Figure 4.53 shows the deterioration of the frame for a temperature gradient along the beam for heat increments of approximately 100 ˚ C up to 1000 ˚ C. It can be seen that the remaining strength of the frame is still approximately 77 % (Figure 4.53) while the remaining strength of the portal frame (model 8) with the beam subjected to uniform temperature increases is at 42 %(Figure 4.34) .

Table 4.14: Summary of the results for model 10 (supports fixed in all directions): beam subjected to gradient temperatures

		Values at 20 °C and percentage increase of values from ambient		Values at 95 °C and percentage increase of values from ambient		Values at 190 °C and percentage increase of values from ambient		Values at 286 °C and percentage increase of values from ambient		Values at 381 °C and percentage increase of values from ambient		Values at 476 °C and percentage increase of values from ambient		Values at 571 °C and percentage increase of values from ambient		Values at 667 °C and percentage increase of values from ambient		Values at 762 °C and percentage increase of values from ambient		Values at 857 °C and percentage increase of values from ambient		Values at 952 °C and percentage increase of values from ambient	
		Value at Ambient(20 °C)	% Increase of value from ambient	Value at 95 °C	% Increase of value from ambient	Value at 190 °C	% Increase of value from ambient	Value at 286 °C	% Increase of value from ambient	Value at 381 °C	% Increase of value from ambient	Value at 476 °C	% Increase of value from ambient	Value at 571 °C	% Increase of value from ambient	Value at 667 °C	% Increase of value from ambient	Value at 762 °C	% Increase of value from ambient	Value at 857 °C	% Increase of value from ambient	Value at 952 °C	% Increase of value from ambient
Beam moments	Connection B	47.20	0.00			55.20	116.95			66.70	141.31			79.90	169.28			91.50	193.86			98.90	209.53
(kNm)	Mid span	-56.00	0.00			-47.90	85.54			-36.40	65.00			-23.30	41.61			-12.10	21.61			-5.90	10.54
	Connection C	47.00	0.00			55.20	117.45			66.70	141.91			79.80	169.79			90.60	192.77			95.60	203.40
Column moment	Support A	-24.93	0.00			-40.00	160.45			-62.30	249.90			-87.82	352.27			-115.07	461.57			-141.30	566.79
(kNm)	Mid span	9.14	0.00			6.00	65.65			0.40	4.38			-6.36	-169.58			-14.71	-260.94			-27.90	-405.25
	Connection B	47.20	0.00			55.20	116.95			66.70	141.31			79.93	169.34			91.55	193.96			98.90	209.53
Beam	Connection B	-1.10	0.00			-1.36	123.64			-1.31	119.09			-1.25	113.64			-1.20	109.09			-0.81	73.64
Y-Deflections	Mid span	-10.91	0.00			-9.31	85.33			-7.10	65.08			-4.70	43.08			-1.40	12.83			2.94	-126.95
(mm)	Connection C	-1.10	0.00			-1.36	123.64			-1.31	119.09			-1.25	113.64			-1.20	109.09			-1.33	120.91
Column	Support A	0.00	0.00			0.00	0.00			0.00	0.00			0.00	0.00			0.00	0.00			0.00	0.00
X-Deflections	Mid span	-1.79	0.00			-3.76	210.06			-6.29	351.40			-9.24	516.20			-12.47	696.65			-15.46	863.69
(mm)	Connection B	-0.52	0.00			-4.81	925.00			-11.30	2173.08			-19.04	3661.54			-27.77	5340.38			-38.17	7340.38

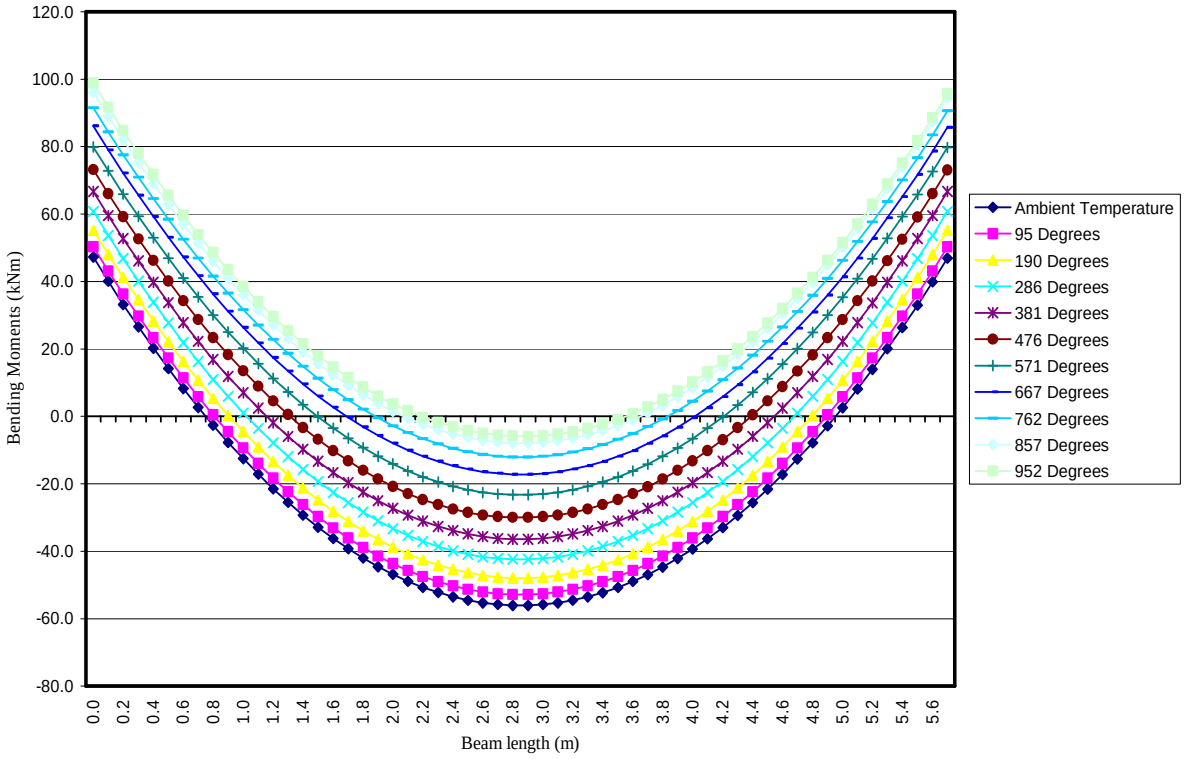

Figure 4.48: Portal beam moments for the beam at gradient temperatures along the length

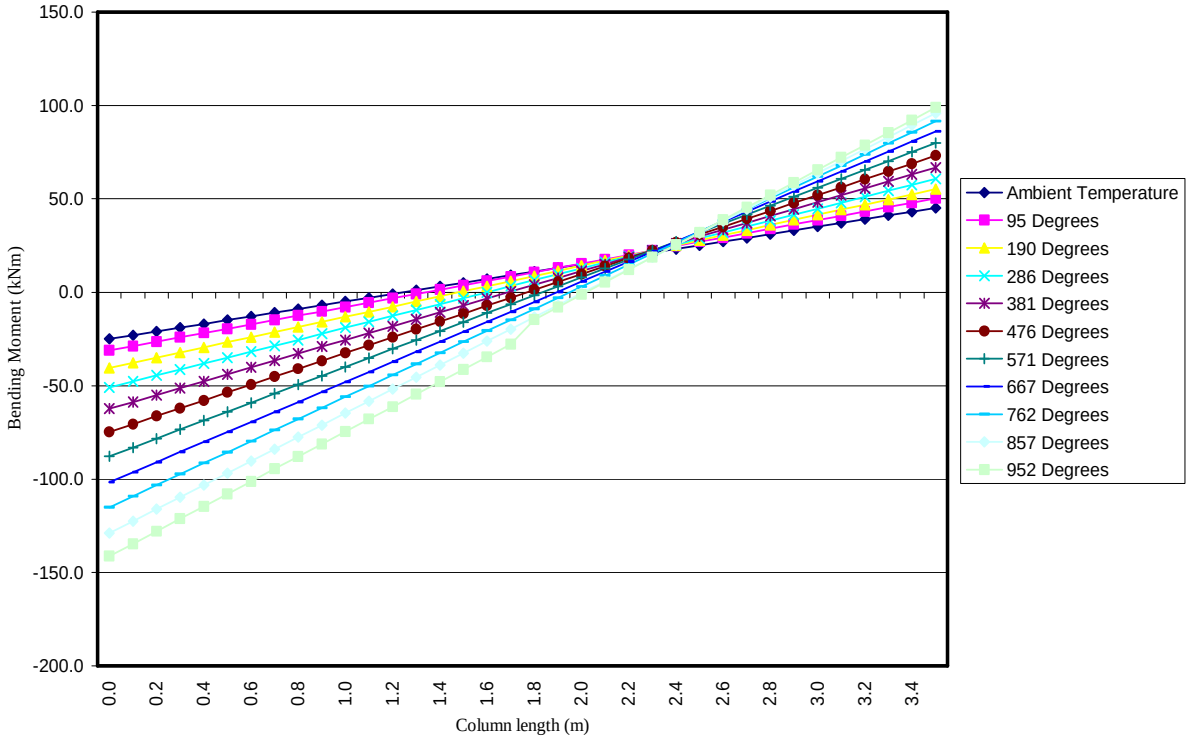

Figure 4.49: Portal column moments for the beam at gradient temperatures along the length

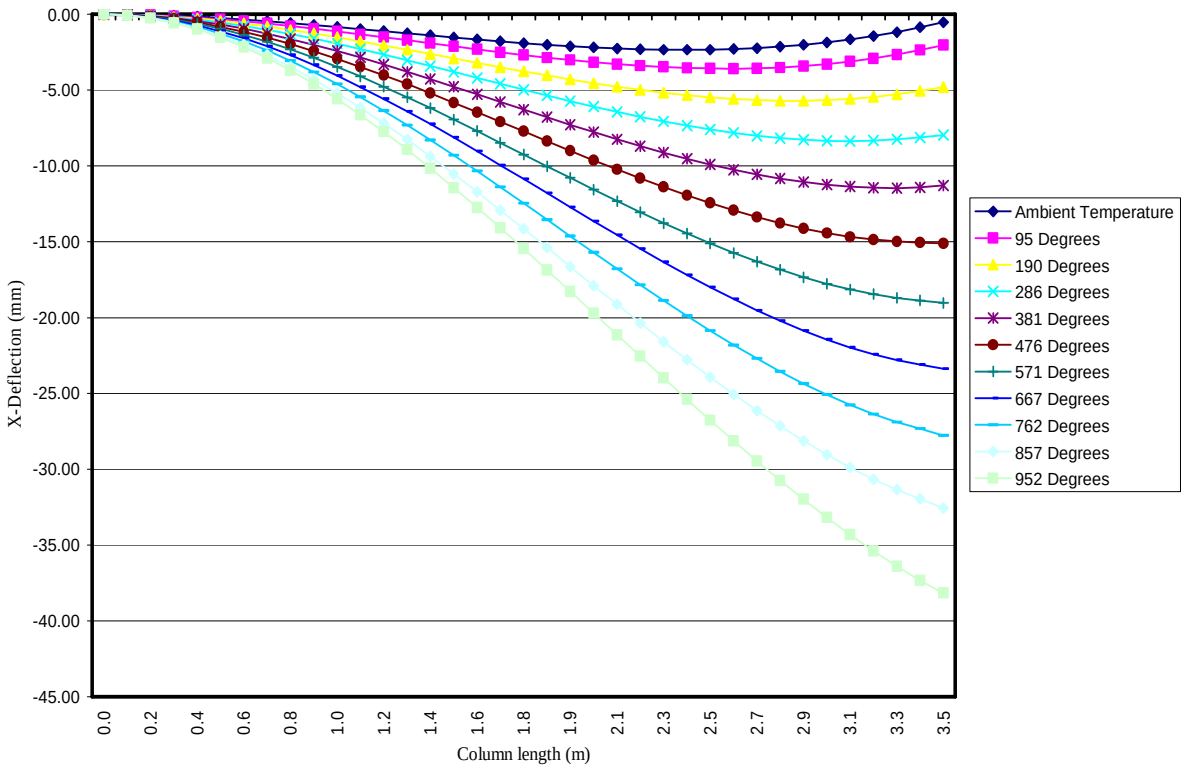

Figure 4.50: Portal column X-deflections for the beam at gradient temperatures along the length

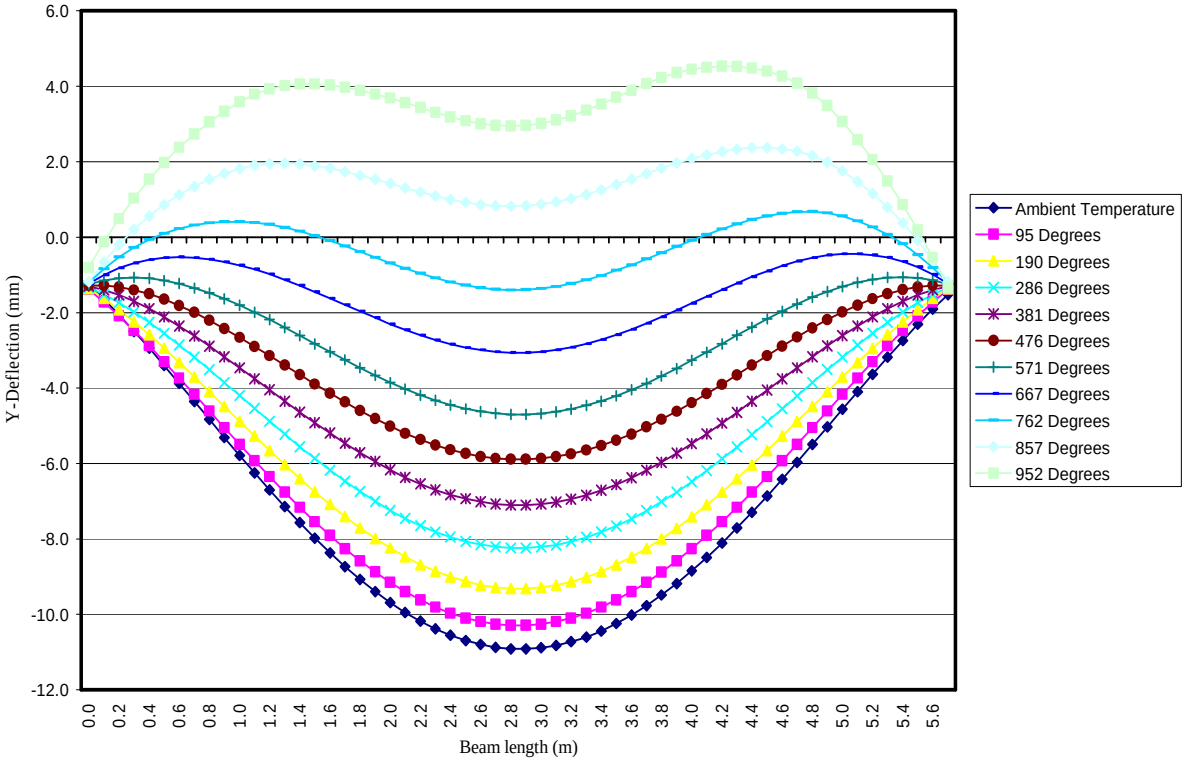

Figure 4.51: Portal beam Y-deflections for the beam at gradient temperatures along the length

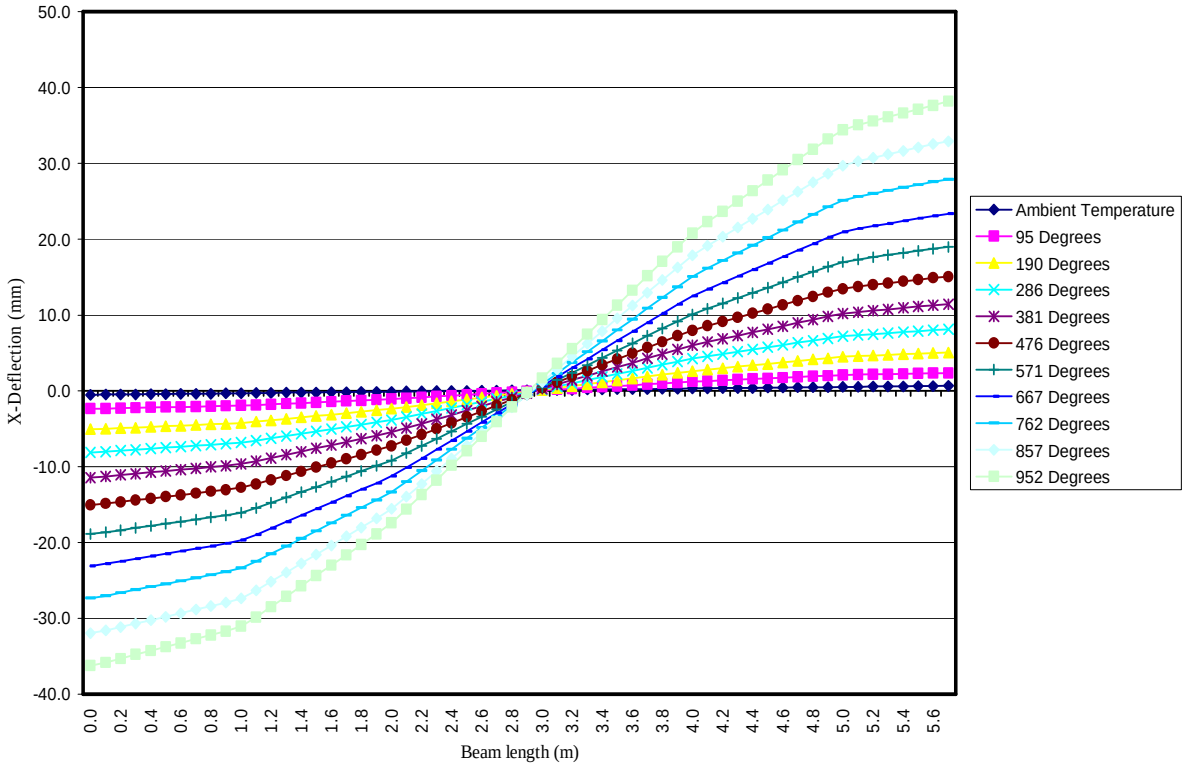

Figure 4.52: Portal beam X-deflections for the beam at gradient temperatures along the length

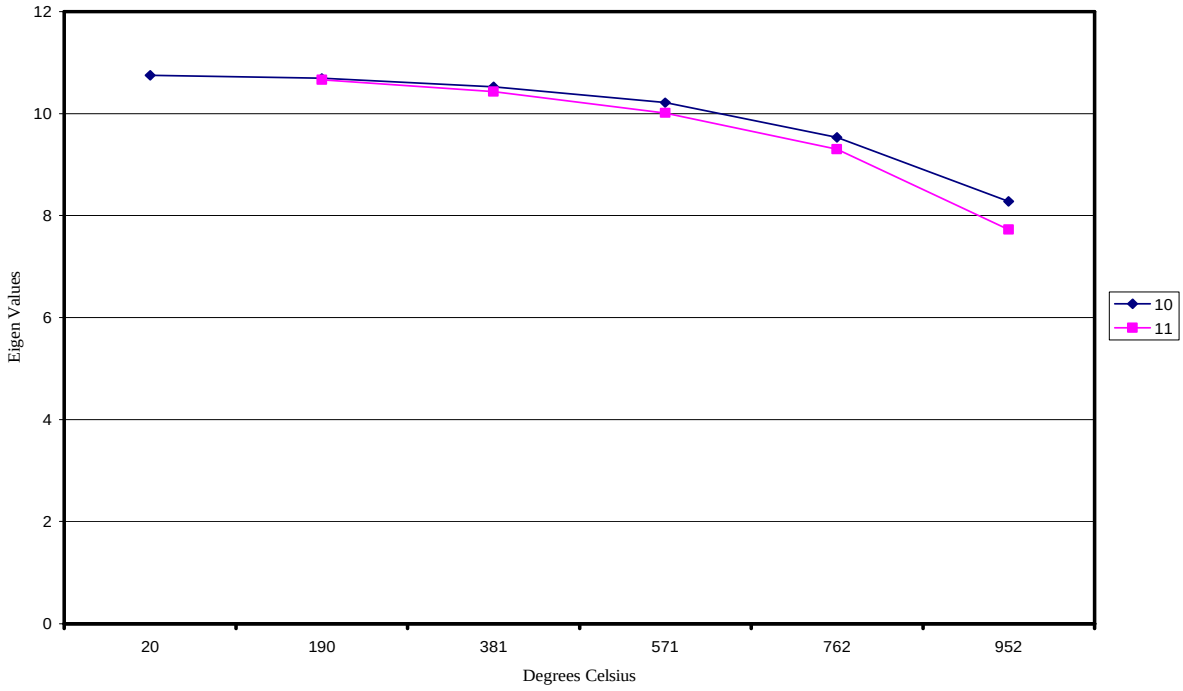

Figure 4.53: Eigen buckling values for the portal frame models 10 & 11

4.4.4.5 Model 11: Gradient heats applied along the LHS column length

The same portal frame with the exact physical dimensions were modelled with line segments for the 305 x 165 x 41 kg/m and 203 x 203 x 52 kg/m beam and column sections respectively (Figure 4.54).

The column was divided into three segments while the beam was divided into two segments. The hermitian beam element group was assigned to the line segments in order to generate the 305 x 165 x 41 kg/m and 203 x 203 x 52 kg/m beam and column sections respectively. An isotropic linear elastic material model was generated for each of the beam or column line segments sharing the same material and cross sectional properties. In this case, it was necessary to generate five material models and five element groups. The supports of the frame were fixed in all degrees of freedom and the beam-column connections were modelled as fixed connections.

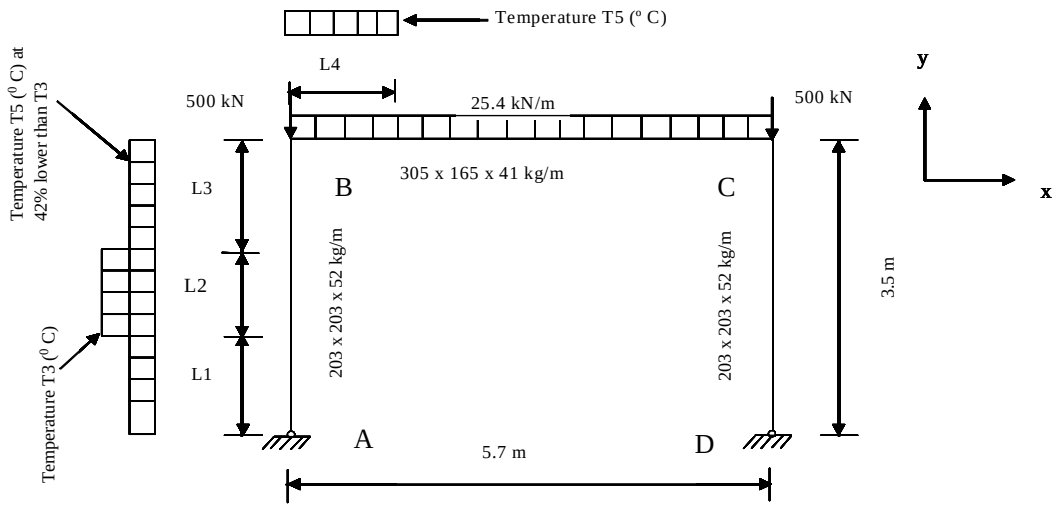

Figure 4.54: Model 11: Portal column with temperature gradients along the length

The values of Young's modulus and the coefficient of thermal expansion corresponding to the applied various uniform temperatures of the beam and column line segments were assigned to the appropriate corresponding material model (Figure 4.54). For this frame, a temperature gradient was applied to the LHS column only. The segment L2 was modelled at the same temperature as for the beam mid span at T3 and the segments L1 and L3 were modelled at 42% lower than T3. For the beam gradient temperature model and values for T3, respectively (Figure 4.4 and Table 4.3). Table 4.15 lists the temperatures used for the column and beam segments.

It can be seen that there is a downward distribution of beam moments at the LHS and RHS column supports of approximately 10 % and 34 % (Figure 4.55 and Table 4.16). Figure 4.56 shows that the moment at the top of the RHS column increases by 10 % up to approximately 600 ˚C and then reduces by approximately 19 % up to 1000 ˚ C. The total decrease in moment is approximately 10 %. The same tendency applies to the base of the column with a decrease of approximately 25 % up to 600 ˚ C and an increase of 29 % afterwards up to 1000 ˚ C (Figure 4.56 and Table 4.16). The column therefore, is distributing its load to the beam mid span.

The column x-deflection is depicted in figure 4.57 and exhibits a half sine profile with a total increase in deflection at mid height of 185 % inwards and a outwards deflection of approximately -1625 % at the top (Figure 4.57 and Table 4.16). The actual deflection is small (8 mm) when compared to the portal frame of model 7 (Figure 4.29) with the uniform temperature increase for all members (90 mm) and compared to the portal frame models with different

heating regimes. This could mainly be due to the portal beam acting as a tie-beam in this case except for model 9 (Figure 4.45) in which the column only was heated uniformly.

Table 4.15: A list of the gradient temperatures that were applied to the LHS column, temperature for L4 and apply to other figures as well.

Segment	Length (m)	Temperature Type	Temperature Range (º C)	Comment
L1	1.167	T5	55 to 545	42% of mid span temperature i.e. temperature for segment L2
L2	1.167	T3	95 to 952	
L3	1.167	T5	55 to 545	
L4	1.167	T6	23.9 to 58.2	Beam segment closest to the support modeled at 7% of L1 plus 20 º C (ambient temperature)
T3	Refers to figures 4.4, 4.11, 4.18, 4.25, 4.47 & 4.54 and to table 4.4			
T5 & T6	Refers to figure 4.54			

The beam y-deflection is shown in figure 4.58 and table 4.16. The beam experiences an upward vertical deflection due to the expansion of the column. This increase of deflection is in the order of approximately 3535 % at 1000 ˚C compared to the ambient temperature (Table 4.16).

The beam x-deflection is slightly restraint by the heated column that is forced outwards and downwards by mainly the axial load. It can be seen in figure 4.59 and table 4.16 that the beam however experiences very little expansion in the order of 8.5 mm (185 % compared to the ambient temperature). Compared to the deflections for the heated beams of model 8 (Figure 4.40) and model 10 (Figure 4.52), this deflection is very small.

Table 4.16: Summary of the results for model 11 (supports fixed in all directions): LHS column subjected to gradient temperatures

		Values at 20 ºC and percentage increase of values from ambient		Values at 200 ºC and percentage increase of values from ambient		Values at 400 ºC and percentage increase of values from ambient		Values at 600 ºC and percentage increase of values from ambient		Values at 800 ºC and percentage increase of values from ambient		Values at 1000 ºC and percentage increase of values from ambient	
		Value at Ambient(20 ºC)	% Increase of value from ambient	Value at 200 ºC	% Increase of value from ambient	Value at 400 ºC	% Increase of value from ambient	Value at 600 ºC	% Increase of value from ambient	Value at 800 ºC	% Increase of value from ambient	Value at 1000 ºC	% Increase of value from ambient
Beam Moments (kNm)	Connection B	47.20	0.00	48.60	102.97	50.80	107.63	51.70	109.53	49.90	105.72	42.70	90.47
	Mid span	-56.00	0.00	-57.00	101.79	-57.40	102.50	-58.50	104.46	-60.90	108.75	-66.10	118.04
	Connection C	47.00	0.00	43.60	92.77	40.50	86.17	37.30	79.36	34.20	72.77	31.20	66.38
Column Moments (kNm)	Support A	-24.90	0.00	-21.00	84.34	-19.00	76.31	-18.60	74.70	-21.20	85.14	-26.20	105.22
	Mid span	9.10	0.00	11.80	129.67	14.00	153.85	14.60	160.44	12.40	136.26	6.30	69.23
	Connection B	47.20	0.00	48.60	102.97	50.80	107.63	51.70	109.53	49.90	105.72	42.70	90.47
Beam Y-Deflections (mm)	Connection B	-1.10	0.00	4.51	-510.00	11.88	-1180.00	20.38	-1952.73	29.71	-2800.91	37.78	-3534.55
	Mid span	-10.91	0.00	-8.22	75.34	-4.58	41.98	-0.53	-95.14	3.62	-133.18	6.46	-159.21
	Connection C	-1.10	0.00	-1.53	139.09	-1.52	138.18	-1.52	138.18	-1.52	138.18	-1.52	138.18
Column X-Deflections (mm)	Support A	0.00	0.00	0.00	0.00	0.00	0.00	0.00	0.00	0.00	0.00	0.00	0.00
	Mid span	-1.79	0.00	-1.36	75.98	-1.12	62.57	-1.10	61.45	-1.60	89.39	-3.32	185.47
	Connection B	-0.52	0.00	1.39	-367.31	3.14	-703.85	5.13	-1086.54	7.14	-1473.08	7.93	-1625.00

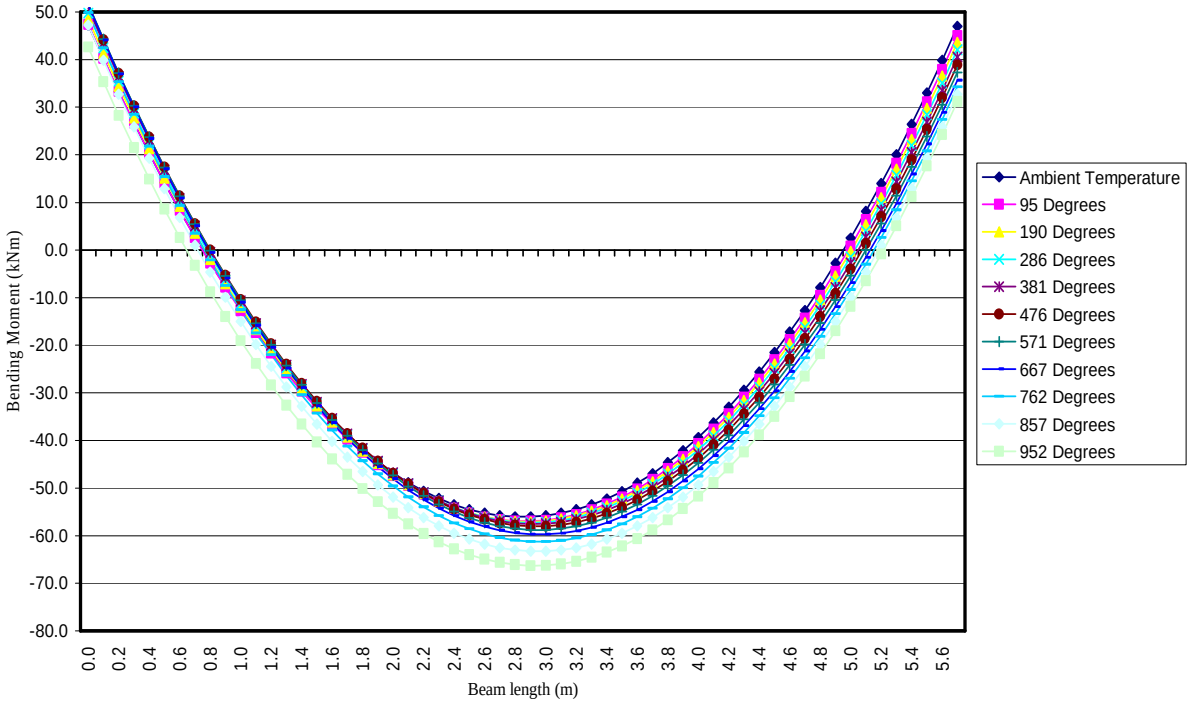

Figure 4.55: Portal beam moments for the column at gradient temperatures along the length

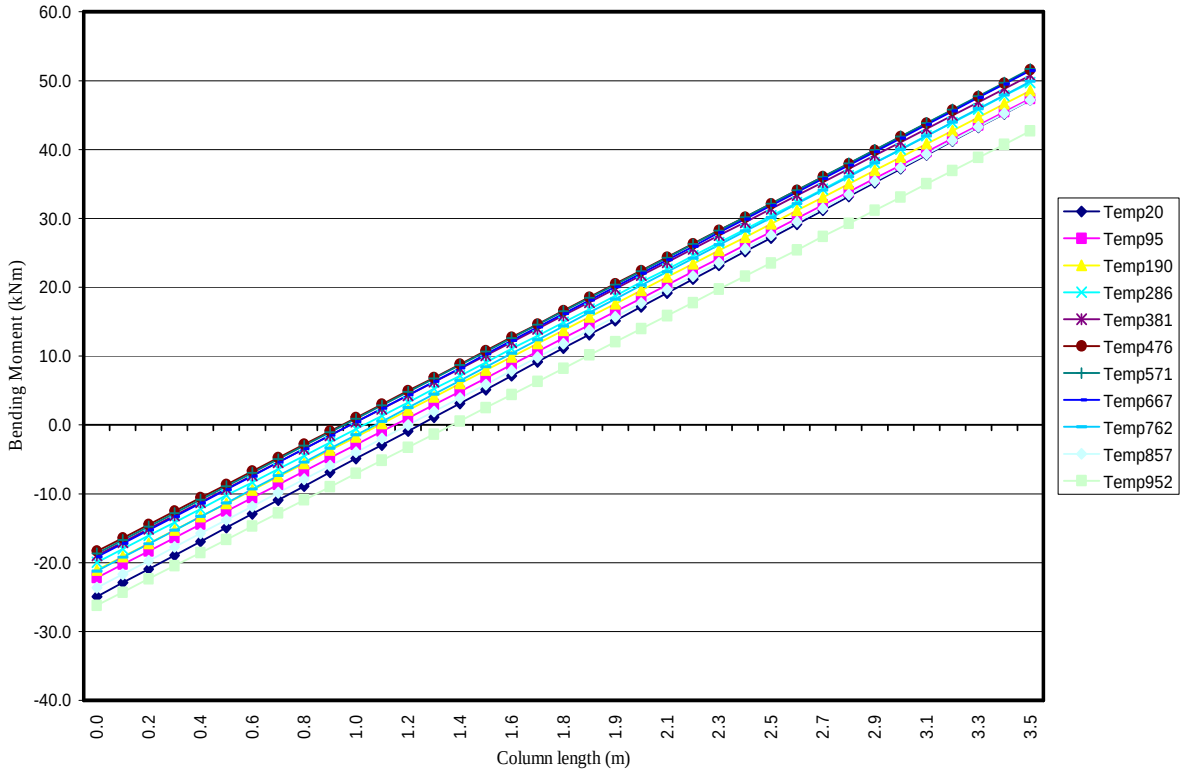

Figure 4.56: Portal column moments for the column at gradient temperatures along the length

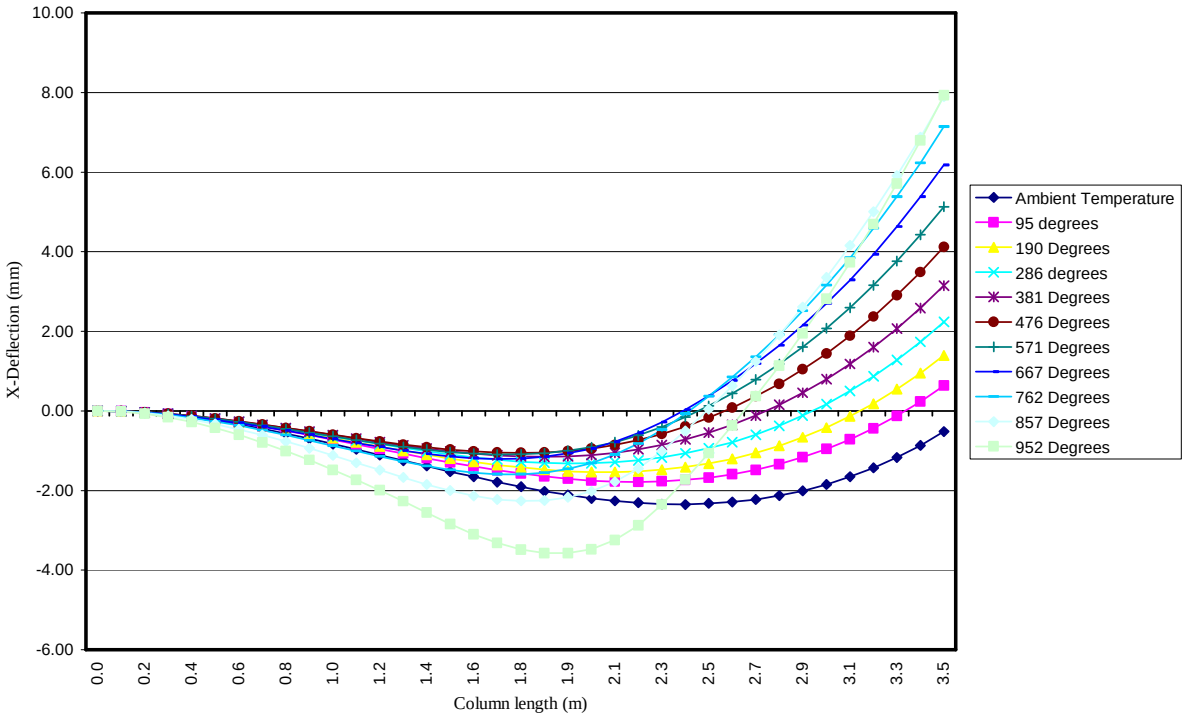

Figure 4.57: Portal Column X-deflections for the column at gradient temperatures along the length

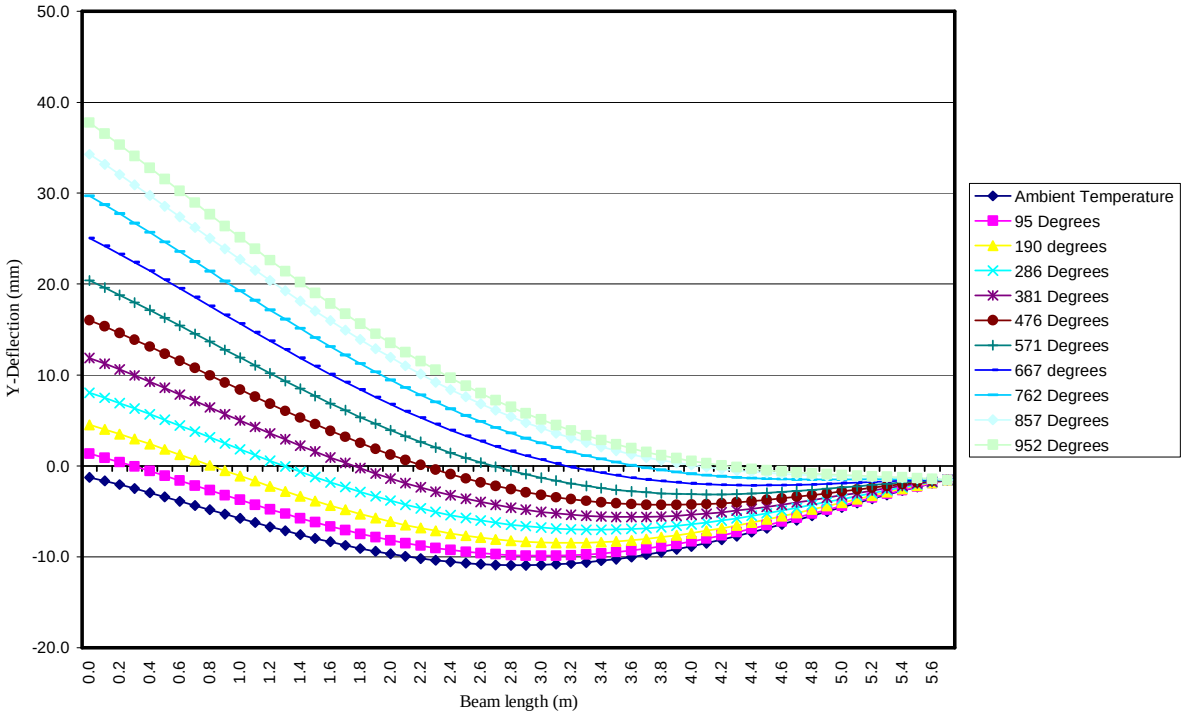

Figure 4.58: Portal beam Y-deflections for the column at gradient temperatures along the length

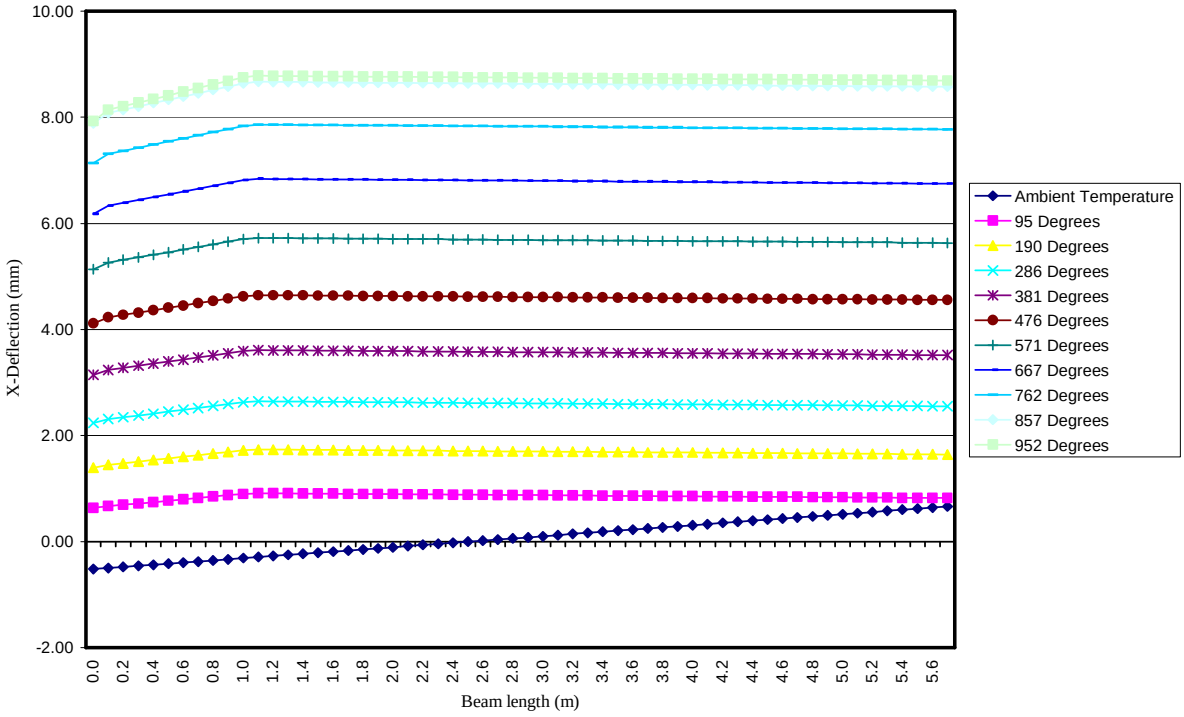

Figure 4.59: Portal beam X-deflections for the column at gradient temperatures along the length

4.4.5 Multi-Storey Frame

4.4.5.1 Model 12: All members of lower LHS compartment heated uniformly

To take the investigations further, a multi-storey frame, three bays with two storeys, was included. The first bay, bottom left hand side, marked ‘Bay 1’was considered as a fire compartment (Figure 4.60). Firstly, all the columns and the floor beam is uniformly heated and each member considered as heated on all four sides. All beams are 5.5 m long and made up of 305 x 165 x 41 kg/m I-beam sections while the columns are 3 m high made up of 203 x 203 x 52 H-column sections. A uniformly distributed load of 25.4 kN/m was applied to all beams with point loads of 75.5 kN and 151 kN (Figure 4.60).

The model was generated with line segments for each column and beam. The hermitian beam elements were used to generate the column and beam sections. For this frame, a total of four element groups and two isotropic linear elastic material models were generated. All the supports and beam-column connections were modelled as fixed.

The values of Young's modulus and the coefficient of thermal expansion corresponding to the applied various uniform temperatures of the beam and column line segments were assigned to the appropriate corresponding material model.

In figure 4.61 and table 4.17 it can be seen that the maximum bending moments are located at the beam-column connections, with the minimum bending moments in the span. The moments in the span is only slightly increased by 21 % up to approximately 800 ˚C and then decreases by 13 % up to 1000 ˚C. The moment at the external beam-column connections is increased by 364 % up to 600 ˚ C before it drops to 169 % up to 1000 ˚ C (Table 4.17). At the internal connection the moments increase by 225 % up to 800 ˚ C before it drops by 11 %. It can be seen that the moments are distributed to both supports (fixed joints) until joints reach capacity limits, for example, internal and external joints.

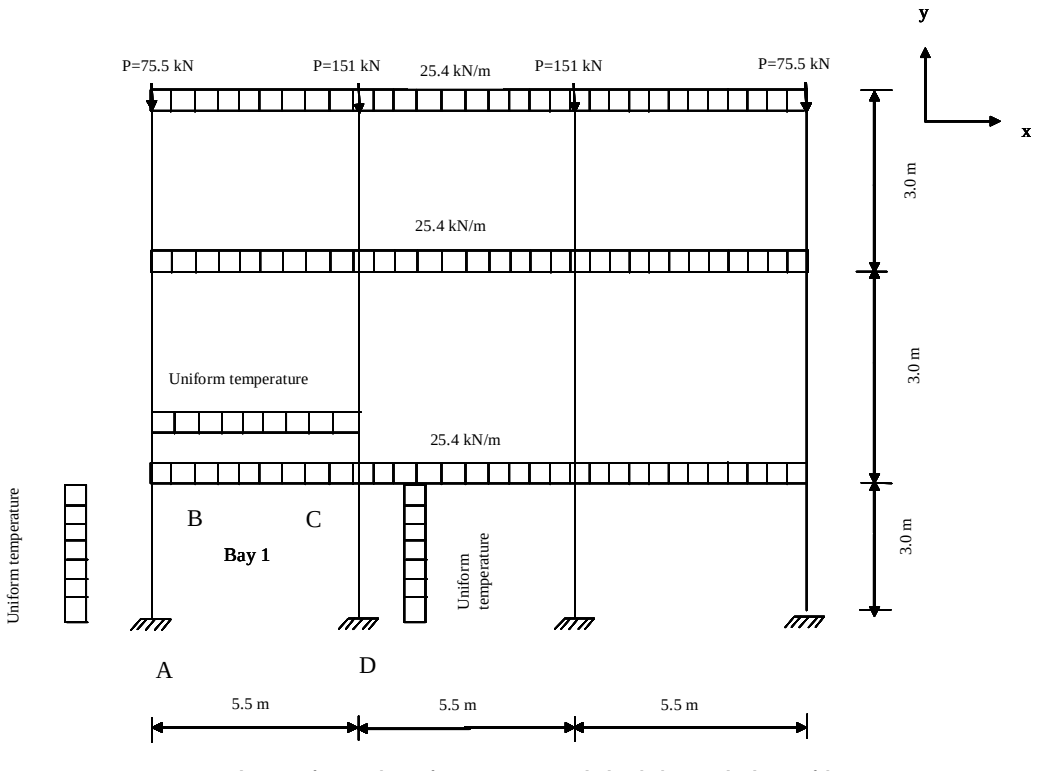

Figure 4.60: Model 12: Multi Storey frame with a uniform temperature applied to the beam and columns of Bay 1

The moment at the top of the external column increased by 387 % and follows exactly the same profile of the joint moments (Figure 4.62 and Table 4.17). It can be seen in figure 4.63 that the column x-deflection of ± 107 mm exceeds the serviceability limit of L/300 (3000/300 = 10 mm) by approximately 100 mm.

The beam y-deflection shows the same tendency as in the portal frame models 8 and 10. The deflection is once again upwards and increases by - 469 % from ambient up to 600 ˚ C before it reduces to a downwards deflection of + 550 % up to 1000 ˚ C (Figure 4.64 and Table 4.17). However, the deflections are just within the serviceability limit of L/300 = 18.3 mm for the downwards deflections but exceeds this limit by approximately 14.5 mm for the upwards deflections (Figure 4.64 and Table 4.17). The beam x-deflection is the most severe at the external joint of the frame (Figure 4.65). It can be seen in figure 4.66 that the strength of the frame reduces to 22.7% at 1000 ˚C of its strength at ambient temperature.

Table 4.17: Summary of the results for model 12 (supports fixed in all directions): beams & column of bay subjected to uniform temperatures

		Values at 20 ºC and percentage increase of values from ambient		Values at 200 ºC and percentage increase of values from ambient		Values at 400 ºC and percentage increase of values from ambient		Values at 600 ºC and percentage increase of values from ambient		Values at 800 ºC and percentage increase of values from ambient		Values at 1000 ºC and percentage increase of values from ambient	
		Value at Ambient(20 ºC)	% Increase of value from ambient	Value at 200 ºC	% Increase of value from ambient	Value at 400 ºC	% Increase of value from ambient	Value at 600 ºC	% Increase of value from ambient	Value at 800 ºC	% Increase of value from ambient	Value at 1000 ºC	% Increase of value from ambient
Beam Moments (kNm)	Connection B	49.00	0.00	84.70	172.86	154.60	315.51	192.30	392.45	178.30	363.88	82.70	168.78
	Mid span	-36.90	0.00	-34.70	94.04	-34.30	92.95	-39.90	108.13	-44.60	120.87	-39.90	108.13
	Connection C	69.50	0.00	78.40	112.81	97.80	140.72	126.90	182.59	156.30	224.89	148.50	213.67
Column Moments (kNm)	Support A	-16.60	0.00	-75.40	454.22	-143.10	862.05	-170.00	1024.10	-147.70	889.76	-64.30	387.35
	Mid span	5.10	0.00	4.60	90.20	5.80	113.73	11.10	217.65	15.30	300.00	9.20	180.39
	Connection B	49.00	0.00	84.70	172.86	154.60	315.51	192.30	392.45	178.30	363.88	82.70	168.78
Beam Y-Deflections (mm)	Connection B	0.07	0.00	7.40	10471.43	17.77	25285.71	30.26	43128.57	44.57	63571.43	56.17	80142.86
	Mid span	-5.04	0.00	2.48	-149.21	12.07	-339.48	18.62	-469.44	16.84	-434.13	-32.77	550.20
	Connection C	-0.64	0.00	6.56	-1125.00	16.63	-2698.44	28.19	-4504.69	39.93	-6339.06	39.96	-6343.75
Column X-Deflections (mm)	Support A	0.00	0.00	0.00	0.00	0.00	0.00	0.00	0.00	0.00	0.00	0.00	0.00
	Mid span	-1.02	0.00	-5.63	551.96	-12.66	1241.18	-23.59	2312.75	-40.26	3947.06	-65.04	6376.47
	Connection B	-0.93	0.00	-10.18	1094.62	-23.76	2554.84	-42.40	4559.14	-67.33	7239.78	-100.00	10752.69

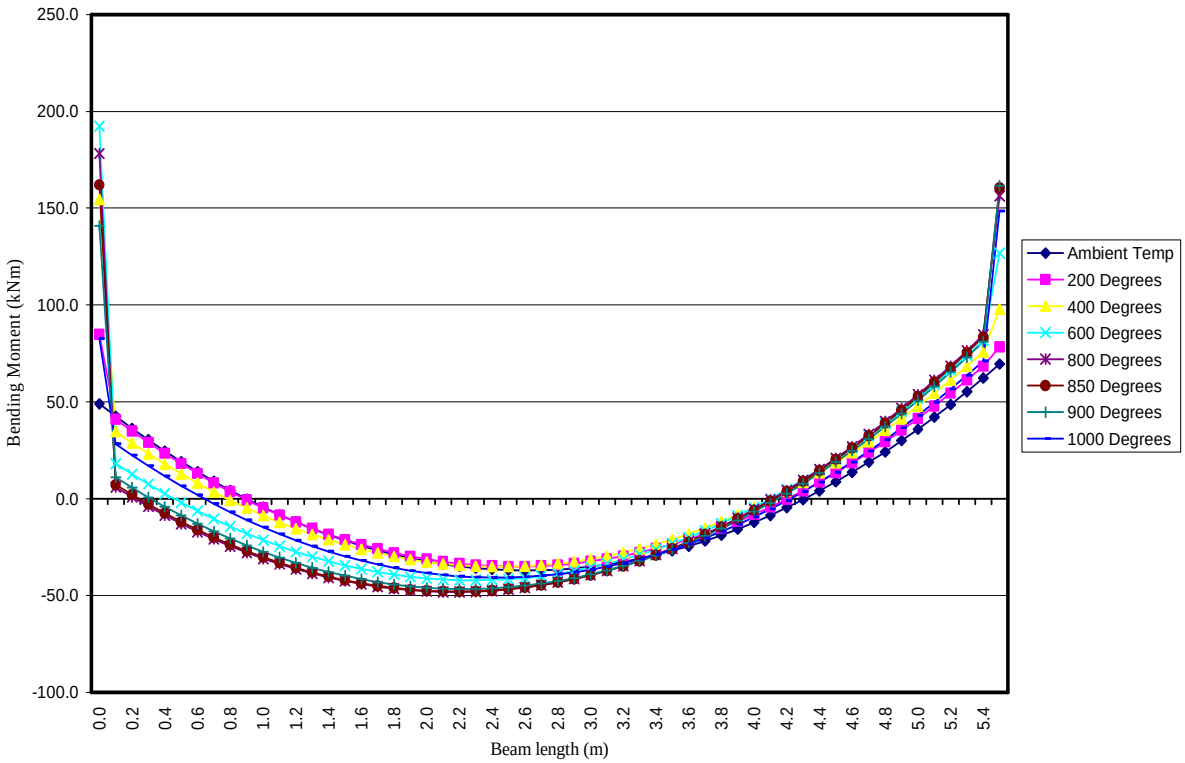

Figure 4.61: M/storey beam moments for the beam and columns at uniform temperatures

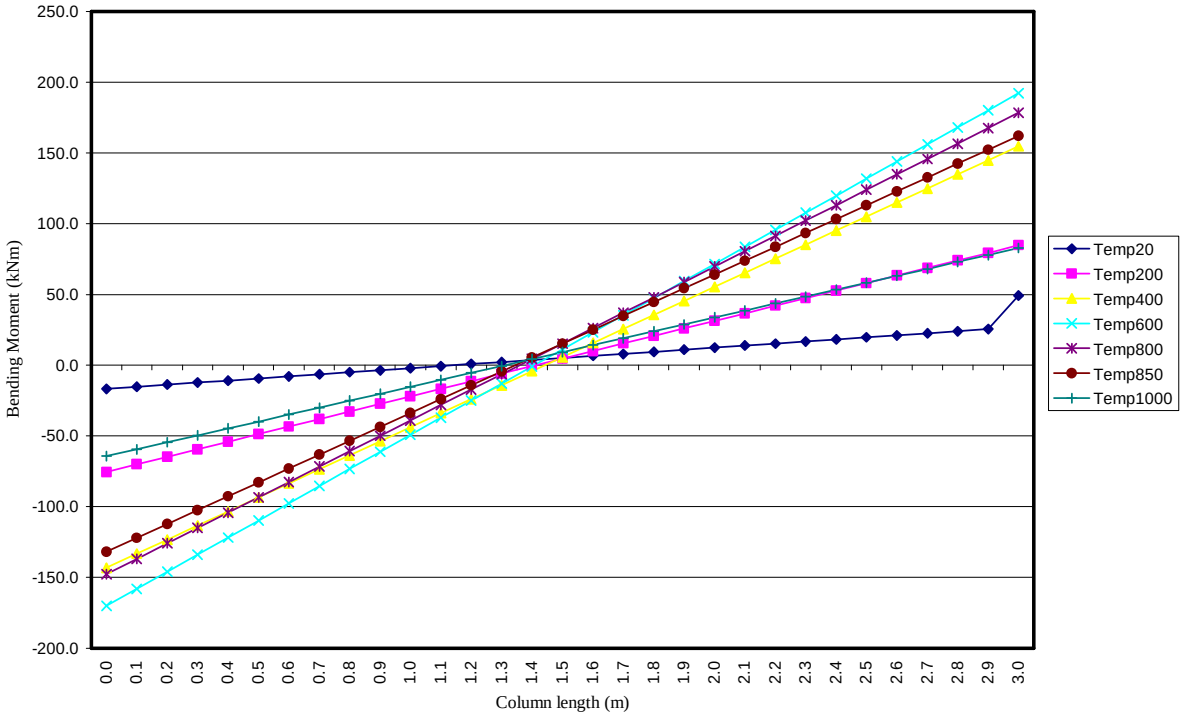

Figure 4.62: M/storey column moments for the beam & columns at uniform temperatures

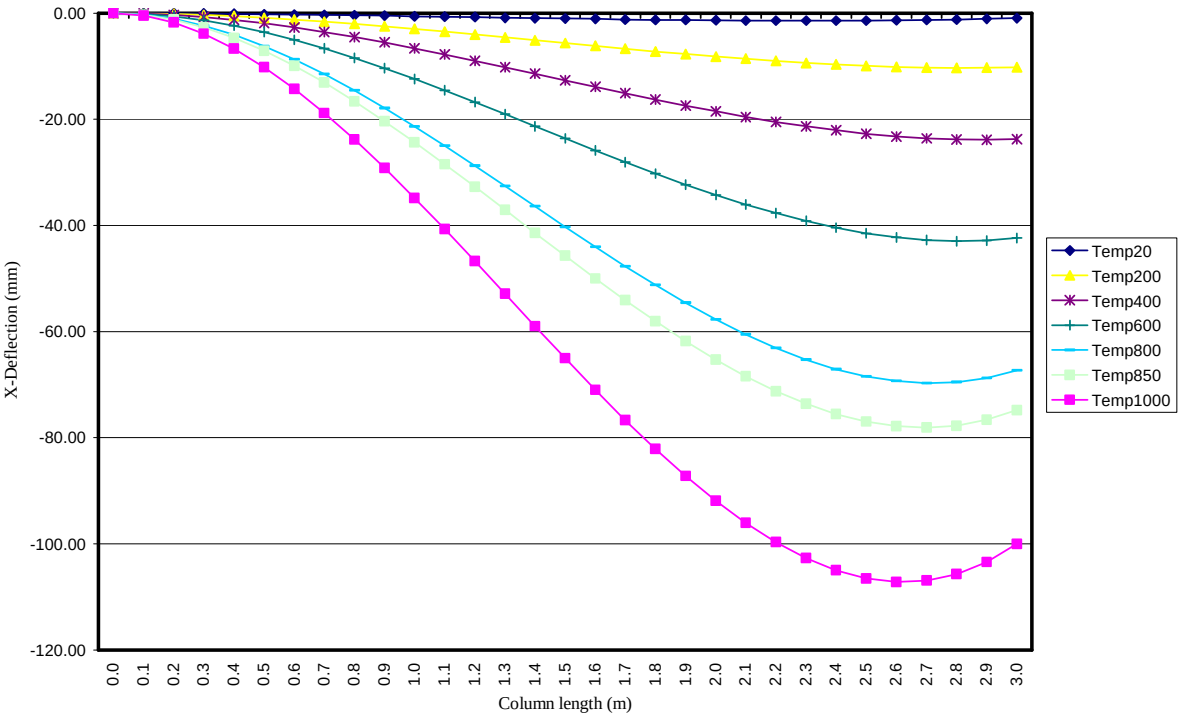

Figure 4.63: M/storey column X-deflections for the beam & columns at uniform temperatures

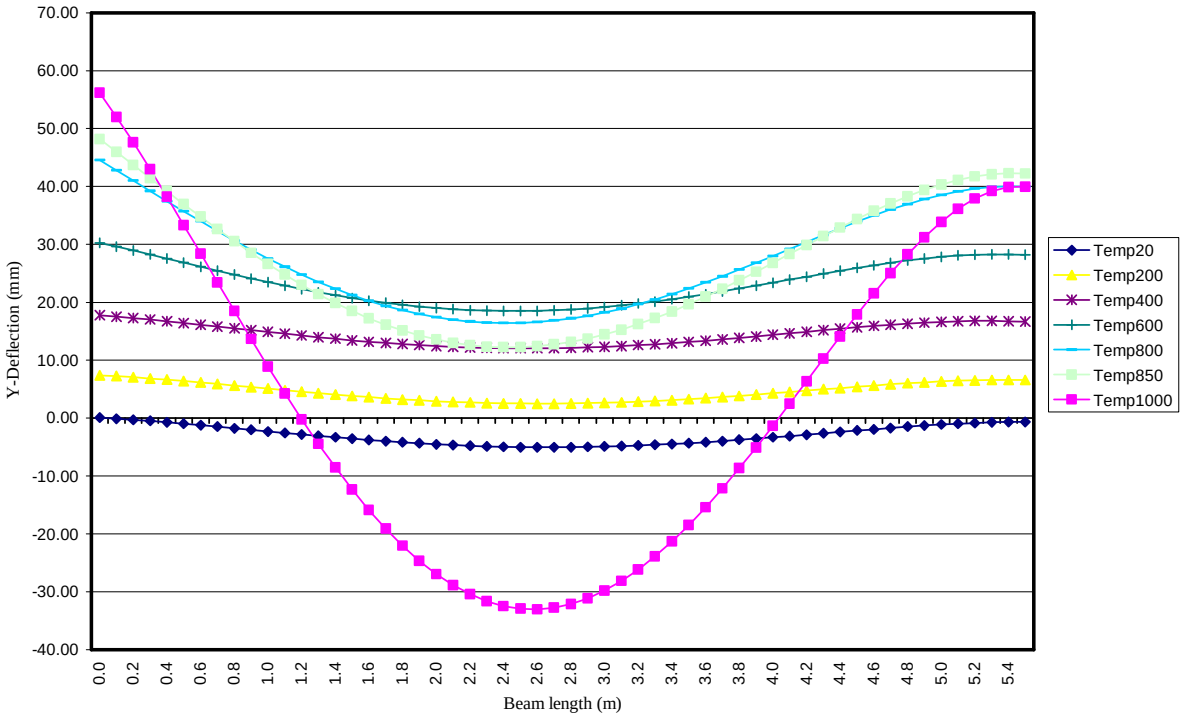

Figure 4.64: M/storey beam Y-deflections for the beam & columns at uniform temperatures

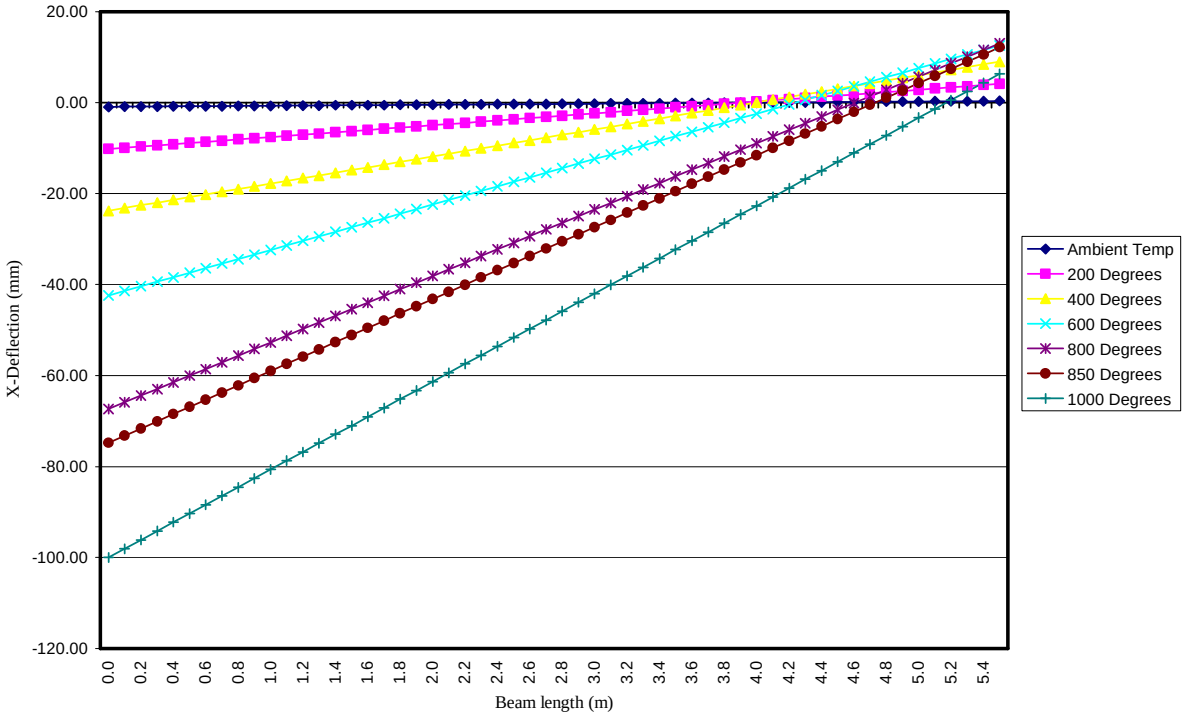

Figure 4.65: M/storey beam X-deflections for the beam & columns at uniform temperatures

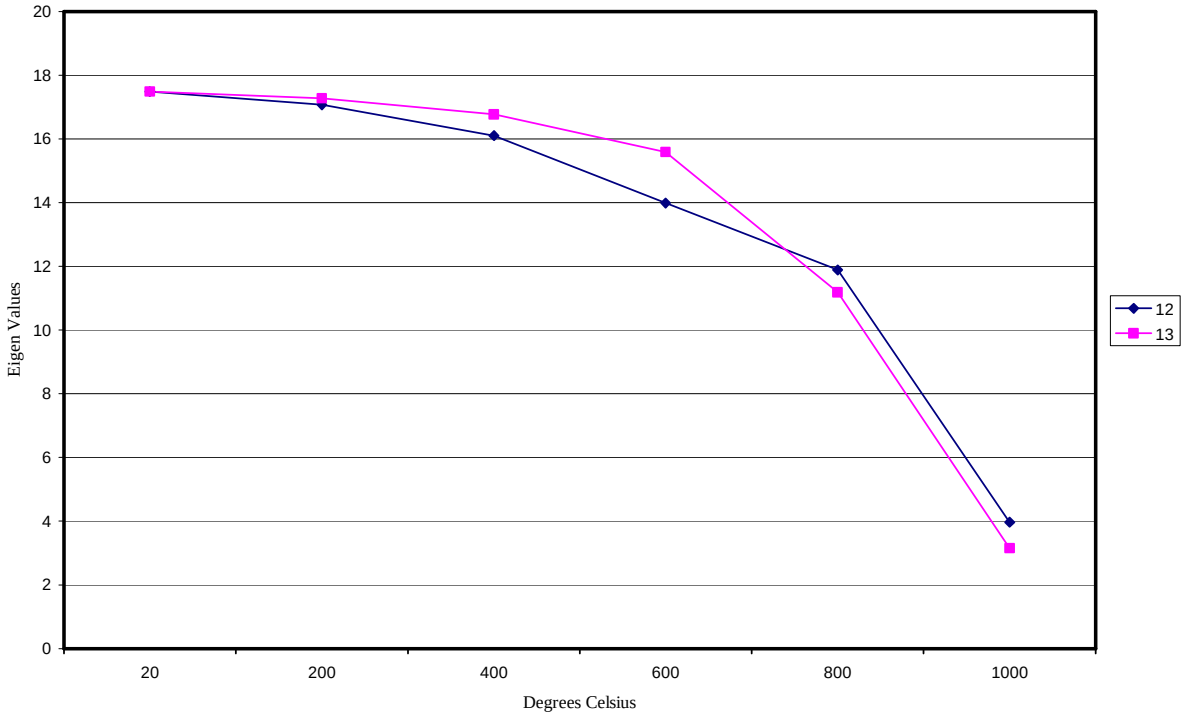

Figure 4.66: M/storey frame Eigen buckling values for models 12 & 13

4.4.5.2 Model 13: Lower LHS compartment beam heated uniformly

The same model as model 12 was used with the same loads and fixed support conditions with fixed beam-column connections (Figure 4.67). The model was generated as line segments representing the beams and columns. The hermitian beam elements were used to generate the column and beam sections. For this frame, a total of three element groups and two isotropic linear elastic material models were generated. The values of Young's modulus and the coefficient of thermal expansion corresponding to the applied various uniform temperatures of the beam line segment were assigned to the appropriate corresponding material model (Figure 4.67).

It can be seen in figure 4.68 and table 4.18 that there is a distribution of moments in the compartment beam to the LHS joint with very little bending moment in the span. The span moments are similar to the multi-storey frame of model 12 with a reduction of approximately 14 %. The external joint increases in moment by 808 % from ambient up to 1000 ˚C while the internal joint reduces in moment by 8 % (Figure 4.68 and Table 4.18). Once again the column moments follow the exact profile of the external joint moments (Figure 4.69 and Table 4.18).

The column x-deflection, as shown in figure 4.70 and table 4.18, is increased by 6417 % up to 1000 ˚ C and is about 40 % less than the deflection of the column for the frame of model 12 (Figure 4.63 and Table 4.17).

The beam y-deflection increases downwards and has a total increase of 1071 % at a temperature of 1000 ˚ C (Figure 4.71 and Table 4.18). This deflection of about 54 mm exceeds the serviceability deflection limit of L/300 = 18.3 mm by 35.7 mm.

It can be seen that the beam x-deflection is large at the external joint (Figure 4.72), but is only approximately 30 % of the beam deflection for the frame of model 12 (Figure 4.63 and Table 4.17).

In figure 4.66, it can be seen how the frame buckling strength deteriorates with temperature up to 18% of ultimate strength at ambient temperature. This is less than the case of the frame with the beams and columns heated uniformly.

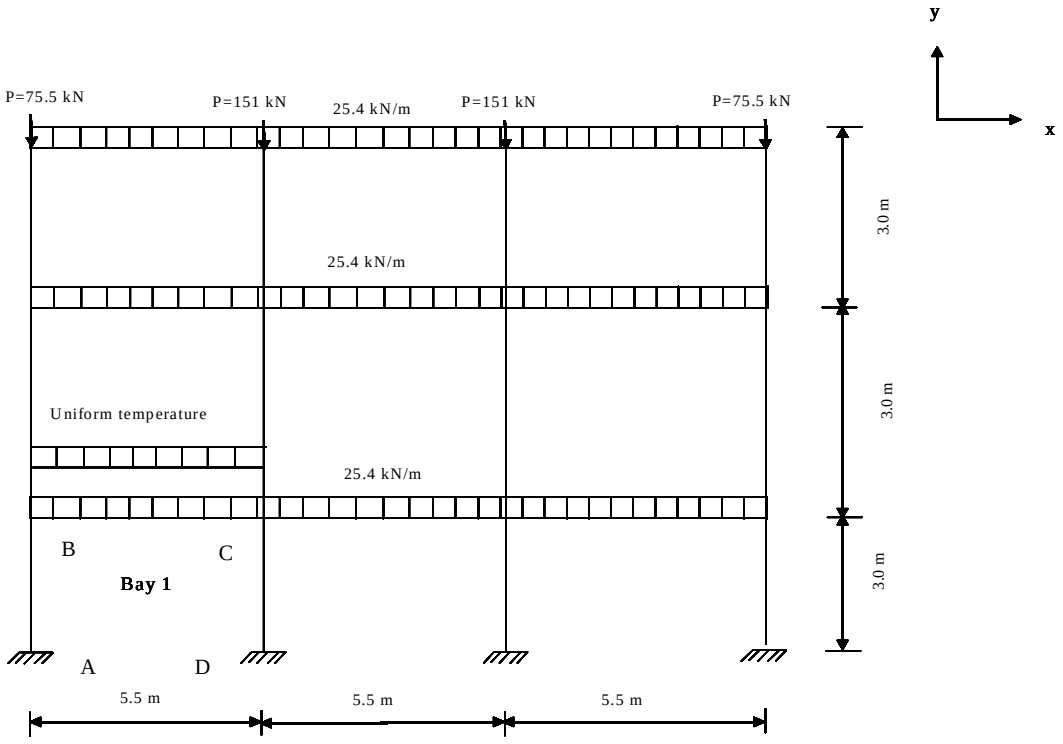

Figure 4.67: Model 13: Multi Storey frame with a uniform temperature applied to the beam only of Bay 1

Table 4.18: Summary of the results for model 13 (supports fixed in all directions): beam of bay subjected to uniform temperatures, only

		Values at 20 ºC and percentage increase of values from ambient		Values at 200 ºC and percentage increase of values from ambient		Values at 400 ºC and percentage increase of values from ambient		Values at 600 ºC and percentage increase of values from ambient		Values at 800 ºC and percentage increase of values from ambient		Values at 1000 ºC and percentage increase of values from ambient	
		Value at Ambient(20 ºC)	% Increase of value from ambient	Value at 200 ºC	% Increase of value from ambient	Value at 400 ºC	% Increase of value from ambient	Value at 600 ºC	% Increase of value from ambient	Value at 800 ºC	% Increase of value from ambient	Value at 1000 ºC	% Increase of value from ambient
Beam Moments (kNm)	Connection B	49.00	0.00	88.70	181.02	175.30	357.76	276.00	563.3	377.00	769.39	395.80	807.76
	Mid span	-36.90	0.00	-35.20	95.39	-32.90	89.16	-31.10	84.3	-30.70	83.20	-31.60	85.64
	Connection C	69.50	0.00	68.30	98.27	67.40	96.98	65.70	94.5	64.30	92.52	64.00	92.09
Column Moments (kNm)	Support A	-16.60	0.00	-81.00	487.95	-171.20	1031.33	-276.50	1665.7	-383.30	2309.04	-403.80	2432.53
	Mid span	5.10	0.00	3.80	74.51	2.10	41.18	-0.20	-103.9	-3.10	-160.78	-4.00	-178.43
	Connection B	49.00	0.00	88.70	181.02	175.30	357.76	276.00	563.3	377.00	769.39	395.80	807.76
Beam Y-Deflections (mm)	Connection B	0.07	0.00	-0.51	-828.57	-0.38	-642.86	-0.26	-471.4	-0.13	-285.71	-0.01	-114.29
	Mid span	-5.04	0.00	-5.50	109.13	-5.55	110.12	-7.46	148.0	-13.86	275.00	-53.98	1071.03
	Connection C	-0.64	0.00	-1.23	192.19	-1.13	176.56	-1.03	160.9	-0.94	146.88	-0.83	129.69
Column X-Deflections (mm)	Support A	0.00	0.00	0.00	0.00	0.00	0.00	0.00	0.0	0.00	0.00	0.00	0.00
	Mid span	-1.02	0.00	-5.73	561.76	-12.33	1208.82	-20.04	1964.7	-27.88	2733.33	-29.40	2882.35
	Connection B	-0.93	0.00	-10.63	1143.01	-24.21	2603.23	-40.13	4315.1	-56.45	6069.89	-59.68	6417.20

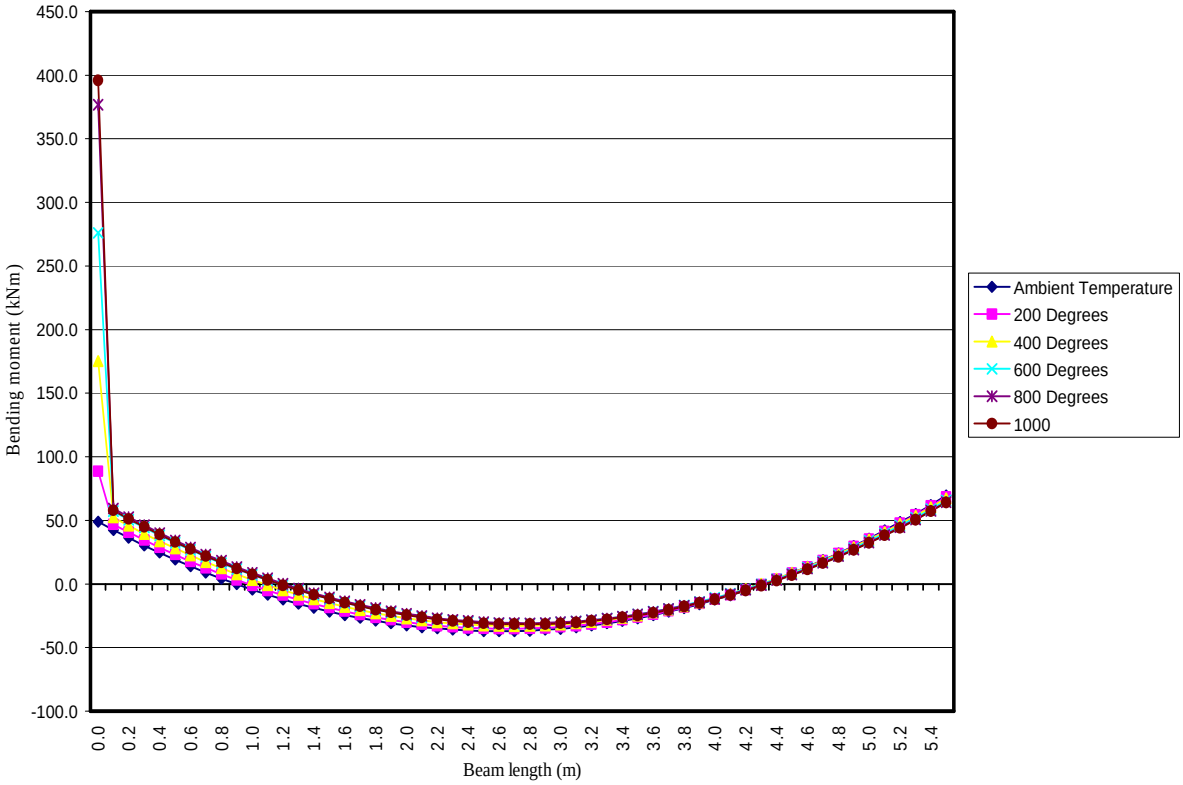

Figure 4.68: M/storey beam moments for the beam at uniform temperatures

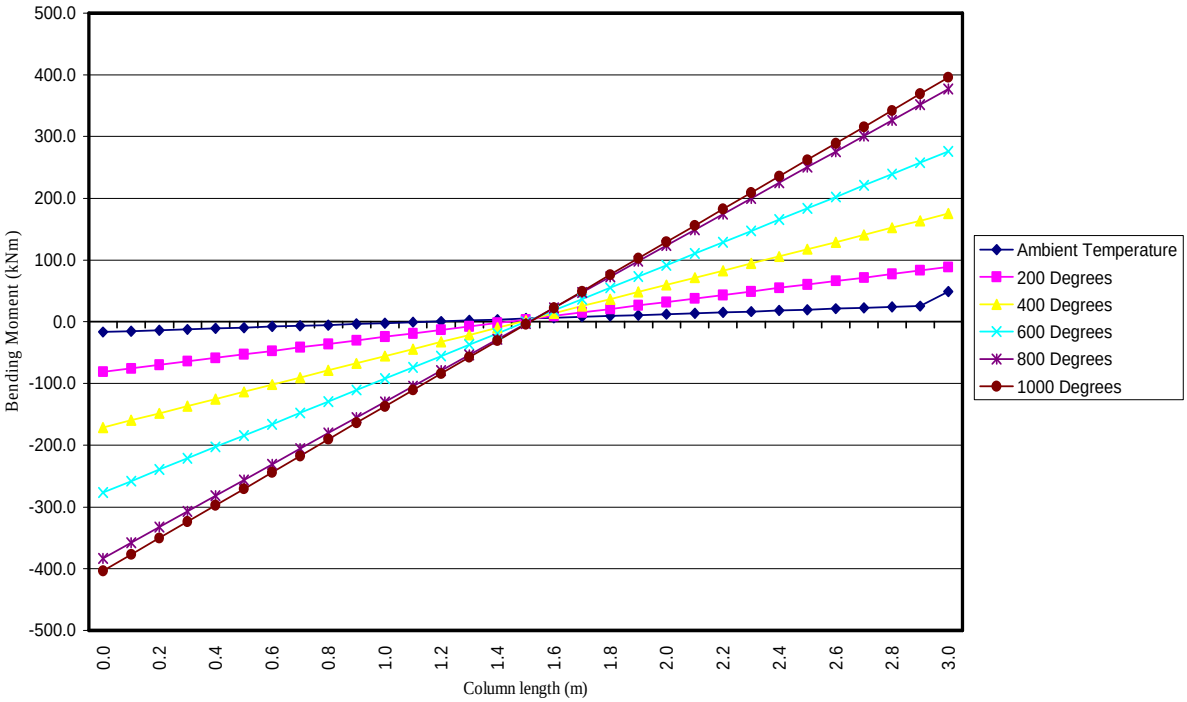

Figure 4.69: M/storey column moments for the beam at uniform temperatures

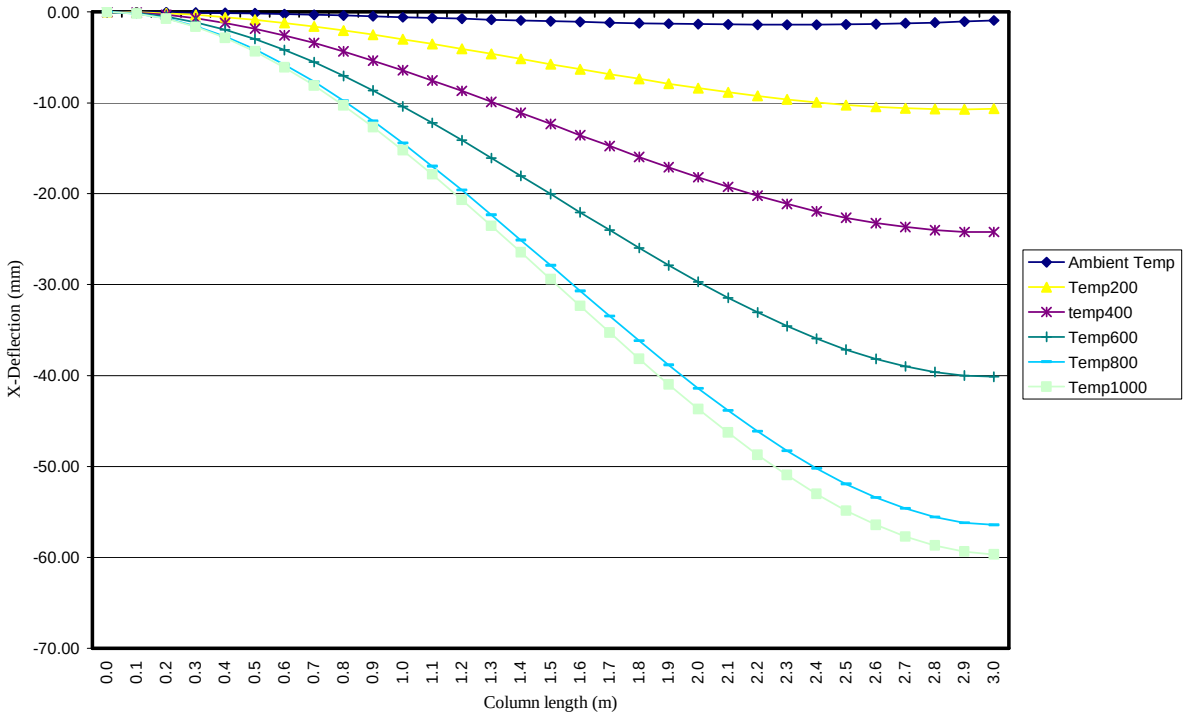

Figure 4.70: M/storey column X-deflections for the beam at uniform temperatures

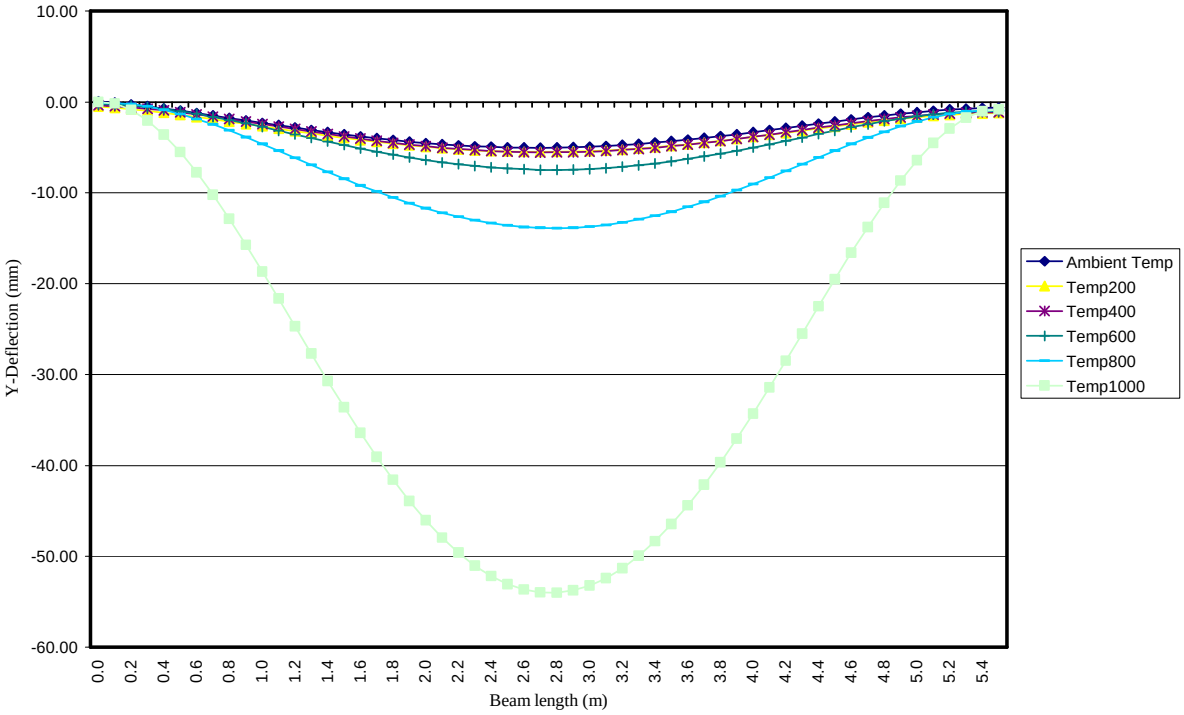

Figure 4.71: M/storey beam Y-deflections for the beam at uniform temperatures

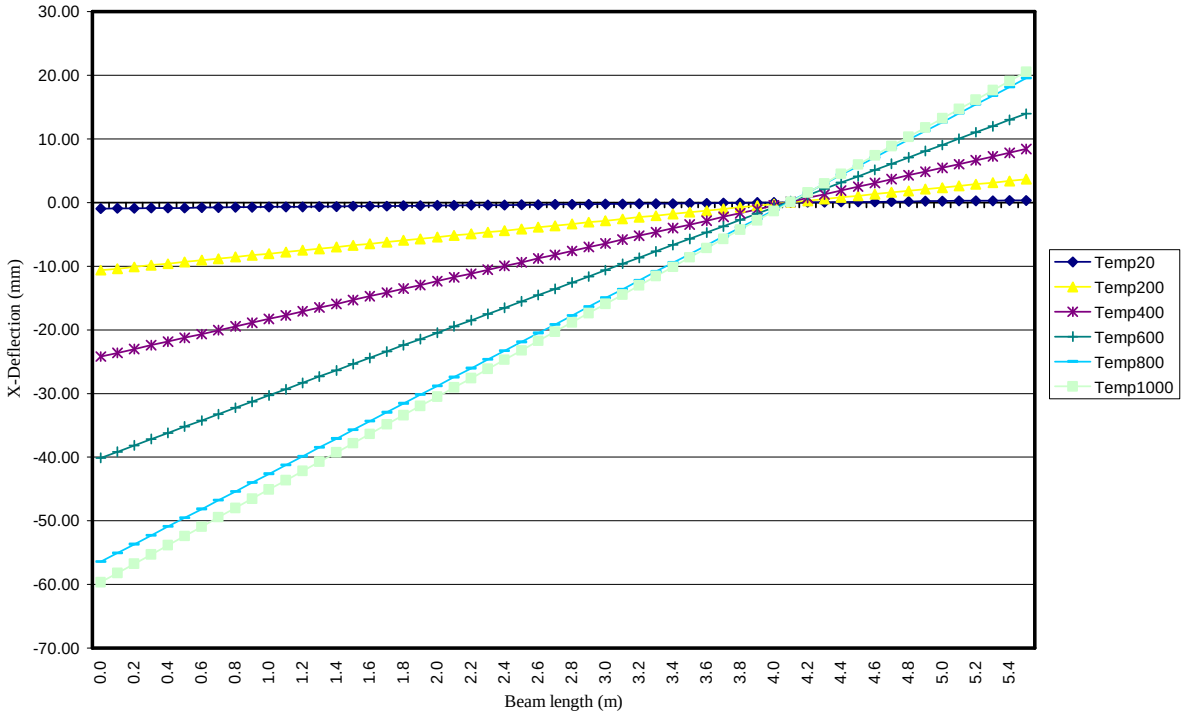

Figure 4.72: M/storey beam X-deflections for the beam at uniform temperatures

4.5 Summary

Beam members spread the moments from the span towards the supports depending on whether the supports are pinned or fixed and fall in the range of 0 to 50 %. The only variance seems to be the isolated fixed end supported members, that is, beams and columns at varying uniform temperatures.

The type of support or connection affects the moment behaviour of the beams. Simply supported beams are unable to spread the applied moments to the stiffer regions i.e. distribute, as their supports cannot absorb moments.

The isolated members, that is, beams and columns, having fixed end support conditions and temperature gradients along the lengths exhibited moment distribution away from the midspan regions to the supports in a range of 15 to 90 %. This gradient temperature seems to enable the distribution of moments in beam/column members. The deflections generated by the thermal expansion are less than the deflections for the beams subjected to uniform temperature increases. This difference is in the order of 38 %. For the columns the y-deflection increase was in the order of 3936 %.

Isolated beam and column members, which have simple and fix end support conditions and are subjected to varying uniform temperatures seem unable to spread the moments from weaker to more rigid sections. The result is a constant bending moment while the extra length that is generated, causes further y-deflections (x-deflections for the column members). The deflections for these beams with simple and fix end support conditions and subjected to uniform temperature increases, are higher than for the beams with the same support conditions but subjected to a gradient temperature. For the columns the y-deflections were negligible.

In the portal frames the beams have a reduction in the mid span moments of 52 to 90 % while the support moments are increased by approximately 60 to 209 %. This is evident in all models where the beam is subjected to heat. In the models where the columns were heated, the moments were spread to the mid span of the beam. The mid span moments increased by 117 to 406 % while the support moments were reduced by 4 to 34 %. The y-deflection of the beam in portal frames with the beam and column subjected to gradient temperatures, increases upwards from – 126 to – 159 %. The upward y-deflection of the beam in portal frames with the column heated uniformly also showed an increase of – 171 %. These upward deflections indicate a stiffening

effect of the beam and column members which is probably reflected in the buckling analysis where some models actually show an increase in strength from 9.44 to 77 %.

For the multi storey frame with all the compartment members heated uniformly, the mid span moments are initially reduced by 8 % and then increased by 20 % before it drops to a final increase of 7 %. For the multi storey frame with the beam heated only, the mid span moments are reduced by 15 % while the LHS support moments increased by 807 %.

The column base moments for the portal frames with heated beams showed an increase of 105 % to 739 % while the moments at the top of the columns were increased by 113 % to 218 %. The portal frames with columns heated showed a decrease of base moments of approximately 70 % except for model 11 which had a slight increase of 105 %. The moments at the top of the columns for these models showed a general decrease of 10 to 70 %. In general columns have showed an increase in moments at the beam-column connections and can be attributed to the thermal expansion of heated beams.

Isolated members and complete frames/structures with increasing gradient temperatures tend to exhibit more strength than isolated members or complete frames/structures subjected to increasing uniform temperature.

5. Conclusions

Clearly beam and beam-column members in frames, with fixed supports, exhibit the ability to spread their loads from weaker midspan sections to more rigid supports or connections. Isolated members with either fixed or pinned supports and subjected to a uniform temperature increase are unable to spread the applied moments. However, isolated fix end supported beams that are subjected to a gradient temperature have the ability to spread the applied moment to the supports. This knowledge implies that steel framed buildings can now be designed for this increased moment at the supports of these members.

Heated beams of portal frames induce moments in the columns of these structures. The increase in the moments in the columns of the investigated systems is in the region of 113 % to 208 %. This means steel structures can now be designed to withstand these induced moments. Alternatively, a bracing system can be employed to counteract these induced moments in columns.

Gradient temperatures applied to individual members of portal frames causes a reduction in the beam mid span deflection and results in an upwards deflection of up to 159 %. This behaviour pattern can be beneficial if the deformation under fire conditions is permanent. It will counteract downward deflections of members under normal loading conditions.

It is clear from the behaviour patterns that it is unrealistic and conservative to consider uniform temperature increases in members as these members will definitely have a temperature gradient along their lengths and even across their cross-sections.

It seems that a large portion of the integrity of the structure hinges on the ability of the joints to absorb the additional moments. Therefore more detailed attention to the connection performance is imperative to ensure the absorption of the additional moments which are in the range of 20 % to 100 % more. Therefore, the applied temperature loading on steel structures under fire conditions should not include the application of uniform cross sectional and longitudinal temperatures on individual or a combination of members forming part of complete frames.

Pattern loading i.e. applying heat to individual or a combination of members forming part of a frame, will result in a combination that will yield the highest stresses for a particular or number of members. This will ensure that steel framed buildings are designed for the highest possible stresses that the building can experience under fire conditions.

Portal frames with members subjected to a gradient temperature increase, seem to have a greater overall strength than portal frames with members subjected to a uniform temperature rise. This improvement in overall strength is in the region of 35 % to 49 %.

However a number of aspects could not be considered in this investigation. These are however important. Some of them are mentioned below;

The analysis of steel structures subjected to fire conditions must take into account the variation of temperature along the length of the individual members of these structures. More investigation is required to determine the effect of a temperature gradient across the cross sections of the individual members of steel framed structures.

The global effect of members that form part of larger structures and that are subjected to localized heating need to be investigated.

Finite element programs need to incorporate the interaction between the temperature model and the structural model to account for the exact distribution of temperature related stresses, strains etc in frame modelling.

Further investigation is required on the effects of pattern loading i.e. applying heat on individual or a combination of individual members forming part of a complete frame, in order to obtain the combination that produces the worst stresses in the members.

References

1 Y.C. Wang and D.B. Moore, Steel frames in fire: analysis. Engineering Structures 17 (6) (1995), pp. 462-472

2 J.A. El-Rimawi, I.W. Burgess & R.J. Plank. The Analysis of Semi-Rigid Frames in Fire-a Secant Approach, J. Construct. Steel Research 33 (1995), pp. 125-146

3 C.G.Bailey & D.B. Moore, The structural behaviour of steel columns during a compartment fire in a multi-storey braced steel –frame. J. Const. Steel Res 52 (2)(1999),pp.137-157

4 K.H. Tan & W.F. Yuan, Buckling of elastically restrained steel columns under longitudinal non-uniform temperature distribution. J Const Steel Res 64 (1) (2008), pp. 51-61

5 Khalifa S. Al-Jabri, J. Buick Davison & Ian W. Burgess, Performance of beam to column joints in fire. Fire Safety Journal Volume 43,Issue No.1(January 2008),pp 50-62

6 D.E.Wainmai and P.A Kirby, Compendium of UK standard fire test data, unprotected structural steel, Vol. 1 Ref. No. RS/RSC/S10328/1/87/B and Vol. 2 Ref. No. RS/R/S1199/88/B, British Steel Corporation, Swindon Laboratories, UK

7 K.J. Bathe, Professor at Massachusetts Institute of Technology, founded ADINA in 1986.

8 T.R. Kay, B.R. Kirby & R.R. Preston, Calculation and the heating rate of an Unprotected Steel Member in a Standard Fire Resistance Test, Fire Safety Journal 26(1996),pp.327-350

9 Eurocode 1: ENV 1991-2-7: Basis of design and actions on structures Part 2: Accidental Actions

10 Eurocode 3 : 2005.Design of steel structures, ENV 1993-1-2: 2005,General rules-structural fire design

11 J.I. Gholel & M.B. Wong, heat transfer model for unprotected steel members in a standard compartment fire with participating medium. J. Const Steel Res 61(6)(2005

12 Kang-Hai Tan, Wee-Siang Toh, Zhan-Fei Huang & Guang-Hwee Phng, Structural responses of restrained steel columns at elevated temperatures. Part 1: Experiments. Engineering Structures 29 (8) (2007), pp. 1641-1652

13 Y.C. Wang & J.M. Davies, An experimental study of non-sway loaded and rotationally restrained steel column assemblies under fire conditions: analysis of test results and calculations. J Const Steel Res 59 (2003), pp. 291-313

14 C.G. Bailey, D.B. Moore and T. Lennon, The structural behaviour of steel columns during a compartment fire in a multi-storey braced steel frame. J Const Steel Res 52 (2) (1999), pp. 137-157.

15 C.G. Bailey, Development of computer software to simulate the structural behaviour of steel-framed buildings in fire. Computers and structures 67 (1998), pp. 421-438.

16 B.R. Kirby and R.R. Preston, High temperature properties of hot-rolled, structural steels for use in fire engineering design studies, Fire Safety J 13 (1988), pp. 27-37.

17 Lyle P. Carden & Ahmad M. Itani, Performance of an unprotected steel structure subject to repeated fire at a fire fighter training facility, Fire Safety Journal 42 (2) (2007), pp.81-90

18 W. Skowronski. Buckling fire endurance of steel columns. J. Structural engineering, ASCE 1993, 119 (6), pp. 1712-1732

19 D.J. Latham, G. Thomson, B.R. Kirby and D.E. Wainman, Second natural fire test on a loaded steel frame at Cardington, RS/RSC/7281/12/86/E. Swindon Laboratories, British Steel Corporation, UK, 1986.

20 M.A. Bradford, T.K. Luu and A. Heidarpour, Generic nonlinear modelling of a steel beam in a frame sub-assembly at elevated temperatures, J Const Steel Res 64 (2008), pp. 732-736.

21 M.B.Wong & .Szafranski,Elastic method for design of 3-D steel structures subject to fire, J Const Steel Res 60 (2004),pp.1095-1108.

22 Y.B. Yang, I.J. Lin, L.J. Leu and C.W. Huang, Inelastic postbuckling response of steel trusses under thermal loadings, J Const Steel Res

23 Y.C. Wang, The Effects of frame continuity on the behaviour of steel columns under fire conditions and fire resistant design proposals, J Const Steel Res 41 (1) (1997), pp. 93-111

24 Commission of the European Community, Eurocode 3: design of steel structures, part 1.4: fire resistance, British Standards Institution, 1994.

25 British Standards Institution, British Standard BS 5959: Structural use of steelwork in buildings, Part 8: code of practice for fire resistant design, British Standards Institution, London, 1990.

26 M. B. Wong & N. Patterson, Unit Load Factor Method for Limiting Temperature Analysis of Steel Frames with Elastic Buckling Failure Mode. Fire Safety Journal 27 (1996), pp. 113-122

27 Y.C. Wang and J.M. Davies, An experimental study of non-sway loaded and rotationally restrained steel column assemblies under fire conditions: analysis of test results and design calculations, J Cont Steel Res 59 (2003), pp. 291-313.

28 K.H. Tan and W.F. Yuang, Buckling of elastically restrained steel columns under longitudinal non-uniform temperature distribution, J Const steel Res 64 (2008), pp. 51-61.

29 ISO 834 (1992) Part 1, Fire resistance test- elements of building construction. Switzerland: International Organisation for Standardisation, 1992.

30 Eurocode 1:1996. Basis of design and actions on structures, ENV1991-2-2: 1996 General actions-Actions on structures exposed to fire.

31 D.K. Edwards and R. Matavosian, Scaling rules for total absorptivity and emissivity of gases. Transactions of ASME, Journal of Heat Transfer 106 (1984), pp. 684-689.

32 J.I. Gholel, A new approach to modelling heat transfer in compartment fires. Fire Safety Journal 31 (1998), pp. 227-237.

33 M.B. Wong and J.I. Gholel, Spreadsheet method for temperature calculation of unprotected steelwork subject to fire. The Structural Design of Tall and special Buildings 12 (2) (2003), pp. 83-92.

34 EN. 1363-1 (1999) Part 1, Fire resistance test- General requirements: European Committee for Standardization, 1999.

35 C. Both and L. Twilt, Report No. BI-89-208. TNO Building and Construction Research, The Netherlands, 1990.

36 Fishenden, M.& Saunders, O.A. An Introduction to Heat Transfer. Clarendon Press,Oxford,UK,1961

37 Lankford, W.T. Samways, N.L, Craven, R.F.& McGannon, H. E., The Making, Shaping and Testing of Steel,10thedn.U.S.Steel,1985

38 J. Thor, Bulletin 29, Institutionen for Byggnadsstatik, Lund, Sweden, 1972.

39 ENV 1993-1-1: Eurocode 3: Design of steel structures Part 1-1: General Rules: Structural Fire design

40 A.S. Usmani, J.M. Rotter, S. Lamont and A.M. Sanad and M. Gillie, Fundamental principles of structural behaviour under thermal effects, Fire Safety Journal 36 (2001), pp. 721-744.

41 A. Hrennikoff, Solution of Problems in Elasticity by the Frame Works Method, Journal of Applied Mechanics, Vol. 8, No. 4, pp. 169-175, Dec. 2001.

42 J.Y. Richard Liew, L.K. Tang, Tore Holmaas and Y.S. Choo, Advanced analysis for the assessment of steel frames in fire, J Const Steel Res 47 (1998), pp 19-45.

43 SANS 0100-1: 2001, Design of Concrete Structures